INITIATION OF SUBCOOLED POOL BOILING DURING PRESSURE TRANSIENTS

by

DONALD L. SCHMIDT

B.S., Kansas State University, 1983

A MASTER'S THESIS

submitted in partial fulfillment of the
requirements for the degree

MASTER OF SCIENCE

Department of Nuclear Engineering

KANSAS STATE UNIVERSITY

Manhattan, Kansas

1985

Approved by:

Richard E Faw

Major Professor

TABLE OF CONTENTS

LIST OF FIGURES

LIST OF TABLES

ACKNOWLEDGEMENTS

The author is greatly indebted to Professor R. E. Faw for his guidance and suggestions throughout the study and the preparation of this thesis. The author also expresses his great appreciation to Mr. W. E. Starr for his assistance in the maintenance and repair of electrical apparatus, and to Mr. R. J. VanVleet for his effort in development of procedures for data collection and analysis. A special thanks is given to Mrs. Connie Schmidt for typing this thesis.

This work was funded in part by National Science Foundation Grant MEA 81-02193.

1. INTRODUCTION

Vapor bubble nucleation and growth phenomena have attracted the attention of researchers for many years. Nearly all of the attention has been placed on saturated nucleate boiling and the transition to film boiling. Studies of boiling under transient conditiona have been devoted primarily to investigations of the transition to film boiling. The nature of boiling phenomena preceding the transition has received little attention. However, these phenomena are important aspects of the broader problem of understanding the sequence of events leading to boiling crises in high-pressure heat exchangers such as nuclear power reactors.

Transient initiation of boiling has been described by steady-state nucleation models, which use the size of active nucleation sites to determine superheats necessary for bubble nucleation from these sites. The required superheats for a simple transient situation can be achieved by an increase in the heater surface temperature or by a decrease in the fluid saturation temperature by means of a reduction in the fluid pressure.

Surface characteristics are important in the description of the sizes of cavities available as nucleation sites. The pressure and temperature conditions experienced prior to the initiation of boiling were also postulated to be of major importance by Fabic (1), since potential sites could be flooded by pre-pressurization. Studies performed to examine transient boiling caused by decompression (2-5) have employed conditions such that bulk liquid flashing occurs by the end of the decompression. Consequently, the behavior when boiling

initiation conditions are not met for the predicted cavity sizes and the reactivation of flooded surface cavities has not been thoroughly investigated.

In this work, the transition from convection to boiling during pressure transients was investigated for a horizontal, cylindrical platinum heating element submersed in a fluid. Maximum overpressures were applied to the system before subjecting the heating element to constant power delivery, maintained during transients by a custom made power supply driven by 12 volt wet cells. Separate runs were necessary to measure the system pressure as a function of time and the element temperature as a function of time. The element temperature was determined using resistance thermometry. The data were recorded using a digital oscilloscope, stored on a floppy disk, then transferred to a computer for analysis. The time at which the first bubble was seen or heard was recorded as the measured boiling initiation time. Initiation times were also estimated based on the point where the analyzed heater temperature began to decrease. Although these two methods did not always produce equivalent time values, ranges for true boiling initiation times were determined from these measurements.

Pressure transients displayed exponential reduction behavior over most of the pressure decrease, and they were reproducible in that region. Boiling initiation times provided conditions which tended to support the cavity deactivation by pre-pressurization hypothesis of Fabic, although the effects of initial pressures were not as pronounced as expected by the model. Boiling was observed even in cases where none was predicted, but subsequent nucleation site reactivation and recovery of the heater temperature to steady-state was impeded by increases in maximum pressure applied.

2. REVIEW OF PREVIOUS WORK

2.1 Convection Heat Transfer

In a system composed of a body immersed in a fluid, convection heat transfer will occur if the body and the bulk fluid temperature are at different temperatures. Quantifying the heat transfer analytically is not a simple matter because of the dependence not only on numerous fluid properties, but also on flow conditions and surface geometry.

Boundary-layer theory has been used to derive numerical solutions for horizontal cylinders. These solutions have been shown to be quite accurate for moderate Rayleigh numbers characterizing cases where the wake is confined to a small region at the rear of the cylinder. Churchill and Chu (6) examined a wide range of data on steady-state convective heat transfer from horizontal cylinders. They recommended the following correlation as being applicable to both constant cylinder surface temperature and constant heat flux for all Rayleigh and Prandtl numbers:

$$Nu^{\frac{1}{2}} = 0.60 + 0.387\ f(Pr)Ra^{1/6} \qquad (2.1)$$

where the Rayleigh and Nusselt numbers are based on cylinder diameter, and

$$f(Pr) = [1 + (0.559/Pr)^{9/16}]^{-8/27}. \qquad (2.2)$$

Morgan (7) also carried out a thorough analysis of published experimental data on steady-state convection from horizontal cylinders, and recommended the following correlation as being applicable for gases and liquids (except liquid metals):

$$Nu = B\ Ra^{m} \qquad (2.3)$$

where values of B and m are given in the following table:

Ra	B	m
$10^{-10} - 10^{-2}$	0.675	0.058
$10^{-2} - 10^{+2}$	1.02	0.148
$10^{2} - 10^{4}$	0.850	0.188
$10^{4} - 10^{7}$	0.480	0.250
$10^{7} - 10^{12}$	0.125	0.333

Fujii, et al. (8) reported that for convection from horizontal cylinders, the following correlation shows good agreement with both calculated and measured heat transfer rates:

$$2/Nu = \ell n\ [1 + 4.918g(Pr)Ra^{-n}], \tag{2.4}$$

where

$$g(Pr) = [1 + (0.492/Pr)^{9/16}]^{-4/9} \tag{2.5}$$

and

$$n = 0.25 + 1.0/(10 + 5Ra^{0.175}). \tag{2.6}$$

Table 2.1 shows a comparison of these three correlations for the Rayleigh number range of interest in this work.

2.2 Boiling Initiation

2.2.1 Steady-State Boiling Initiation

Many theoretical analyses and interpretations of experimental data on boiling initiation have been based on concepts introduced by Griffith and Wallis (9) and embellished by Hsu (10), Bergles and Rohsenow (11),

Table 2.1. Comparison of predictions of Churchill-Chu, Fujii, and Morgan correlations for natural convection heat transfer from a 0.25 mm diametric cylinder. Ambient conditions: T_a = 20°C. Fluid properties are evaluated at the mean temperature between T_w and T_a.

$T_w - T_a$ (°C)	Heat Flux (kW/m^2)		
	Churchill-Chu	Morgan	Fujii, et al.
10	26.2	29.4	31.1
20	60.3	68.0	72.5
30	100	113	121
40	145	163	176
50	195	218	237
60	249	278	304
70	308	341	376
80	371	409	453
90	438	483	535
100	509	564	622

Han and Griffith (12), Madejski (13), and Cole and co-workers (14, 15, 16). In its simplest form, the concept may be described as follows.

Consider present within a fluid a heating element within the surface of which is an active boiling initiation site with a circular aperture of radius r_c (Fig. 2.1). As the temperature of the heating element is increased beyond the saturation temperature of the fluid, a vapor bubble emerges from the aperture. The surface of the bubble is spherical shaped due to the effect of surface tension. The minimum radius of curvature of the bubble is r_c, the radius of the aperture. At this minimum radius, surface forces are maximum, and the excess of the vapor pressure within the bubble over the static fluid pressure must be maximum.

If the fluid surrounding the bubble is at temperature T_w, the excess pressure is given by

$$p_v(T_w) - p_v(T_s) = 2\sigma(T_w)/r_c, \tag{2.7}$$

in which T_s is the saturation temperature of the fluid at system pressure $p = p_v(T_s)$, $p_v(T_w)$ is the vapor pressure of the fluid at temperature T_w, and σ is the fluid-vapor surface tension evaluated at temperature T_w. The excess temperature of the fluid at the fluid-vapor interface of the bubble can be related to the excess pressure in the bubble through use of the Clausius-Clapeyron relation. Application of this relation leads to the approximation that

$$T_w = f_1(r_c) \equiv T_s + \frac{2\sigma T_s}{\lambda \rho_v r_c}, \tag{2.8}$$

where ρ_v is the vapor phase density, assumed to be much less than that of the liquid phase, and λ is the latent heat of vaporization. This is the

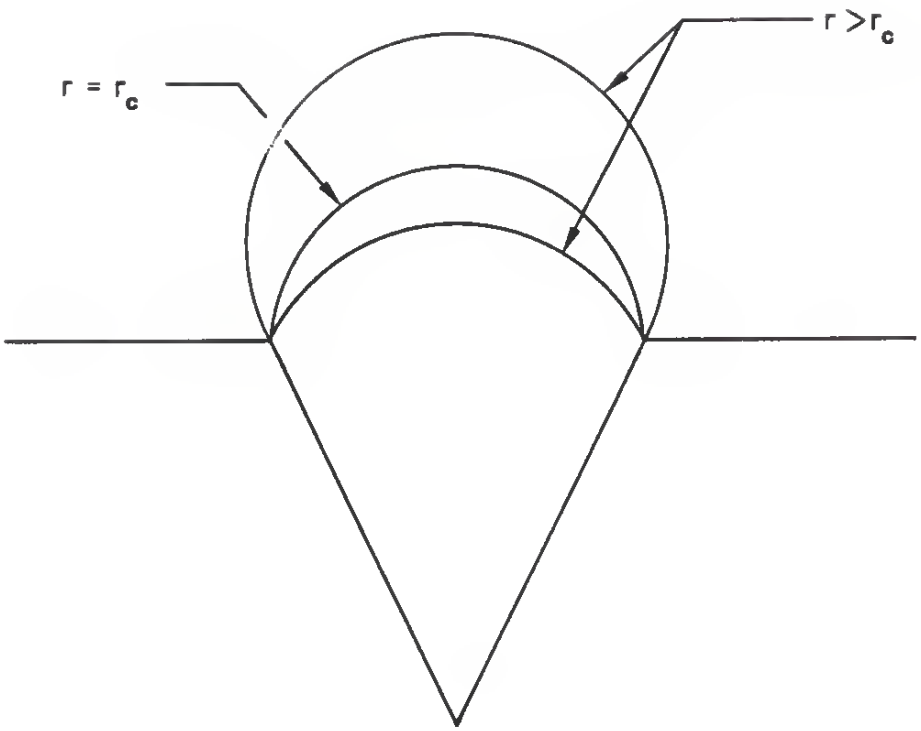

FIG. 2.1. Illustration of bubble growth from an active nucleation site.

threshold temperature which must be exceeded for the bubble to grow beyond radius r_c.

Now suppose that the fluid surrounding the heating element has a temperature distribution $T(r) = f_2(r)$, a function of distance r from the surface. Let T_w and T_a represent the surface temperature and the ambient temperature respectively. If q is the heat flux from the surface to the fluid, then approximately

$$f_2'(r) = dT/dr = -q/k, \tag{2.9}$$

and

$$f_2(r) = T(r) = T_w - qr/k, \tag{2.10}$$

where k is the thermal conductivity of the fluid.

Griffith and Wallis argued that for a bubble to grow in size beyond the radius r_c, the surface temperature of the heating element must exceed the threshold temperature, i.e., that $f_2(0) = f_1(r_c)$. Hsu contended that for the bubble to grow, it is necessary that the fluid temperature, not at the heating-element surface or base of the bubble, but at the cap of the bubble, exceed the threshold, i.e., that $f_2(r_c) = f_1(r_c)$. Han and Griffith argued that neither the temperature at the bubble base nor that at the bubble cap controlled the bubble growth. Rather, it was reasoned, the average liquid temperature surrounding the bubble was the controlling factor. This led to the criterion $f_2(ar_c) = f_1(r_c)$, where it was argued that $a = 3/2$. Sakurai and Shiotsu (17) accommodated in their arguments an empirical relationship between the cavity radius and the bubble radius at boiling inception, namely that the bubble radius is br_c. Allowing for this empericisim, the boiling initiation criterion may be stated as $f_2(ar_c) = f_1(br_c)$, or

$$T_w - T_s = \frac{qar_c}{k} + \frac{2\sigma T_s}{\lambda \rho_v b r_c} . \tag{2.11}$$

For the Griffith and Wallis approach, a = 0 and b = 1. For that of Hsu, a = 1.6 and b = 1.25. For that of Han and Griffith, a = 1.5 and b = 1. Sakarai and Shiotsu recommended that a = 1.8 and b = 1.67.

Suppose now that there are present on the heating element surface nucleation sites of a wide variety of radii. Cole (18), following the prescription of Bergles and Rohsenow (11), showed that, as the heat flux or surface temperature is increased, the first nucleation site to become active, i.e., from which the first bubble will emerge, is that one for which $r_c = r_*$ determined by $f_2'(ar_*) = f_1'(br_*)$. From Eqs. (2.8) and (2.9),

$$r_* = (2k\sigma T_s/\rho_v \lambda b^2 q)^{\frac{1}{2}}. \tag{2.12}$$

Substitution of this value into Eq. (2.11) leads to the following expression for the minimum surface superheat required for boiling from a surface with a full size range of nucleation sites:

$$(T_w - T_s)_{min} = (8\sigma T_s q/k\lambda\rho_v)^{\frac{1}{2}}. \tag{2.13}$$

Bergles and Rohsenow offered the following correlation of computed values for water over the pressure range 15 to 2000 psia:

$$q = 1.55 \times 10^4 \, p^{1.156} \, [1.8(T_w - T_s)]^{2.047/p^{0.0234}} \tag{2.14}$$

where q is measured W/m^2, T is K, and p is MPa. If, on the other hand, the largest nucleation site present has $r_c = r_m < r_*$, then the minimum surface superheat required for boiling initiation is the greater value

$$(T_w-T_s)_{min} = \frac{qar_m}{k} + \frac{2\sigma T_s}{\lambda\rho_v b r_m} . \qquad (2.15)$$

Selected values of minimum boiling superheat for H_2O are given in Table 2.2. For each saturation temperature, the last four values of r_m listed are the r_* values for the heat fluxes listed. Thus, superheats above and to the left of the horizontal lines are for the cases $r_m < r_*$.

One may ask how the superheat at boiling inception is affected by the subcooling of the ambient liquid. Suppose that a full range of initiation sites is available, so that the boiling superheat is governed by Eq. (2.13). Suppose that natural convection is the heat transfer mechanism, so that

$$q = C(T_w-T_a)^n \qquad (2.16)$$

where $n \sim 1.2$. By equating the heat fluxes in Eqs. (2.13) and (2.16), and noting that $T_w-T_a = T_w - T_s + \Delta T_{sub}$, one can show that $(T_w - T_s)_{min}$ is given by solution of the equation

$$(T_w - T_s)_{min} = C'[(T_w - T_s)_{min} + \Delta T_{sub}]^{n/2} \qquad (2.17)$$

where $C' = (8\sigma T_s C/k\lambda\rho_v)^{1/2}$. Evaluation of $(T_w-T_s)_{min}$ is illustrated in Fig. 2.2 where it may be seen that, as ΔT_{sub} increases, so also does the minimum boiling superheat. For example, for water at $T_s = 100°C$, an increase in ΔT_{sub} from 10 to 30°C causes an increase of about 5°C in the minimum boiling superheat.

Madejski (13) developed a model for boiling initiation which allows for a non-spherical bubble shape and avoids specification of the distance from the heating surface at which the superheat criterion must be applied. As corrected by Schmidt and Cole (14), the result of the

Table 2.2. Minimum boiling superheat as a function of maximum cavity radius.

T_s (°C)	r_m (μm)	q(MW/m²)	Minimum Boiling Superheat (K) for a=b=1			
			0.1	0.2	0.5	1.0
100	1		32.9	33.1	33.5	34.3
	2		16.7	17.0	17.9	19.3
	4.73		7.6	8.3	10.4	13.8
	6.69		5.9	6.9	9.8	13.8
	10.6		4.7	6.2	9.8	13.8
	15.0		4.4	6.2	9.8	13.8
150	0.5		15.4	15.5	15.7	16.1
	1		7.8	8.0	8.4	9.1
	2.31		3.7	4.0	5.0	6.6
	3.26		2.8	3.3	4.7	6.6
	5.16		2.2	3.0	4.7	6.6
	7.30		2.1	3.0	4.7	6.6
195	0.5		5.1	5.2	5.4	5.8
	1		2.7	2.8	3.3	4.0
	1.31		2.1	2.3	2.9	3.9
	1.86		1.6	1.9	2.7	3.9
	2.93		1.3	1.7	2.7	3.9
	4.15		1.2	1.7	2.7	3.9

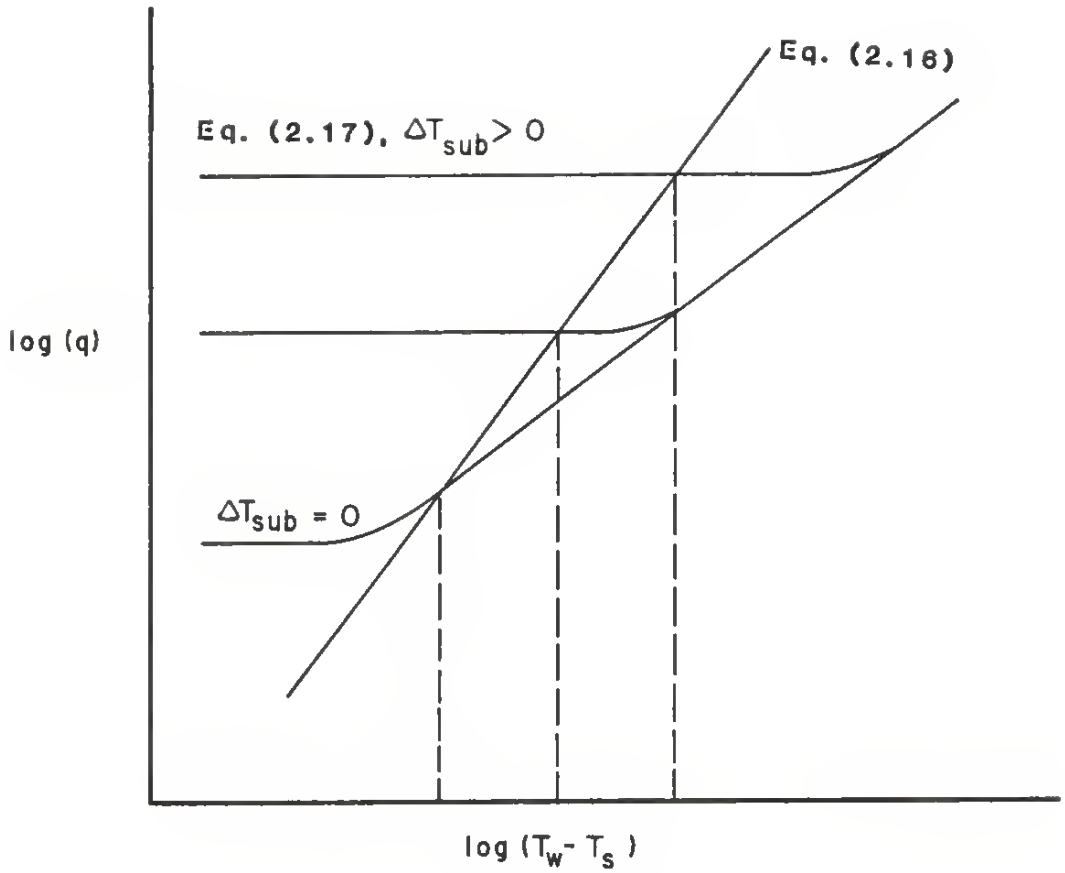

FIG. 2.2. Determination of boiling initiation superheat requirements based on Eqs. (2.13) and (2.16).

analysis is expressed as the ratio of the minimum surface superheat in a variable temperature situation to that required if the liquid were uniformly superheated, namely

$$\frac{(T_w-T_s)_{min}}{(T_w-T_s)_\infty} = \text{fctn}[r_m k(T_w-T_a)/q]. \qquad (2.18)$$

The function increases monotonically with its argument, reaching a value of about 4.5 at an argument of 3. The utility of the Madejski approach is limited by the availability of data for boiling initiation temperatures in uniformly superheated liquids.

2.2.2 Transient Boiling Initiation

Most of the work performed concerning transient boiling phenomena has focused on constant pressure systems subjected to transient heating. Few are of interest here because pressure effects generally were not considered. Those studies that used pressure as a parameter (e.g., references 19, 20, and 21) reported that the superheat required for boiling initiation decreased with increasing pressure. However, these studies examined boiling at various constant system pressures and did not test the effects of applying a temporary overpressure before an experimental run.

Fabic (1) thoroughly examined the consequences of the pressure-temperature history of a heating element on boiling initiation. He argued that the maximum radius of an active (unflooded) initiation site at the time of a test is governed by the maximum value of the ratio $(p-p_v)/\sigma$ experienced prior to the test. Here p is the system pressure and p_v the fluid vapor pressure. Call this maximum ratio $(p_o-p_{vo})/\sigma_o$. The maximum cavity radius is

$$r_c^+ = 2\sigma_o \frac{\cos(\pi-\theta_a)}{p_o - p_{vo}} \tag{2.19}$$

where θ_a (>90°) is the contact angle between the cavity wall and the vapor-liquid interface within the cavity. The value of θ_a is taken as 108° for water at all temperatures and pressures. Values of the ratio and r_c^+ are given in Table 2.3 for water under various conditions.

Fabic noted that most test fluids at some time are at 20°C and atmospheric pressure. This leads to an upper bound of $r_c \equiv \hat{r}_c = 0.5$ μm, for radii of nucleation cavities. He argued that boiling initiation takes place with a contact angle θ_r between 0 and 66°, and at a surface temperature T_w which satisfies the equation

$$p_v(T_w) - p = 2\sigma\cos\theta_r / r_c^+, \quad r_c^+ \leq \hat{r}_c, \tag{2.20}$$

$$= 2\sigma\cos\theta_r / \hat{r}_c, \quad r_c^+ > \hat{r}_c, \tag{2.21}$$

where σ is evaluated at T_w. Upper and lower limits on T_w would depend on the choice of 0° or 66° for θ_r. If, in fact, the largest potential initiation site had a radius $r_m < r_c^+$, then that radius would apply.

One may inquire of the effect of boiling from the heating surface at test conditions for purposes of degassing the surface. Fabic argued that the process would "arm" previously inactive (flooded) sites with vapor and thus that the pressure and temperature under which the degassing took place would define r_c^+.

One may also inquire of the effect of degassing at saturation conditions. Fabic is silent on this point. Presumably sites of all sizes would be activated and r_m would govern subsequent boiling initiation.

Table 2.3. Maximum active site radius as a function of temperature and pressure, computed using the Fabic Model [1].

Fluid Temp. (°C)	Pressure (MPa)	$(p-p_v)/\sigma$ (μm^{-1})	r_c^+ (μm)
20	0.101	1.35	0.46
	1.398	19.1	0.032
70	0.101	1.08	0.57
90	0.101	0.51	1.21
95	0.101	0.28	2.22
100	0.476	6.33	0.098
100	1.123	17.3	0.036
100	1.398	21.9	0.028
120	0.476	5.02	0.12
140	0.476	2.24	0.28
145	0.476	1.21	0.51
165	1.398	15.2	0.041
185	1.398	6.64	0.093
190	1.398	3.55	0.17

Winterton (2) also developed an expression for conditions at nucleation based on the pressure-temperature history of the heater,

$$p_v + p_g - p = \frac{1}{\gamma} \frac{\sigma}{\sigma_o} (p_o - p_{vo} - p_{go}) , \tag{2.22}$$

where p_g is the partial pressure of noncondensible gas, and γ is defined as

$$\gamma = \frac{\cos (\pi - \theta_a + \frac{\alpha}{2})}{\cos(\theta_r - \frac{\alpha}{2})} , \tag{2.23}$$

where α is the included apex angle of the cavity. It will be noted that Eq. (2.22) reduces to Eq. (2.20) for the case of a well degassed system and a cylindrical cavity ($\alpha = 0$). Winterton performed a number of experiments using vertical tubes to test theories of nucleation by surface cavities. He examined both transient heat flux - constant pressure and constant heat flux - transient pressure cases. Liquid pressures were in the range of approximately 0.01 to 0.1 MPa for both cases and true heat fluxes in the transient heat tests were 10 kW/m^2 maximum, resulting in a rate of rise in temperature of less than 1°C/s. For the transient heat case, he reported that the vapor pressure at nucleation increased with increasing overpressures, but that the effect was not as pronounced as indicated by the theory with γ set equal to unity. He reported that the order of magnitude of γ was 1, but his experiments indicated that the value was not constant. Instead, γ increased as the overpressure increased. The limitations of his experimental apparatus precluded making conclusions about the effect on the transient pressure case. However, for the conditions under which he was able to make both transient heat and transient pressure measurements,

he found no significant difference in the calculated cavity radius required for nucleation, thus confirming the equivalence of the two methods of nucleation. Gallagher and Winterton (4) performed a study which expanded on the power transient boiling work of Winterton. Again, a very low heat flux was used, and overpressures up to 0.7 MPa were applied before performing tests at 0.0122 MPa. They found that special preparation of the test section was necessary to produce consistent results. They reasoned that this preparation was associated with obtaining suitable and consistant values of contact angles within the surface cavities. Their results show a strong effect of pressure on deactivating cavities. They reported good agreement between their results and Eq. (2.22) using a constant value for γ of 5.4.

Faw and VanVleet (22), investigating boiling initiation from a horizontal wire in a subcooled pool of water, reported initiation conditions that were not consistent with any single size-distribution of nucleation sites. However, nearly all results were consistent with predictions made using Fabic's model. They also found that pre-pressurization well above saturation pressure led to greatly increased superheat requirements at boiling initiation consistent with the model. They noted that only the first test after pressurization was so affected; subsequent tests in the series had boiling initiation superheats approximately those expected in the absence of pre-pressurization. They postulated that the first test reactivated previously flooded sites.

Investigation of boiling phenomena during transient pressure conditions has been prompted by desire to determine the response of a high pressure, high temperature heat exchanger system (e.g., a nuclear

reactor) to a loss of pressure. Since the mechanical integrity of such a system can be breached by events resulting from inadequate heat transfer, most studies have examined the transition from nucleate to film boiling and critical heat fluxes (e.g., references 23, 24, and 25).

The initiation of boiling during decompression has received limited attention. Fabic argued that his pressure-temperature history modeling of boiling initiation would also apply to the pressure transient case. He noted that the nucleation event could occur due to a decrease in system pressure even if the surface temperature T_w did not change. In this case the system pressure p necessary for vapor nucleation could be predicted from Eqs. (2.20) and (2.21). Values of the boiling initiation pressure in water, based on the Fabic model, are given in Table 2.4 for water under various conditions.

It can be expected from Fabic's model that an increase in the initial overpressure applied to a system should cause an increase in the instantaneous surface superheat $[T_w-T_s(p)]$ necessary to initiate boiling. This increase would manifest itself by producing a measurable delay between the time boiling initiation is predicted by steady-state considerations and when it is actually observed. Hooper and Abdelmessih (26) observed just such an occurrence in a study of liquid flashing. However, Kenning and Thirunavukkarasu (27) found no indication of delay in bubble growth in their study of bubble nucleation characteristics of surfaces.

Weisman, et al. (3), in a study of boiling initiation using heated and unheated ribbons, found that measurable delays in boiling initiation could be encountered under appropriate conditions. They suggested that the results of Kenning and Thirunavukkarasu could be explained by the

Table 2.4. Boiling initiation system pressure values prescribed by the Fabic model (1) at T_a = 100°C and using θ_r = 66°.[a] $T_w = T_a$ until after initial pressure is applied.

p_i (MPa)	T_w (°C)	p_b (MPa)
0.239	140	0.204
0.273		0.165
0.308		0.125
0.308	150	0.250
0.377		0.175
0.411		0.137
0.377	160	0.330
0.446		0.258
0.515		0.186
0.584		0.114
0.515	170	0.380
0.584		0.312
0.653		0.243
0.790		0.106
0.584	180	0.546
0.653		0.481
0.790		0.350
0.997		0.155

fact that the pressure was released very rapidly to well below saturation pressure, thus activating unflooded cavities and allowing bubble growth to begin almost immediately. In their own investigation, the authors also found that the superheat required to initiate boiling on an unheated ribbon increased with increasing rate of depressurization. This is consistent with results obtained in studies of the response of hot water to rapid depressurization (28)(29). Furthermore, Weisman et al. found that at low decompression rates the superheats required to initiate boiling showed no effects due to the pressure history, and instead approached steady-state values. These superheats, in the 3 - 4°C range, were substantially below those predicted for the pressure-time histories considered. The authors reasoned that small bubbles of noncondensible gas could remain at a cavity base after application of an overpressure. As pressure is reduced, vapor diffuses into the bubble, which then fills the cavity. Thus, an active cavity is present with a radius larger than the maximum unflooded radius predicted, and boiling is possible at a superheat below that predicted using the maximum unflooded radius. The authors speculated that the finite time to fill such a cavity could be the reason for the delay. Heated ribbons were used to verify that the first boiling in the system occurred on the ribbon. The authors noted that the superheats were higher than for the tests without heating, but they did not comment on how these superheats compared to predicted values.

Sakurai, et al. (5), examined transient boiling of a test heater caused by depressurization with near-exponential reduction periods ranging from 3 to 60 ms. The platinum wire test heater was initially in a nonboiling state in a pool of water, and the heat generation rate at

the heater was held constant throughout the experimental run. They used initial pressures of 0.59, 1.08, and 1.9 MPa with water temperatures of 353 and 373 K. Rapid decompression was achieved using a rupture disc device to vent the test section to atmosphere. The authors found that the heater surface temperature and true heat flux remained constant until boiling initiated. The incipient boiling point was assumed to have been reached at the time the heater temperature began to decrease. They argued that this gave the criterion for boiling initiation even if it may not have been the true incipient boiling point. They found that the pressure p_b, and the instantaneous surface superheat, ΔT_b, at the incipient boiling point depended upon the heat flux, even if the initial overpressure and the reduction period were the same. They noted that ΔT_b increased with decreasing p_b and was little dependent on the pressure reduction period, consistent with the incipient boiling model of Sakurai and Shiotsu [Eq. (2.11)].

2.3 Nucleate Boiling

A well-known correlation for fully-developed subcooled and saturated nucleate pool boiling is that of Rohsenow (30), which may be expressed in the form

$$q = C_1(T_w - T_s)^3. \tag{2.24}$$

The factor C_1 is a function of pressure (fluid properties evaluated under saturation conditions) and fluid-surface combination, namely

$$C_1 = [(\rho_f \rho_v) g/\sigma]^{\frac{1}{2}} \mu\lambda Pr^{-3n} (c/\lambda C_2)^3, \tag{2.25}$$

where g is the acceleration of gravity, μ is the viscosity of the fluid, and c is the heat capacity of the fluid. The constant n and the value

of C_2 depend on the fluid-surface combination (18), and take the values 1.0 and 0.013 respectively for a platinum surface in water. Unless otherwise indicated, properties are those of the liquid phase. For example, for platinum-water at atmospheric pressure, $C_1 = 140\ Wm^{-2}K^{-3}$.

Stephan and Abdelsalam (31) carried out an exhaustive investigation of experimental data on pool boiling in various fluids and recommended the following correlation as being applicable to water

$$q = C_3(T_w - T_s)^{3.06} \tag{2.26}$$

in which C_3 is a function of saturation temperature. Based on data in the paper, C_3 may be expressed empirically, in S.I. units, as

$$C_3 = 229\ p^{0.649} \tag{2.27}$$

where p is in units of MPa for the range 0.1 to 20. As an example, for boiling at atmospheric pressure, $C_3 = 52\ Wm^{-2}K^{-3.06}$. Thus, for a given surface superheat, this correlation predicts a much lower heat flux than that predicted by the Rohsenow correlation.

3. THEORY

3.1 Determination of Largest Potentially Active Cavity

In the absence of free gas bubbles, nucleation sites for boiling initiation will be located at surface cavities which have vapor trapped in them. The rate of boiling heat transfer is governed by the spatial distribution and the size spectrum of nucleation sites. Heat flux and superheat required to initiate boiling generally depend on the size of the largest site. The largest potential nucleation site, i.e., a cavity, idealized by a conical shape, containing vapor, can be determined by considering the pressure-temperature history of the surface along with the fluid-surface wetting characteristics.

Consider an arbitrary surface cavity, idealized by a conical shape, containing vapor with a fluid of infinite extent covering the surface (Fig. 3.1). Assume a well degassed fluid so that the partial pressure of noncondensible gas is negligible compared to vapor pressure and fluid pressure. The system is initially at pressure p_{f1} and at temperature T_1 at which the vapor pressure is p_{v1} less than p_{f1} and the surface tension is σ_1.

When a pressure $p_{f2} >> p_{v1}$ is applied, the fluid will enter the mouth of the cavity. Mechanical equilibrium across the meniscus requires

$$p_{f2} - p_{v1} = \frac{2\sigma_1}{R_M} , \tag{3.1}$$

where R_M is the radius of curvature of the meniscus (see Fig. 3.1). From a geometric consideration, the cavity radius r at the meniscus line of contact is given by

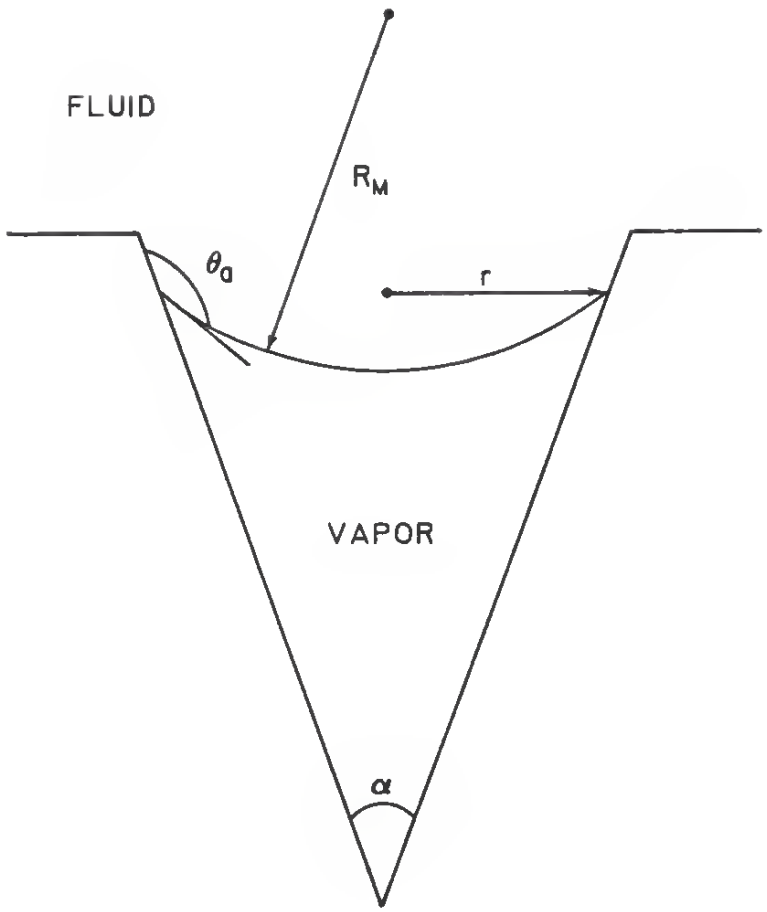

FIG. 3.1. Illustration of vapor entrapment at a potential nucleation site.

$$r = R_M \cos(\pi - \theta_a + \frac{\alpha}{2}),$$

or

$$r = \frac{2\sigma_l}{p_{f2} - p_{vl}} \cos(\pi - \theta_a + \frac{\alpha}{2}) \qquad (3.2)$$

where θ_a is the advancing contact angle between the fluid and the cavity wall, and α is the included angle of the cavity apex. The minimum pressure necessary for the meniscus to enter a cavity with mouth radius r_c can also be obtained from Eq. (3.2). If this requirement is not met, then the contact angle is less than θ_a and the meniscus is at the mouth or the cavity is flooded.

The argument of the cosine must fall between 0 and $\frac{1}{2}\pi$ since r must exist for vapor to be trapped in the cavity. This provides a maximum value for the apex angle of the cavity,

$$\alpha_{max} < 2\theta_a - \pi. \qquad (3.3)$$

If α is greater than this value, the cavity will flood with fluid and become deactivated. It is also apparent from Eq. (3.3) that θ_a must be greater than $\frac{1}{2}\pi$ for vapor to be trapped in the cavity.

Equations (3.1), (3.2), and (3.3) describe the potential nucleation sites available for the pressure-temperature history of the system when p_{f2} equals $p_{f,max}$. Cavities with mouth radii greater than or equal to the critical radius $r = r_c$ when $p_{f2} = p_{max}$ and apex angles less than α_{max} will have the meniscus located at the position inside the cavity where the local cavity radius is equal to r_c. Cavities with apex angles greater than α_{max} will be flooded, while cavities with mouth radii less than r_c will not be affected.

The description of the meniscus behavior as conditions leading to nucleation are imposed depends on the manner in which these conditions arise. Boiling can be initiated by decreasing the fluid pressure, increasing the vapor pressure by heating, or a combination of these two actions.

3.2 Activation of a Nucleation Site

3.2.1 Decrease in Fluid Pressure

If the fluid pressure is released to a value p_f such that $p_{v1} \leq p_f \leq p_{f2}$, the radius of the meniscus will change to a new value given by

$$R_M = \frac{2\sigma_l}{p_f - p_{v1}} . \tag{3.4}$$

The radius of the meniscus line of contact remains constant at the value given by Eq. (3.2), and the contact angle θ must satisfy

$$r = \frac{2\sigma_l}{p_f - p_{v1}} \cos(\pi - \theta + \frac{\alpha}{2}) = r_c . \tag{3.5}$$

As p_f approaches p_{v1}, the contact angle θ must decrease so that r remains constant. However, as long as p_f is greater than p_{v1}, the meniscus will be concave on the fluid side.

When p_f becomes less than p_{v1}, the meniscus radius becomes negative by Eq. (3.4), i.e., the meniscus flips from concave to convex on the fluid side. From the force balance,

$$R_M = - \frac{2\sigma_l}{p_f - p_{v1}} . \tag{3.6}$$

With no boiling, r remains constant at the value determined by Eq. (3.2). However, r can also be defined by

$$r = R_M \cos(\theta - \frac{\alpha}{2})$$

$$= - \frac{2\sigma_1}{p_f - p_{v1}} \cos(\theta - \frac{\alpha}{2}) \qquad (3.7)$$

Equation (3.7) shows that r will remain constant as θ decreases to the value of the receding contact angle θ_r. When θ equals θ_r the fluid will begin to recede over the previously wetted cavity wall and the meniscus line of contact will move towards the cavity mouth. This will occur when

$$p_{v1} - p_f' = \frac{2\sigma_1}{r_c} \cos(\theta_r - \frac{\alpha}{2}). \qquad (3.8)$$

When the meniscus is at the cavity mouth, boiling inception will take place when the meniscus radius of curvature is at a minimum, i.e., at the cavity mouth radius, $\hat{r}_c$. This will occur at a pressure p_f'' such that

$$p_{v1} - p_f'' = \frac{2\sigma_1}{\hat{r}_c} \qquad (3.9)$$

The application of these equations to a range of cavity sizes will be discussed later. However, it is apparent that $p_f'' < p_f'$ when $r_c = \hat{r}_c$.

3.2.2 Increase in Vapor Pressure

If a temperature $T_2 > T_1$ is applied at pressure p_f, where $p_{v1} \leq p_f \leq p_{f2}$, the surface tension and the vapor pressure will assume new values σ_2 and p_{v2}, respectively. If T_2 is less than the saturation

temperature at p_f the meniscus radius of curvature will change, but the line of contact will not, and the radius r at the line of contact will remain constant at the value given by Eq. (3.2). Here,

$$R_M = \frac{2\sigma_2}{p_f - p_{v2}}, \tag{3.10}$$

and

$$r = R_M \cos(\pi - \theta + \tfrac{\alpha}{2})$$

$$= \frac{2\sigma_2}{p_f - p_{v2}} \cos(\pi - \theta + \tfrac{\alpha}{2}) = r_c. \tag{3.11}$$

Again, the interface is stable with the meniscus concave on the fluid side for $(p_f - p_{v2}) > 0$.

When the applied temperature T_2 becomes greater than the saturation temperature at p_f, the meniscus radius of curvature becomes negative by Eq. (3.10) and the meniscus flips from concave to convex on the fluid side. The force balance in this case requires

$$R_M = -\frac{2\sigma_2}{p_f - p_{v2}}. \tag{3.12}$$

The radius of the meniscus line of contact is given by

$$r = R_M \cos(\theta - \tfrac{\alpha}{2})$$

$$= -\frac{2\sigma_2}{p_f - p_{v2}} \cos(\theta - \tfrac{\alpha}{2}) = r_c. \tag{3.13}$$

The meniscus radius of contact remains constant as θ decreases to the value of the receding contact angle θ_r. Movement of the meniscus line of contact towards the cavity mouth will commence when

$$p'_{v2} - p_f = \frac{2\sigma'_2}{r_c} \cos(\theta_r - \frac{\alpha}{2}) \ , \tag{3.14}$$

corresponding to a temperature T'_2. Again, boiling will initiate when the meniscus radius of curvature reaches a minimum equal to the cavity mouth radius $\hat{r}_c$. This will occur at a temperature T''_2 such that

$$p''_{v2} - p_f = \frac{2\sigma''_2}{\hat{r}_c} \ . \tag{3.15}$$

Although σ decreases with increasing temperature, under usual conditions $p''_{v2} > p'_{v2}$ or $T''_2 > T'_2$ when $r_c = \hat{r}_c$.

3.3 Cavity Geometry

Consider now a broad size range of active cavities present on the surface. The system has experienced conditions such that the meniscus radius of curvature is convex on the fluid side. If the meniscus line of contact is below the cavity mouth, an increase in $p_v - p_f$ can not be balanced in Eq. (3.8) or (3.14), and the line of contact will move towards the cavity mouth. First boiling will then occur from a cavity with mouth radius $\tilde{r}_c$ such that

$$\tilde{r}_c = \hat{r}_c \sec(\theta_r - \frac{\alpha}{2}) \ , \tag{3.16}$$

since the threshold conditions for meniscus motion will also satisfy the requirement for nucleation from a cavity with mouth radius $\tilde{r}_c$.

The effect of the cavity apex angle in determining potential nucleation sites is revealed by Eq. (3.2), which shows that vapor can be trapped at lower liquid temperatures as α decreases. In other words, given two cavities with the same mouth radius, the cavity with the

smaller apex angle will boil first. Therefore, a cylindrical cavity ($\alpha = 0$) will be the largest potentially active nucleation site available, and the superheat required to achieve the receding contact angle θ_r will be less than for a conical cavity. The meniscus will rush out of the cylindrical cavity for an increase in $p_v - p_f$, and the relation of Eq. (3.9) or (3.15) must be satisfied to initiate boiling if the entrance angle to the cavity mouth is 90°. The superheat in this case may be higher than that required for a conical cavity with mouth radius $\tilde{r}_c$ if α is sufficiently small. However, Fabic (1) argued that the cavity mouth would be rounded, and appropriate rounding at the entrance would allow boiling to initiate after the meniscus flip with no additional superheat. This special rounding would also apply to conical cavities, but the only effect would be to allow the superheat necessary for boiling inception in a cavity with mouth radius $\hat{r}_c$ to approach the value for $\tilde{r}_c$. Since Fabic's argument provides the lower limit for boiling initiation, further discussion will consider cylindrical cavities where $r = r_c$ is the radius of the largest active cylindrical cavity according to Eq. (3.2).

3.4 Effect of Contact Angles

The contact angles used in this work are the same as those adopted by Fabic. He selected an advancing contact angle $\theta_r = 108°$ for water on metal for all values of system pressures and temperatures. This value is based on reported findings that the largest contact angle water can make with a solid surface is $\theta_a = 105°$ to 110°. His selection of the receding contact angle $\theta_r = 66°$ was more arbitrary since it was a best fit value for his work. However, it also agreed with the observance of a 40° maximum difference between θ_a and θ_r.

Consider a horizontal surface immersed in well degassed water of infinite extent. The surface and the fluid are initially at uniform temperature T_1 when an initial pressure p_{f2} is applied. The surface is then heated to temperature $T_w = T_2$ such that no boiling occurs. Beginning at time $t = 0$, the system is subjected to a time-dependent decrease in the fluid pressure $p_f(t)$. No boiling will occur until p_f reaches the value necessary for boiling initiation.

The radius of the largest active cylindrical cavity is obtained from Eq. (3.2) for the conditions T_1 and p_{f2},

$$r_c = \frac{2\sigma_1}{p_{f2} - p_{v1}} \cos(\pi - \theta_a). \tag{3.17}$$

Since r_c remains constant until boiling is initiated, Eq. (3.13) also applies,

$$r_c = -\frac{2\sigma_2}{p_f - p_{v2}} \cos(\theta_r). \tag{3.18}$$

The fluid pressure necessary for boiling initiation, p_b, can be obtained by combining Eqs. (3.14) and (3.15),

$$p_b = p_{v2} - \frac{\sigma_2}{\sigma_1} \frac{\cos(\theta_r)}{\cos(\pi - \theta_a)} (p_{f2} - p_{v1}). \tag{3.19}$$

Figure 3.2 shows the effect of surface temperature on the incipient boiling pressure, where it is observed that increasing T_w causes p_b to increase. The figure also shows that for appropriate extreme conditions of initial pressure, no boiling is predicted.

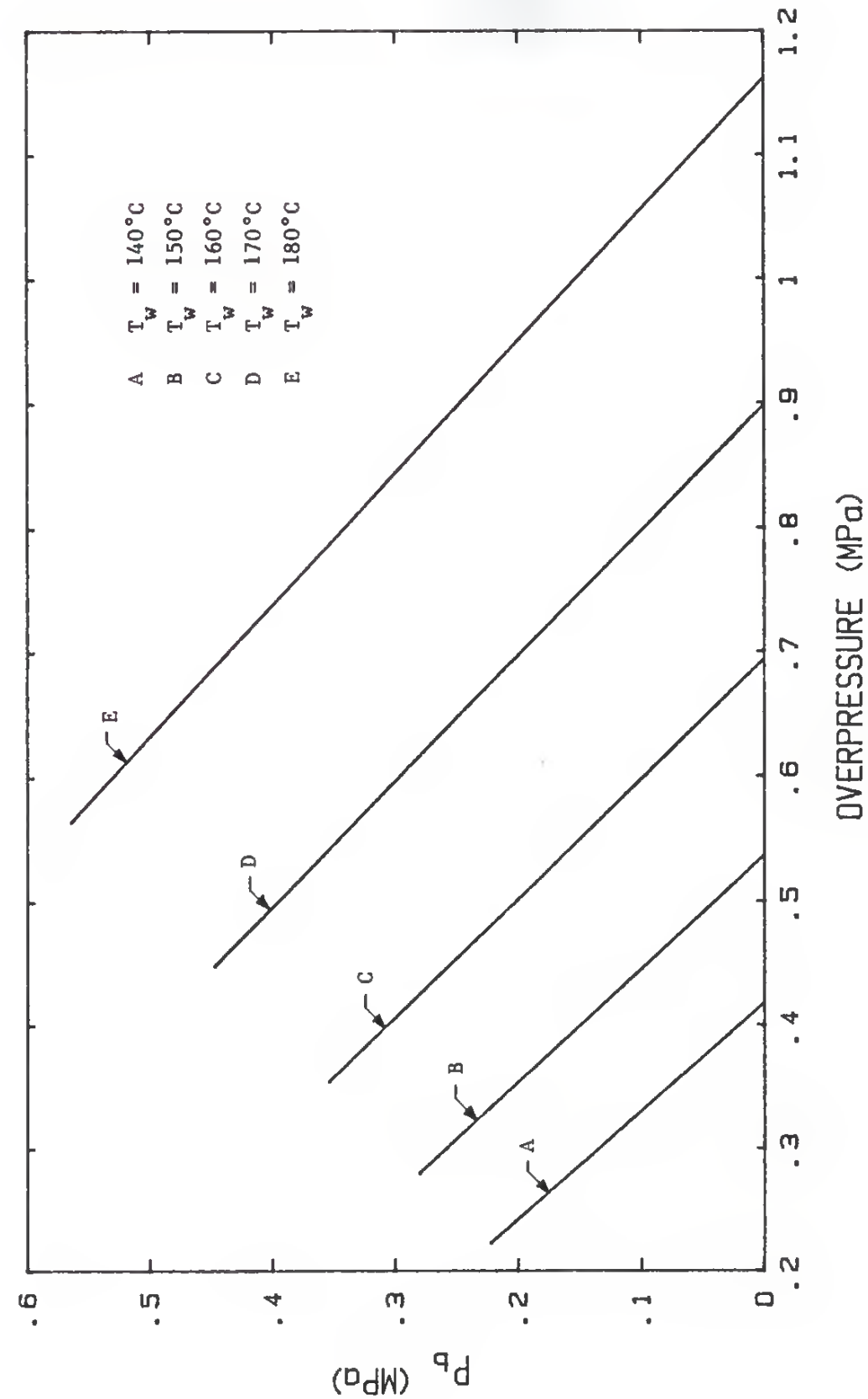

FIG. 3.2. Effect of surface temperature on incipient boiling pressure with θ_a = 108° and θ_r = 66°. Overpressure is applied at ambient temperature T_a = 100°C.

The influence of the advancing and receding contact angles on the boiling initiation pressure can be examined using Eq. (3.19). Increasing the ratio of the cosine terms, by decreasing θ_r or increasing θ_a, requires a lower value of p_b (and hence a higher superheat) to satisfy the condition for nucleation. Decreasing the ratio of the cosine terms has the opposite effect. The effect of selected changes in contact angles on the ratio of the cosine terms is shown in the following table, and the effect on p_b for a representative case is shown in Fig. 3.3. It is apparent that the value of p_b is very sensitive to small changes in the value of either contact angle.

θ_a	θ_r	$\frac{\cos(\theta_r)}{\cos(\pi - \theta_a)}$
108°	66°	1.316
110°	63.25°	1.316
106°	68.73°	1.316
106°	66°	1.476
108°	62.86°	1.476
108°	68.45°	1.189
110°	66°	1.189

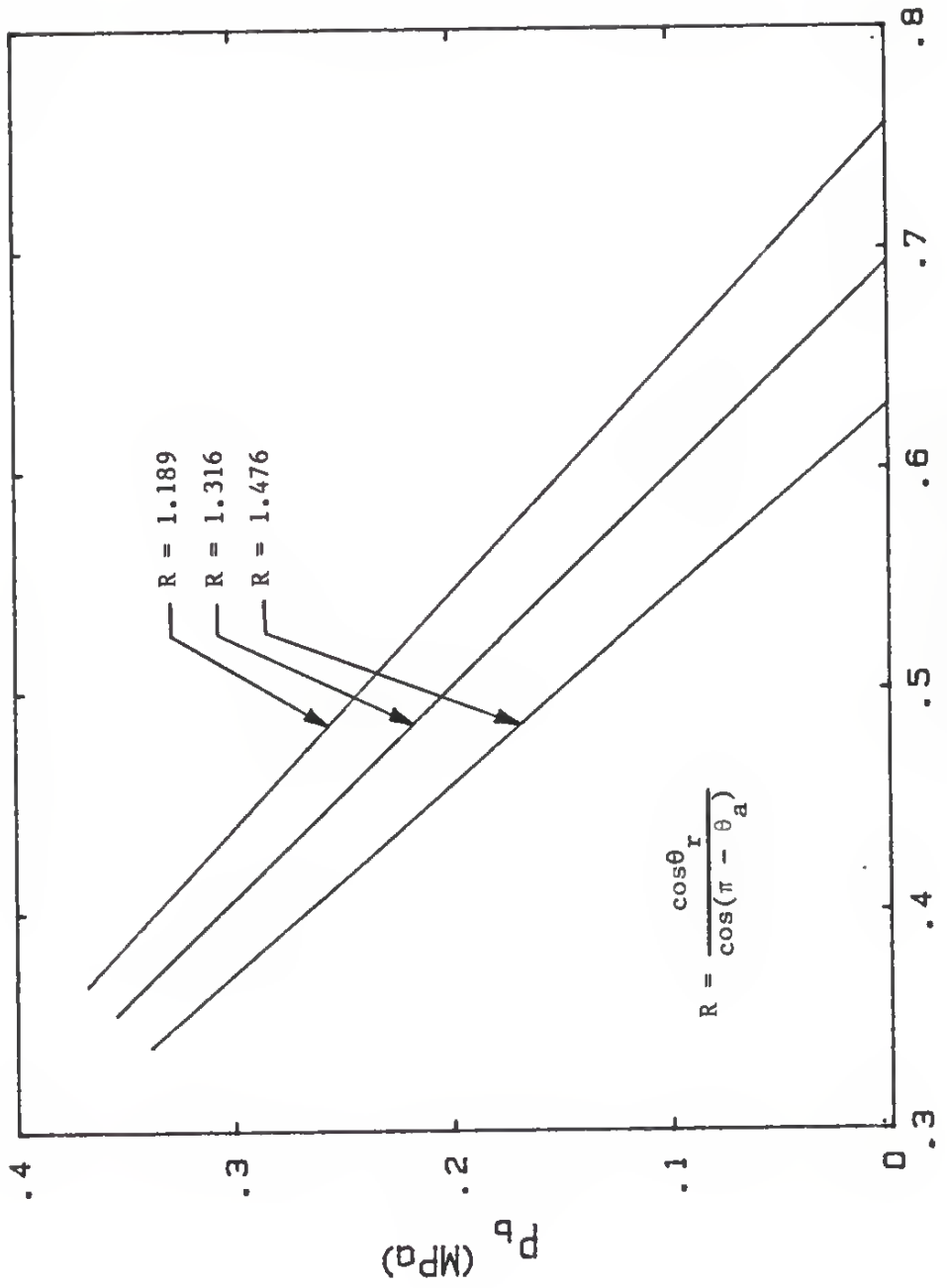

FIG. 3.3. Effect of selected changes in contact angle on incipient boiling pressure. Overpressure is applied at T_a = 100°C before the surface temperature is raised to T_w = 160°C.

4. APPARATUS AND EXPERIMENTAL PROCEDURE

4.1 Pressure System

4.1.1 Pressure Vessel

The test vessel, shown in Fig. 4.1, is made of type 316 stainless steel. The vessel is 40.64 cm in length with an outer diameter of 12.065 cm and an inner diameter of 9.8425 cm. The end flanges are sealed with Ultek oxygen free hardened copper O-rings Model 2 68-4000, from Perkin-Elmer Corp. One end flange is penetrated by a 2 kW Firerod electrical heater, Model N6A22, from Watlow, Inc. This heater is used to maintain the ambient temperature of the test fluid. The other end flange is penetrated by the electrode assembly. A stainless steel-sheathed copper-constantan thermocouple from Watlow, Inc. penetrates the cylinder wall to provide constant monitoring of the bulk fluid temperature.

The two optical ports are essential to the observation of bubble growth behavior on the electrically heated test element. The design of the window housing is shown in Fig. 4.2. The windows are of T08 commercial grade clear fused quartz obtained from Amersil, Inc. The discs are 4.445 cm in diameter and 1.5 cm thick and, as estimated by Amersil, a pressure of 13.6 MPa may be used with an approximate safety factor of 3.5. The cushions and seals for the windows are fabricated of teflon.

4.1.2 Pressure Measurement System

A Kistler Quartz Miniature Pressure Transducer Model 603A penetrates the cylinder wall to provide the means to measure the pressure history during a transient. The point of penetration is between one of the optical ports and the end flange containing the electrode assembly, and

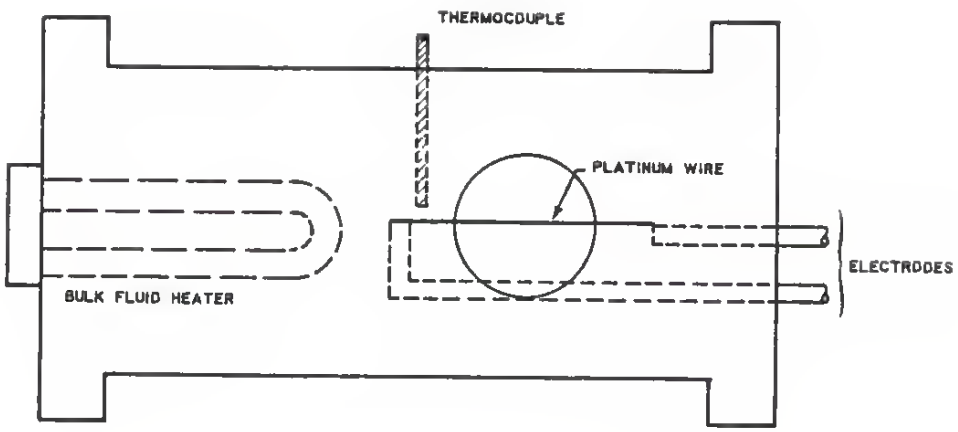

FIG. 4.1. Schematic diagram of the pressure vessel.

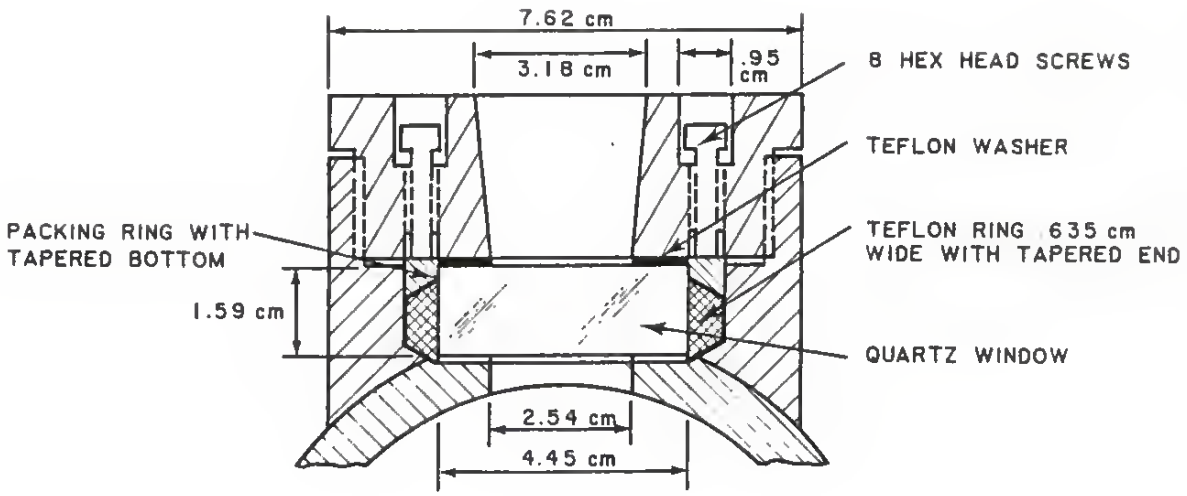

FIG. 4.2. Pressure vessel window housing.

on the horizontal plane through the test element. This location places the pressure transducer in closest proximity to the test element so that recorded information represents the actual pressure history of the test element during the experiment. Although the transducer will withstand sustained temperatures of up to 260°C without damage, its temperature must be limited to about 120°C to minimize drift and ensure good low frequency response. A water cooling adapter designed by Kistler provides this cooling capability, as well as being a most convenient means of attachment to the pressure vessel. Figure 4.3 shows details of the cylinder wall where the adaptor is mounted, and Fig. 4.4 shows the cooling adaptor design from Kistler. Since this design is for a physically larger transducer, an adaptor was designed to mount the Model 603A pressure transducer in the cooling jacket. The design of the second adaptor is shown in Fig. 4.5. Both adaptors were fabricated by machine shop personnel in the Department of Physics.

The quartz sensing element in the pressure transducer is oriented such that increasing applied pressure results in a negative-going charge signal that is inverted to a positive-going voltage signal by Kistler charge amplifiers. The Kistler Model 504E Dual Mode Amplifier is designed to develop the full capabilities of the quartz transducer while eliminating the attenuating effects of the cable and transducer capacitance.

Three factors must be considered when setting up the pressure measurement system for optimum performance: the system transfer function (i.e., volts output per measurand unit input), the correct time constant for the event, and the amplifier drift. All are directly affected by the settings on the dual mode amplifier.

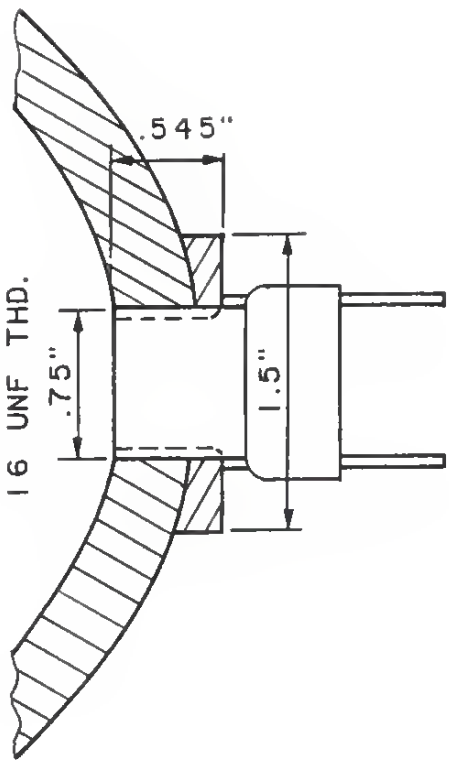

FIG. 4.3. Pressure transducer cooling adaptor mounting to the pressure vessel.

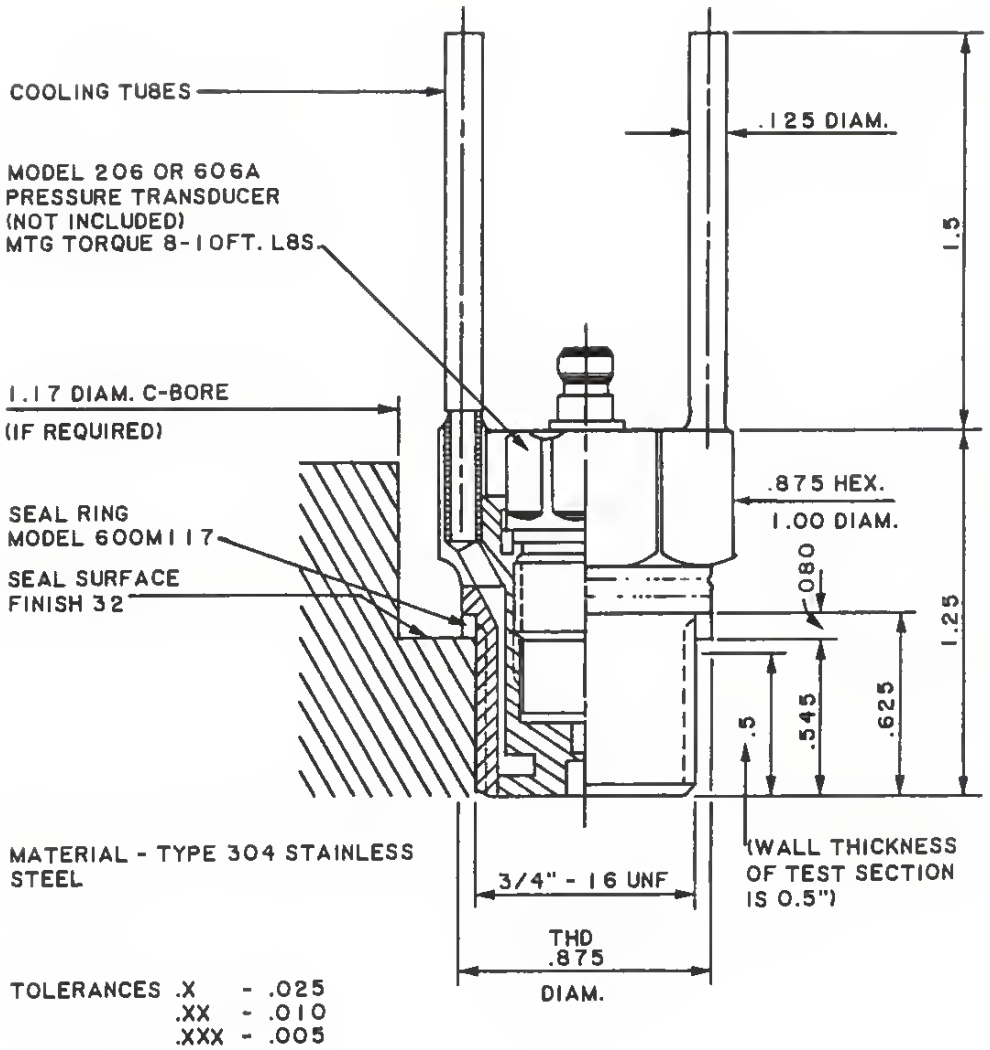

FIG. 4.4. Pressure transducer cooling adaptor, designed by Kistler.

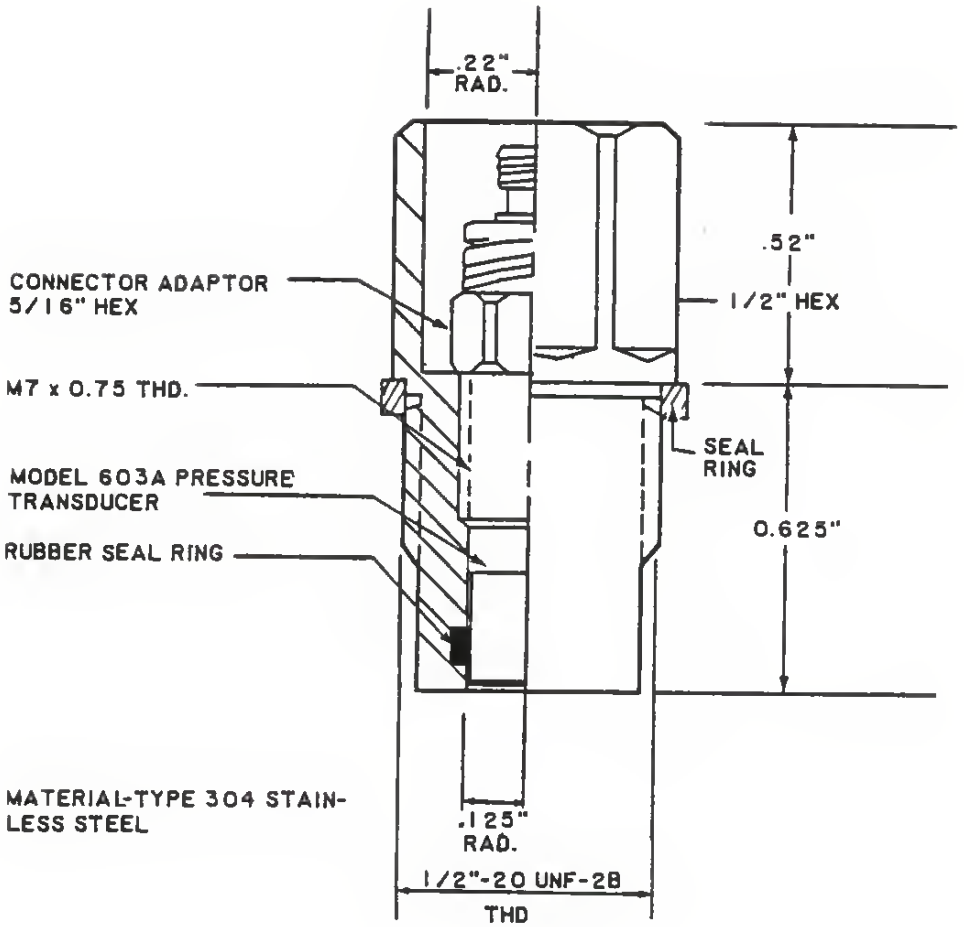

FIG. 4.5. Pressure transducer adaptor for mounting the Model 603A to the cooling adaptor.

The system transfer function is inversely proportional to the transducer sensitivity, which is set on the dual mode amplifier as a value between 1.00 and 11.00. Since the pressure transducer used in this study has a sensitivity less than 1.00 pC/psi, a range multiplier of 10 is automatically required in determining the transfer function. The transfer function is also dependent on the amplifier gain, which varies directly with the range switch position.

The time constant is selected according to the temporal behavior of the input signal. Since the depressurization rates used in this study were small, the long time constant setting was chosen to avoid signal decay before the end of the transient. Unfortunately, the improvement in low frequency response allowed by the long time constant setting is at the expense of amplifer drift as a function of time.

Amplifier drift is inversely proportional to the range setting. For the long time constant the drift is measured in millivolts per second. Thus the need to minimize drift must be balanced against the desire to establish a system transfer function that provides maximum deflection of the output signal for a given pressure change.

4.1.3 Pressurizer

The pressurization system, as shown in Fig. 4.6, consists of a bottle of commercial nitrogen, the pressurizer, Model 30A-10WS, from Greer Hydraulics, Inc. and the pressure vessel. Seamless stainless steel tubing (0.635 cm) with 0.635-cm taper-seal valves from High Pressure Equipment Company is used for gas delivery. The high pressure nitrogen enters one side of the pressurizer and inflates a neoprene rubber bag. This bag presses against the water in the other half of the pressurizer. Thus, pressure can be applied to the test fluid without having the

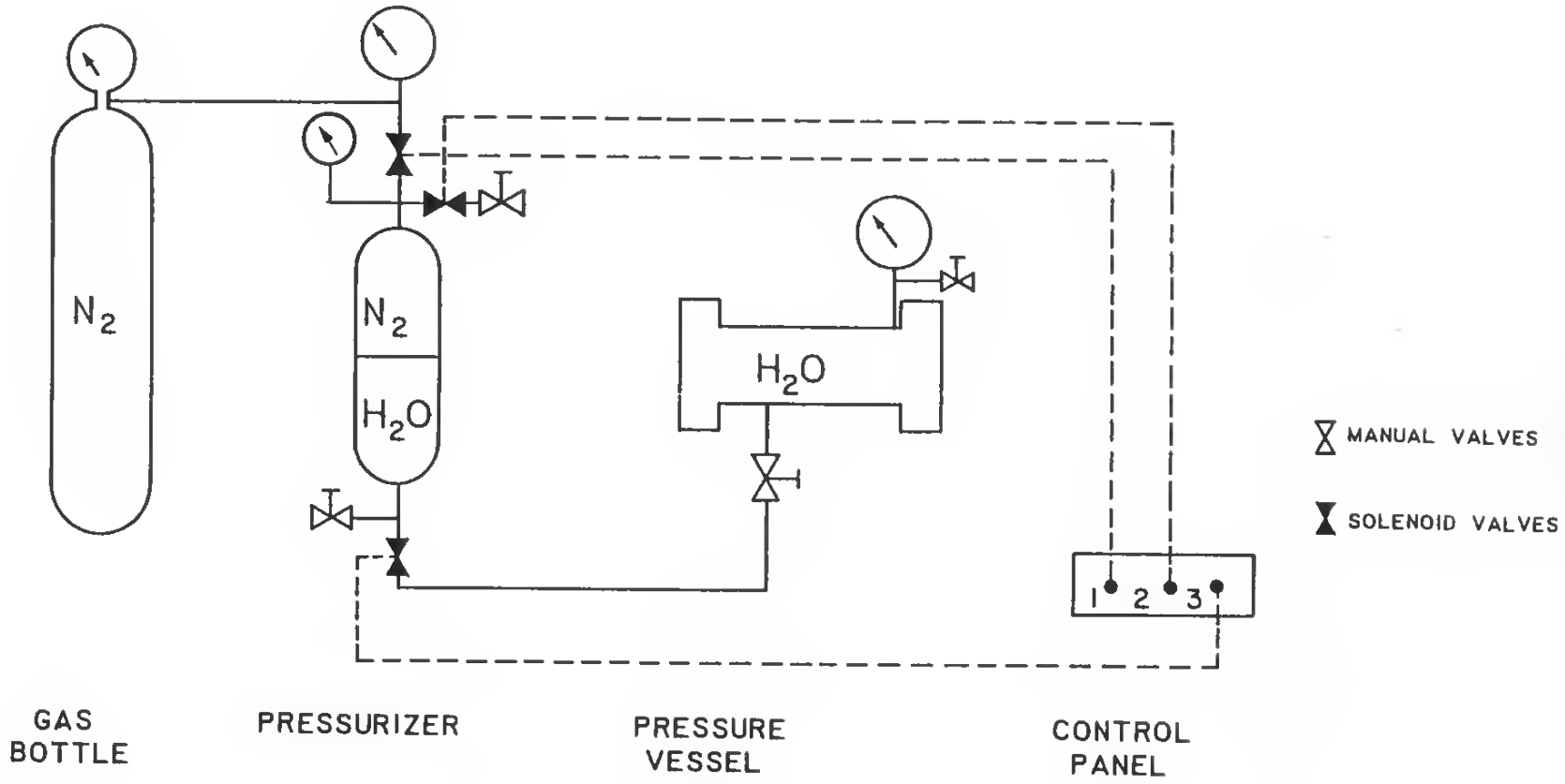

FIG. 4.6. Pressurization system.

pressurizing gas dissolve in the test fluid. The pressure vessel is also connected to the water side of the pressurizer using seamless stainless steel tubing. On the gas side, there are two Asco Red Hat solenoid valves, Model 8262A214 from Automatic Switch Co., one to control inflow of gas and another solenoid valve to control the flow of gas to the atmosphere. On the fluid side of the system, there is another solenoid valve. Once the system is pressurized, this valve can be closed so that the pressure in the pressure vessel remains constant while the pressure on the gas side of the bladder is raised or lowered. Then the valve can be opened causing an instantaneous compression or decompression. There are also two Model 63-5622 pressure gauges from Matheson Corp. and one Model 7108P-200 pressure gauge from Transcat associated with the system. One Matheson gauge is on the pressure vessel itself and the other is on the supply line of the nitrogen gas, while the Transcat gauge is on the gas side of the pressurizer.

4.2 Heating Element

The test element, shown in Fig. 4.7, consists of two brass rods each 0.6350 cm in diameter and a teflon block. The teflon block is used to prevent the rods from sagging. The vertical support assembly can be adjusted to provide for different lengths of platinum wire. The teflon seals at the penetration points of the electrodes served a double purpose of providing a water tight seal and also providing insulation between the electrodes and the pressure vessel.

The heating element is of pure platinum wire (SPPL-010 from Omega Engineering, Inc.) of diameter 2.50×10^{-4} m and is mounted horizontally. The maximum length of the heating element is 9.6 cm. The spring attachment provides tension across the wire. The platinum wire not only

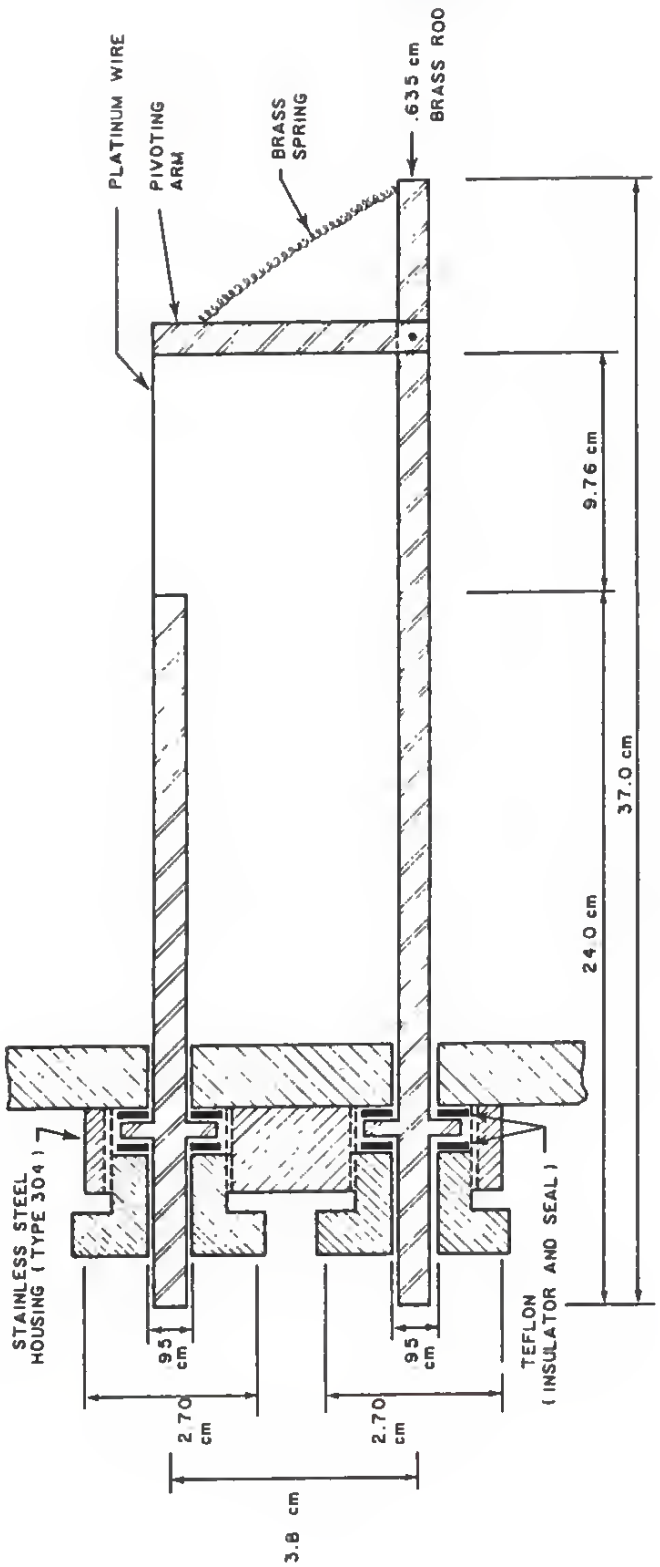

FIG. 4.7. Heating element construction.

acts as the test element but also as a temperature sensor. The resistance, $R(\theta)$, of pure platinum has a well characterized temperature dependence, (32)

$$R(\theta) = R_0 (1 + \alpha\theta + \beta\theta^2),$$

where

$\alpha = 3.92 \times 10^{-3}$

$\beta = -5.5 \times 10^{-7}$

θ = the temperature of the platinum wire in°C,

$R(\theta)$ = the resistance of the wire at temperature θ in ohms,

R_0 = the resistance of the platinum wire at 0°C.

Once the resistance is measured, the average temperature of the platinum wire can be calculated.

4.3 Electrical System

The electrical system consists of two twelve volt storage batteries, a control system, and a voltage bias system. The two storage batteries are wired in parallel and provide the dc current to the test element. The control system regulates current to the test element such that the power delivered remains constant with time. Figure 4.8 is a schematic diagram of the control system circuit. The voltage bias system is an EAI Analog Computer, Model TR-10. Simple linear summing circuits apply bucking voltages to the test voltages across the standard resistor and the test element so that only the variations in these voltages are recorded by the oscilloscope.

4.4 Data Measurement System

Data for the experimental runs are taken on a Nicolet Explorer III Digital Oscilloscope equipped with a floppy disc storage system and a

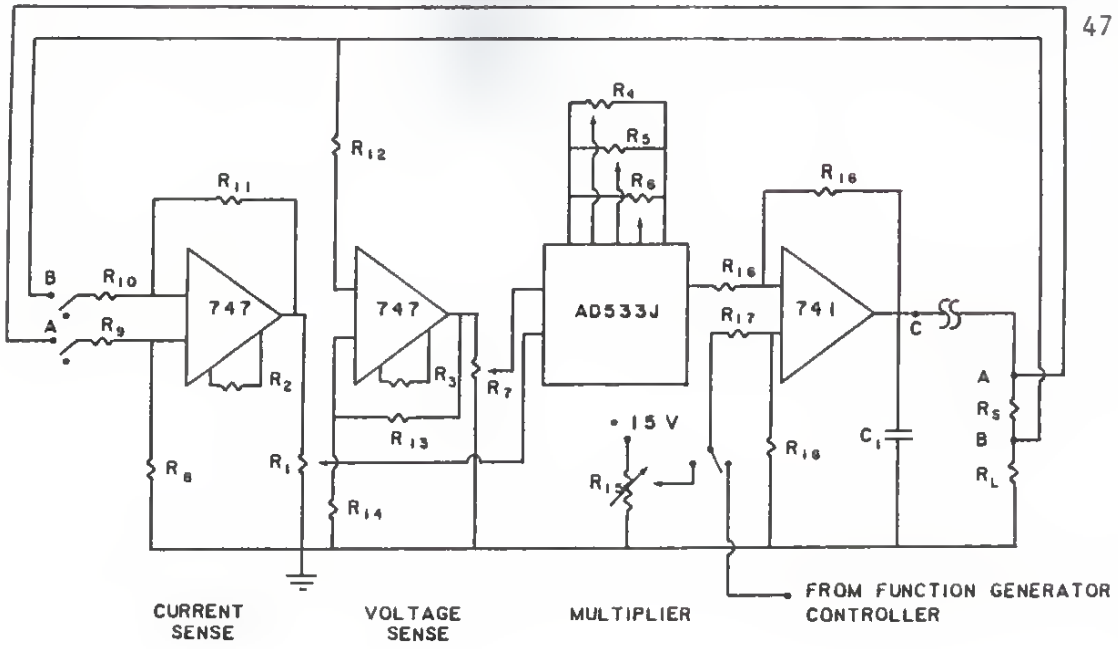

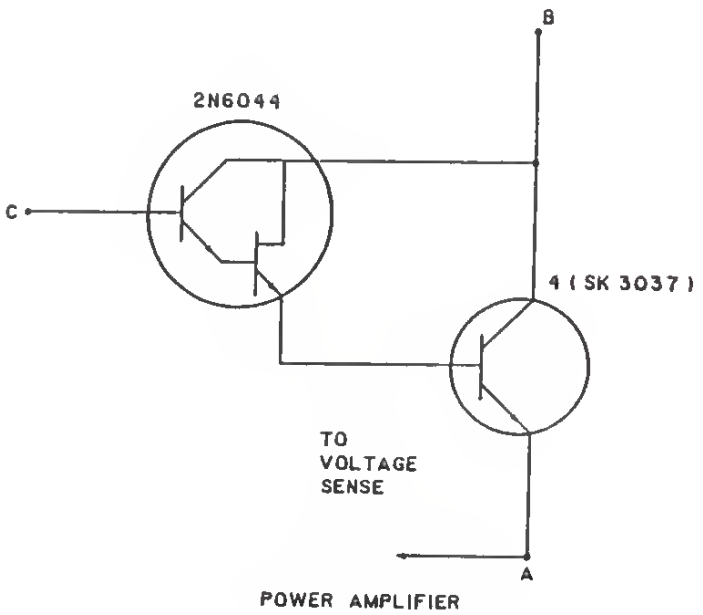

FIG. 4.8. Control system and power amplifier schematic diagrams.

RS-232C serial interface port for transmission of the stored data to other devices. The oscilloscope has two inputs, each with separate smplifying circuits. The oscilloscope is set in Cursor mode for triggering. In this mode the trigger source signal is continuously monitored until the triggering conditions are met or exceeded. At this instant the designated storage channel is assigned trigger time zero, and input signal regions both preceding and following the trigger time are stored for observstion. Thus, although the event time zero may not correspond to the trigger time zero, the entire transient can be captured by judicious choice of the storage channel for trigger time zero. Any difference between trigger and event time zero can be accounted for in analysis.

Three voltage signals are available during a transient: one relating to pressure vessel pressure, and two relating to test element temperature. Experimental runs to determine the pressure history during decompression are performed by recording the voltage signal from the pressure transducer amplifier, with the oscilloscope triggered by this signal. The unused input channel is turned off so that the total recording capacity of the oscilloscope is utilized for recording the single input voltage. This signal provides the information necessary for determining the pressure history of the test element during the transient. Experimental runs to determine the test element temperature history during decompression are performed by recording the variations in both the voltage across the test element and the voltage across a stsndard resistor, Model 79 21 from Ohmite, with the oscilloscope triggered by the latter signal. The two source signals sre fed to the voltage bias system, where the voltages induced by the application of

power at initial conditions are cancelled by applying bucking voltages. The two recorded signals, together with their respective bucking voltages, provide the information necessary for determining the resistance of the test element and thus its temperature, as well as the power delivered to the test element. The computer code used in the analysis of temperature data is provided in Appendix A, and the computer code used in the analysis of pressure data is provided in Appendix B.

4.5 Test Element Installation

The test vessel is cleaned using acetone and then rinsed with the test fluid. The optical ports require special attention during cleaning to keep the windows clear of spots and also free from scratches.

The test element is soldered to the brass electrodes of the test section. The entire test section is then cleaned with acetone to remove excess flux or other contamination arising from the soldering process. The test section is then installed in the pressure vessel and the mounting bolts torqued to 80 to 110 Nm. A small voltage is applied across the test element in such a way that the wire glows cherry red. The air heating is done for approximately ten minutes. The heating of the wire tends to anneal the surface of the wire thus leading to consistent surface properties.

After the initial preparation of the test element, the test fluid is poured into the pressure vessel. The wire is then conditioned by applying a small voltage across it until boiling initiated. The wire is operated at this voltage for approximately ten minutes, then the voltage is increased slightly. This is repeated until the voltage across the wire reaches a maximum of 10 V. The purpose of this conditioning is to activate the cavities on the wire by driving out any trapped gas.

Each time a new test element is installed, the power supply must be calibrated. The following steps are used:

1. Set V_a and V_b equal to zero by grounding.
2. Adjust R_2 until the output of V_x is equal to zero.
3. Adjust R_3 until the output of V_y is equal to zero.
4. Adjust R_6 until the output of V_o is equal to zero.
5. Set V_a and V_b equal to each other and adjust R_4 so that the output of V_o is equal to zero.
6. Set V_b to zero (leaving V_a alone), then adjust R_5 so that the output of V_o is equal to zero.
7. Set V_a equal to zero and re-adjust R_6 so that the output of V_o is again equal to zero.
8. Set V_a equal to 8.245 V and V_b equal to 4.588 V.
9. Adjust R_1 until V_x is equal to 10.00 V.
10. Adjust R_7 until V_y is equal to 10.00 V.

4.6 Procedures

4.6.1 Preliminary Procedures

These steps are followed before each experimental session:

1. The test fluid is heated to boiling and boiled for one hour to remove dissolved gases.
2. A voltage is applied to the test element until vigorous boiling has commenced. The boiling from the element is continued for ten minutes.
3. The pressure vessel is refilled with de-gassed, near-boiling test fluid, and all valves to atmosphere are closed.
4. All associated electronic equipment is allowed to warm up for the hour required for de-gassing.

5. The oscilloscope Channel B trigger level is adjusted using a Wavetek Digital VCG Model 113.

4.6.2 Experimental Procedures

Since the oscilloscope has only two input channels for recording data, pressure data and temperature data must be recorded in separate experimental runs. However, most procedural steps are the same.

These steps are followed to set up each experimental run:

1. Vigorous boiling from the test element is achieved and continued for ten minutes at atmospheric pressure and the desired bulk fluid subcooling. This allows activation of the full size range of bubble nucleation sites.
2. The test element is allowed to cool to test fluid bulk temperature.
3. The system is slowly pressurized to the desired pressure while holding the bulk temperature constant. The system is maintained at this condition for ten minutes to allow it to stabilize.
4. Power is applied to the test element until the desired test element temperature is achieved.
5. The zero settings on the active input amplifiers of the oscilloscope are adjusted and the trigger time zero is checked. These settings are important for proper triggering of the oscilloscope and for use in the computer analysis of the run.
6. Voltage signals from the standard resistor and the test element are fed to the voltage bias system. Bucking voltages are applied such that the signals from the voltage bias system to

the oscilloscope are nominally zero. (This step is performed only if recording temperature data.)

If the boiling initiation time is not desired when performing a run to record pressure data, steps 1, 2, and 4 may be disregarded.

After the run has been set up, these steps are followed to continue the experiment:

7. Equipment settings are checked and recorded as necessary, and test fluid pressure and temperature are recorded. The gas supply solenoid valve is then closed.
8. The decompression is initiated and the oscilloscope is triggered by the appropriate input signal.
9. The recorded data are stored on floppy disc for later transmission to the computer.
10. Manually observed boiling initiation time is recorded (if measured).
11. Steps 1 through 10 are repeated until all data for this combination of test parameters are acquired.

The above steps are repeated for other test parameter combinations of interest.

5. RESULTS

5.1 Boiling Initiation

The initiation of boiling at a surface is governed by the size distribution of potential nucleation sites and the fluid temperature profile adjacent to the surface. The largest site will be the first to become active since it requires the least superheat for boiling. The mouth diameter of the largest potentially active site is estimated to be 0.35 μm. This value was obtained from photo-micrographs of the surfaces of similar heating elements used in the concurrent study of pressure effects on boiling initiation during transient heating (22). As discussed in Chapter 3, the activation of a cavity occurs when the superheat has reached a prescribed magnitude at a distance from the surface comparable to the radius of the cavity mouth.

Natural convection determines the temperature gradient in the fluid adjacent to the surface before decompression. After natural convection is fully established, the thermal boundary layer and the temperature profile do not change significantly until the fluid is agitated, either by boiling or by bulk fluid movement. The increase in superheat necessary to initiate boiling arises from the decrease in the bulk fluid saturation temperature associated with the decrease in system pressure.

The temperature of the test element should behave in a simple manner when a constant power is applied and natural convection from the surface to the fluid is fully established. The temperature would be constant before a pressure transient is initiated, and would remain so during the transient until the inception of boiling. At this point the test element temperature would begin to decrease. Thus, finding this

point of time in the temperature history and the pressure at this time from the pressure history of a test would establish the conditions for boiling inception.

In this study of boiling initiation during pressure transients, three voltage signals, one for pressure and two for temperature, were available for each test. However, the digital oscilloscope could only record two of these simultaneously. Since both temperature signals had to be recorded for quantitative results, the nature and reproducibility of the decompression event had to be investigated.

The system was prepared for experimental runs by bulk boiling of the water in the pressure vessel for one hour at atmospheric pressure, after which the fluid lost through evaporation was replaced with degassed water at near-boiling temperature. The pressure vessel vent to the atmosphere was closed after bulk boiling, and subsequent system venting to the atmosphere was accomplished by opening the gas side of the pressurizer to atmospheric pressure. This was followed by vigorous boiling from the platinum test element for ten minutes. Pressure and temperature runs were then conducted to examine the effect of the pressure-temperature history on boiling initiation.

5.2 Pressure Runs

The program used to analyze the pressure runs is provided in Appendix B. The choice of amplifier time constant and the effect of system temperature on the pressure signal is discussed in Appendix C. Representative results from the program are provided in Appendix D. All pressure runs are described in Table 5.1.

The reproducibility of the decompression was of primary importance. In all runs the ambient temperature was 100°C, and the decompression

Table 5.1. Results of measurements made to determine the behavior of the pressure transients.

Run	p_a (MPa)	Drift (V/s)	Transfer Function (MPa/V)
AP2-2	0.377	-0.005246	0.7942
AP2-6	0.377	-0.005246	0.8654
AP2-7	0.515	-0.0096	0.7798
AP2-8	0.515	-0.0096	0.7908
AP3-4	0.515	-0.0096	0.8131
AP3-5	0.446	-0.007801	0.7631
AP3-6	0.446	-0.007632	0.7705
AP4-2	0.446	-0.005812	0.7748
AP4-3	0.584	-0.006913	0.7631
AP4-7	0.584	-0.005800	0.7771
AP4-8	0.584	-0.005295	0.7690
AP7-5	0.377	-0.003981	0.9952
AP7-8	0.377	-0.003926	1.0297
AP8-6	0.377	-0.002703	0.8536
AP9-2	0.377	-0.004091	0.9432
AP9-8	0.377	-0.002093	0.8248

ended at atmospheric pressure. The pressure histories for decompressions from initial pressures of 0.377-0.584 MPa are illustrated in Figs. 5.1 - 5.4, where it is seen that the decompression event is reproducible over most of the initial pressure drop.

The results of runs AP2-7, AP2-8, and AP3-4 require special comment. For unknown reasons, analysis of the raw data indicated negligible drift and a pressure transducer sensitivity greater than the manufacturer's specification. Since this was not characteristic of previous experience, a drift value was arbitrarily specified to give a transfer function reasonable with expectations. However, results with this data should be viewed with caution.

The pressurizer tended to back-fill with water from the pressure vessel in the course of the repeated fluid temperature cyclings experienced. This process was slow enough that little effect on depressurization was observed until the pressurizer was almost completely full of water. When this occurred the decompression event became erratic and unreliable. When approximately two liters of water were removed from the pressurizer, allowing a larger gas volume for pressurization, the rate of decompression changed significantly (Fig. 5.5). However, the partial removal of water did not affect the reproducibility of subsequent pressure runs, as shown in Figs. 5.6 and 5.7.

The decompressions displayed near-exponential behaviors over the reproducible portions of the transients. Figures 5.8 and 5.9 illustrate this behavior for representative pressure runs, and Table 5.2 lists their approximate reduction periods. These periods were on the order of 4 s before the pressurizer was partially drained and on the order of 6.6 s afterward.

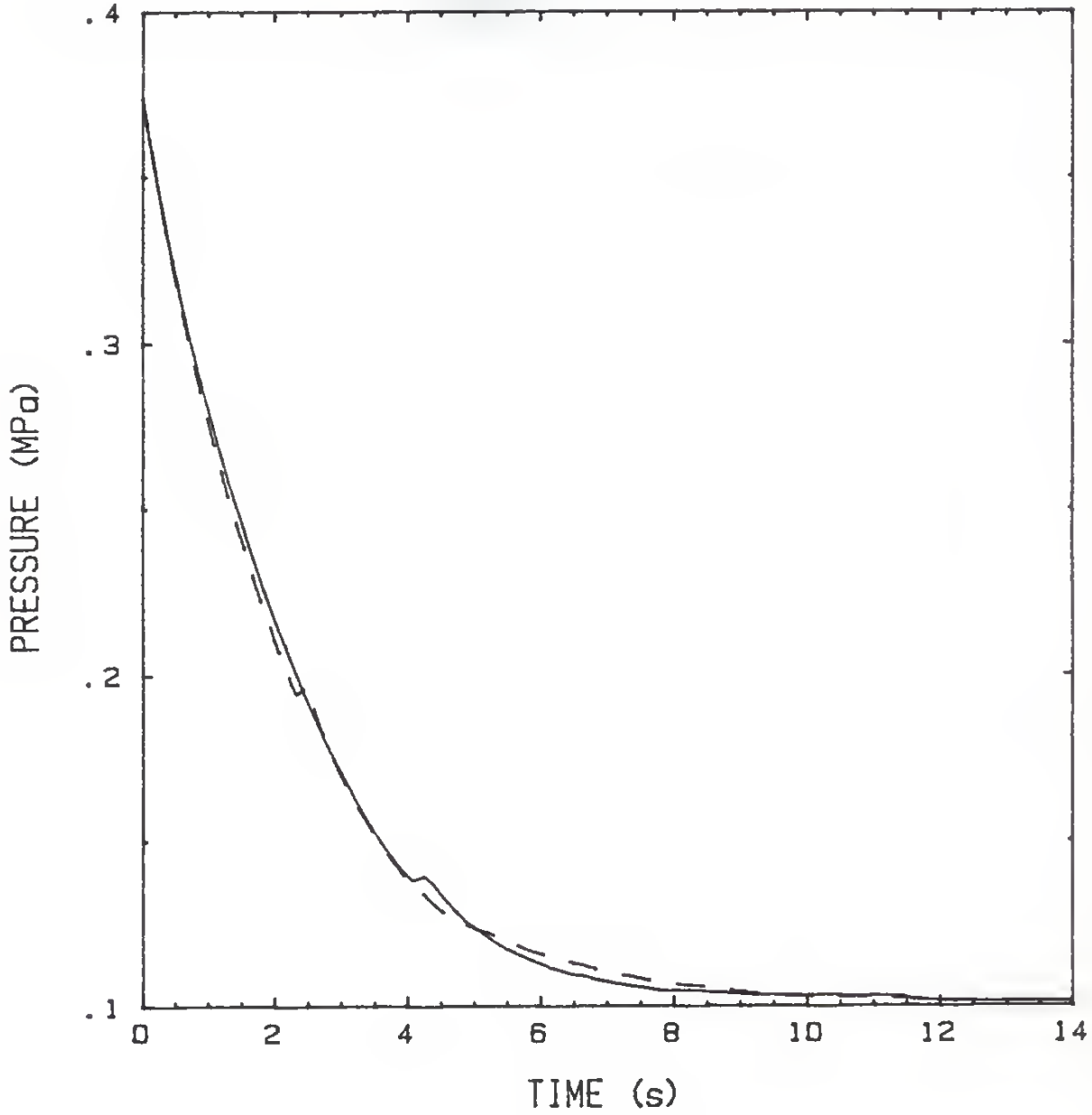

FIG. 5.1. Experimental pressure results for decompression from 0.377 to 0.101 MPa at T_a = 100°C. The solid line represents results from run AP2-2. The dashed line represents results from run AP2-6.

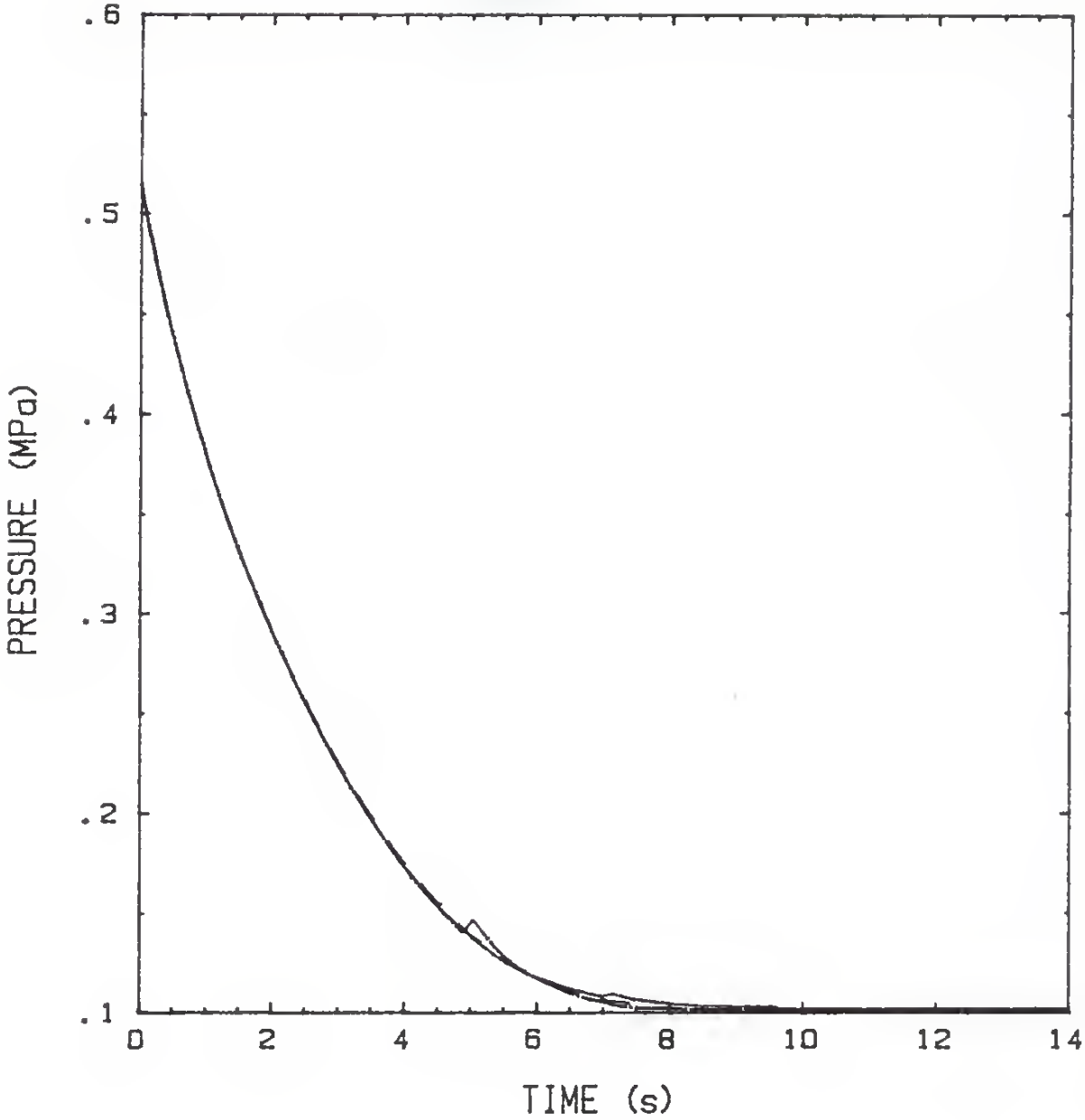

FIG. 5.2. Experimental pressure results for decompression from 0.515 to 0.101 MPa at T_a = 100°C. The dashed line represents results from run AP2-7, the solid line represents results from run AP2-8, and the dot-dashed line represents results from run AP3-4.

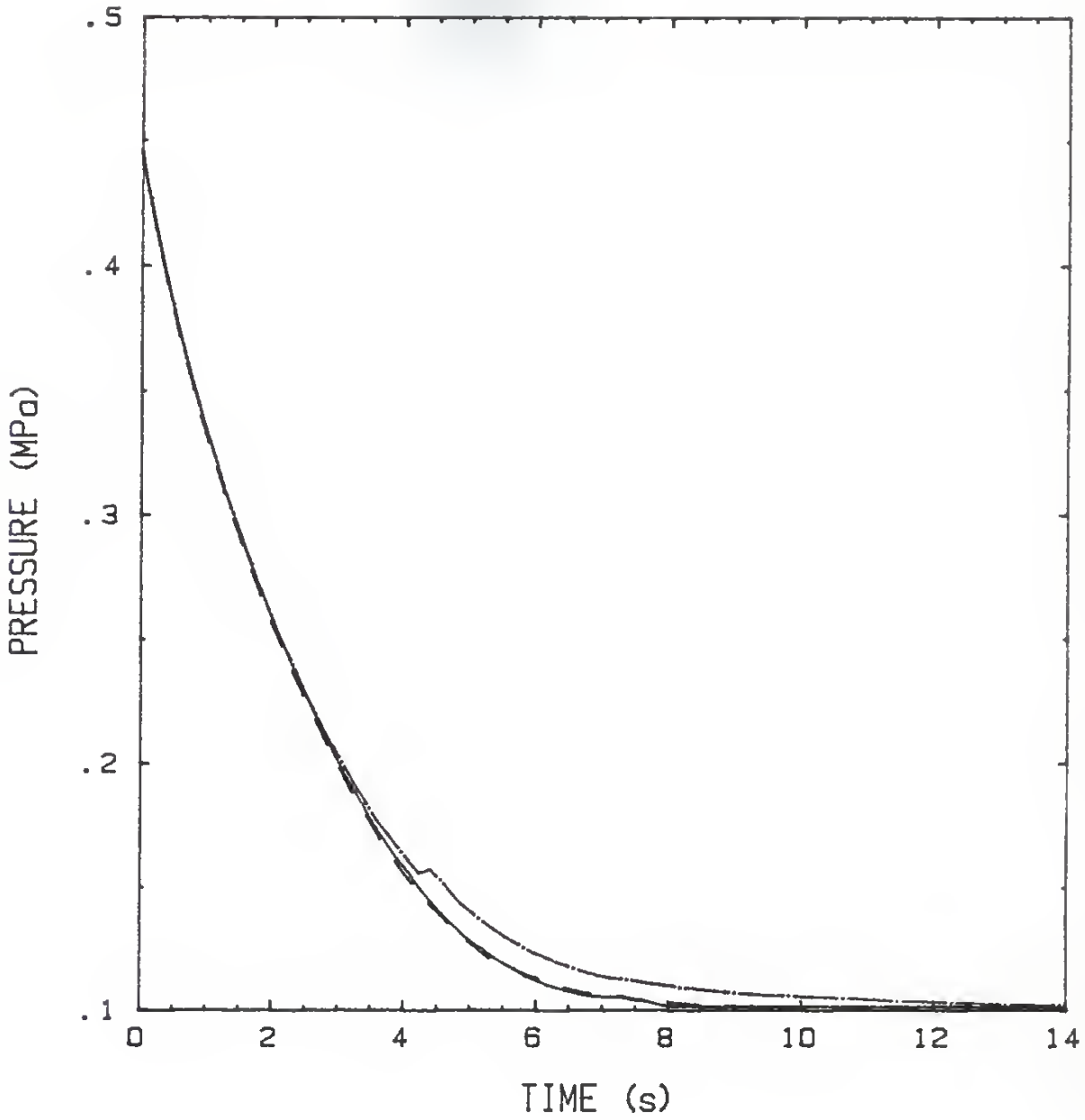

FIG. 5.3. Experimental pressure results for decompression from 0.446 to 0.101 MPa at T_a = 100°C. The solid line represents results from run AP3-5, the dashed line represents results from run AP3-6, and the dot-dashed line represents results from run AP4-2.

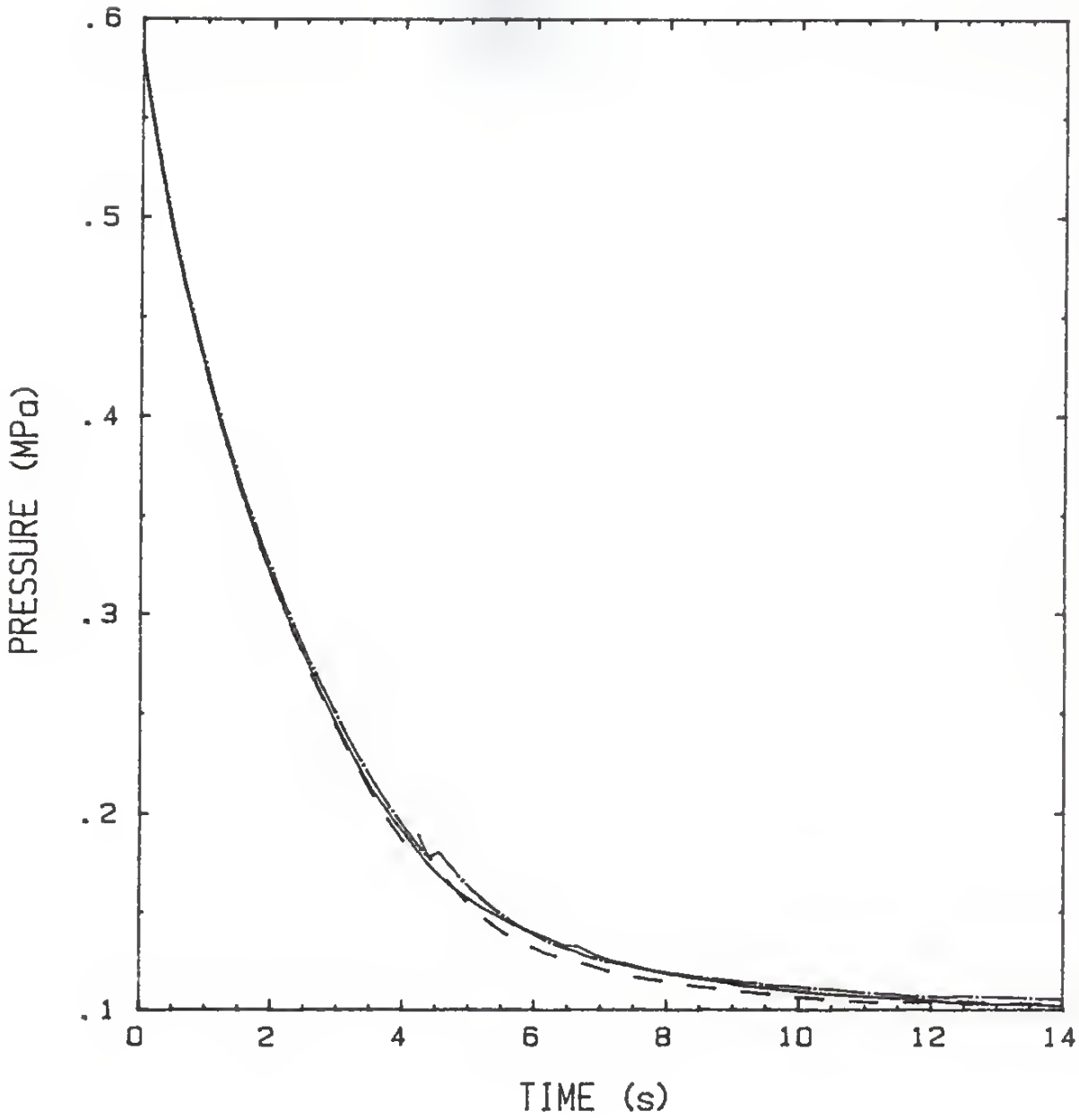

FIG. 5.4. Experimental pressure results for decompression from 0.584 to 0.101 MPa at T_a = 100°C. The solid line represents results from run AP4-3, the dashed line represents results from run AP4-7, and the dot-dashed line represents results from run AP4-8.

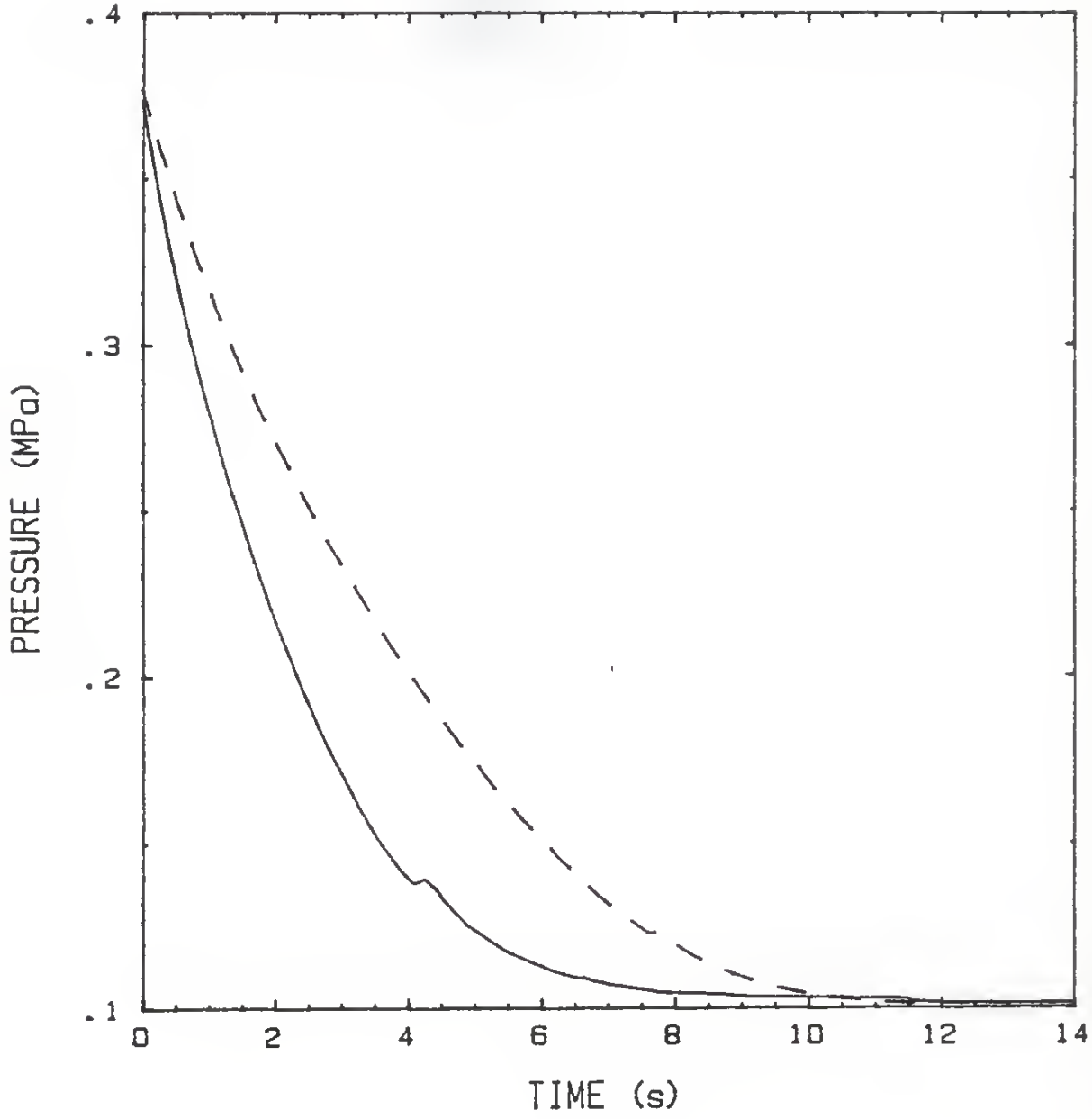

FIG. 5.5. Comparison of experimental pressure results for decompression from 0.377 to 0.101 MPa at T_a = 100°C before and after partial draining of the pressurizer. The solid line represents run AP2-2, performed before approximately 2 liters of water were removed from the pressurizer. The dashed line represents run AP8-8, performed after the quantity of water was removed.

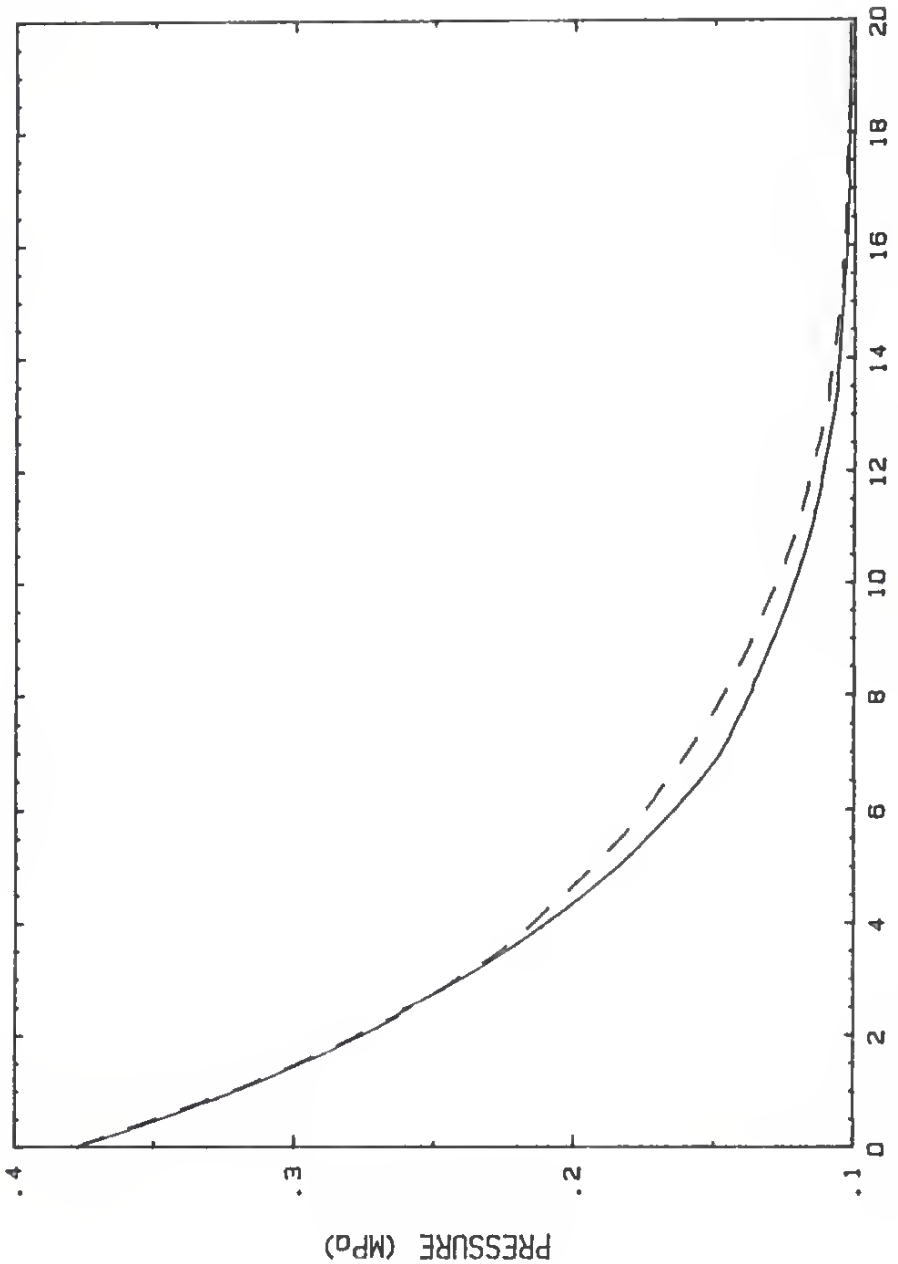

FIG. 5.6. Experimental pressure results for decompression from 0.377 to 0.101 MPa at T_a = 100°C. The maximum system pressure was 0.377 MPa. The solid line represents results from run AP7-5. The dashed line represents results from run AP7-8.

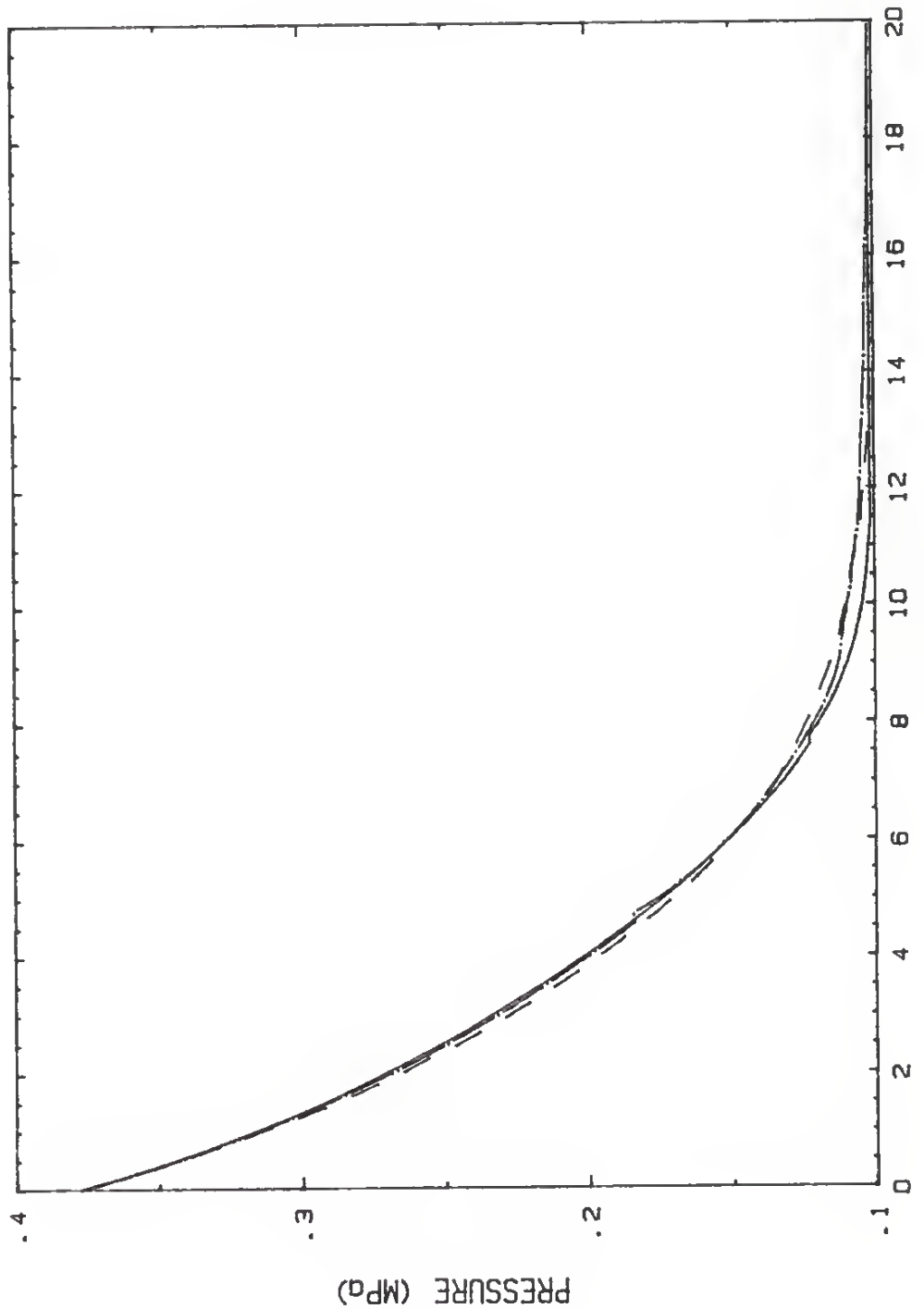

FIG. 5.7. Experimental pressure results for decompression from 0.377 to 0.101 MPa at T_a = 100°C after application of a maximum pressure greater than 0.377 MPa. The solid line represents results from run AP8-6, the dashed line represents results from run AP9-2, and the dot-dashed line represents results from run AP9-8.

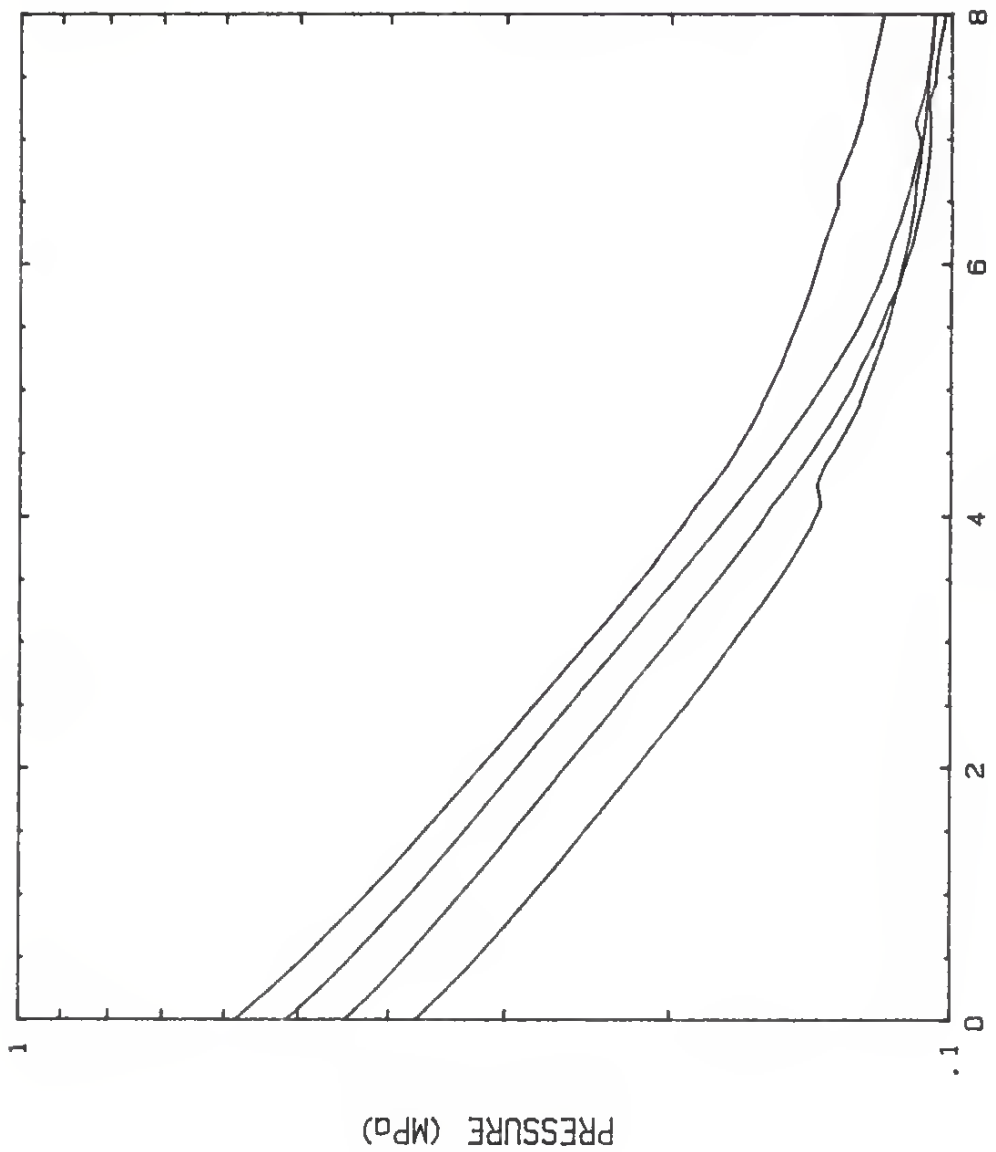

FIG. 5.8. Experimental pressure results for decompressions to 0.101 MPa at T_a = 100°C. Initial pressures were 0.377 to 0.584 MPa. Results are from representative runs performed before removal of a quantity of water from the pressurizer.

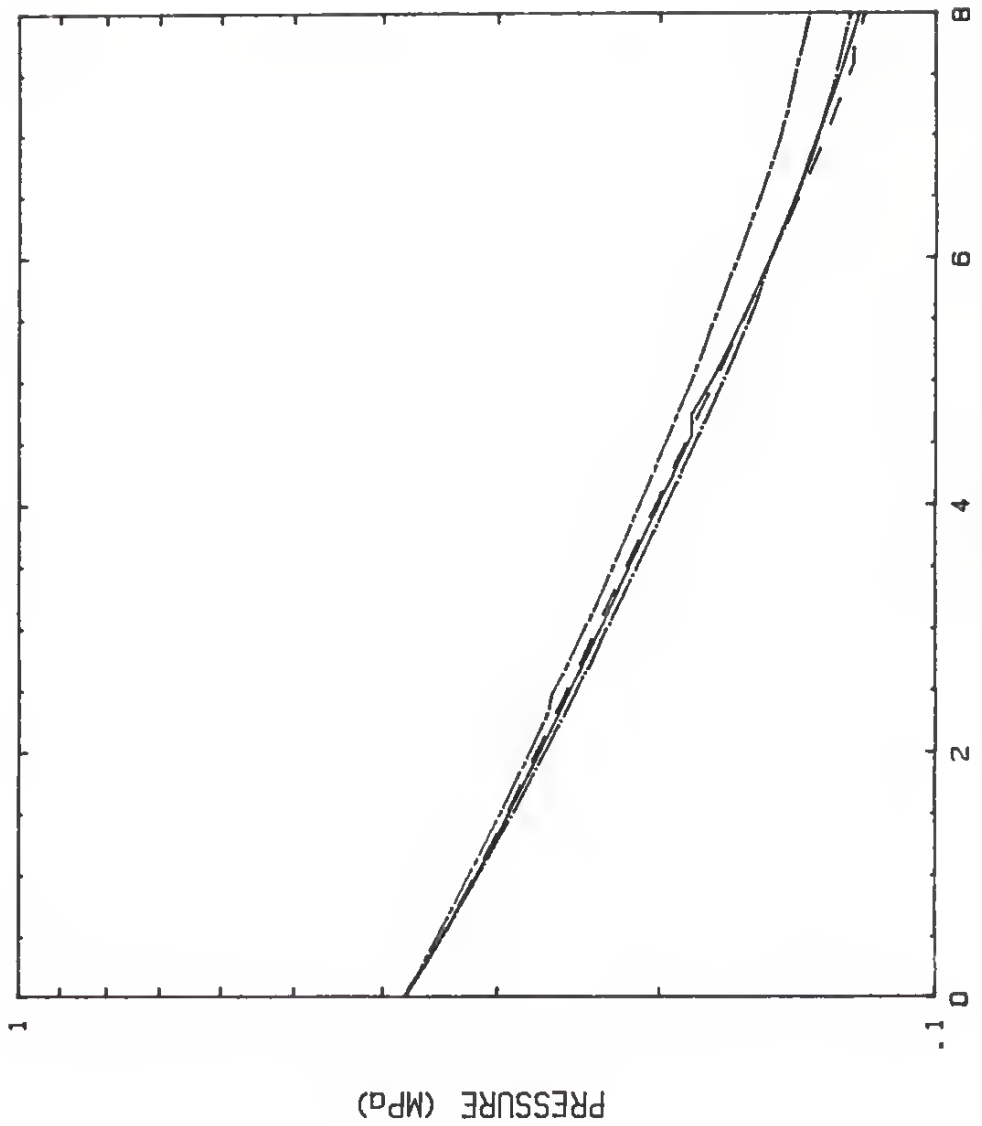

FIG. 5.9. Experimental pressure results for decompression from 0.377 to 0.101 MPa at T_a = 100°C after application of a maximum pressure $p_{a,max} \geq 0.377$ MPa. Results are from representative runs performed after removal of a quantity of water from the pressurizer.

Table 5.2. Approxmiate reduction periods for representative pressure runs.

Series	Run	t_1 (s)	t_2 (s)	$p(t_1)$ (MPa)	$p(t_2)$ (MPa)	τ (s)
1	AP2-2	0.56	3.60	0.3153	0.1496	4.078
2	AP2-8	0.56	3.60	0.4300	0.1921	3.773
3	AP3-5	0.56	3.60	0.3764	0.1733	3.920
4	AP4-3	0.56	3.60	0.4822	0.2089	3.634
5	AP7-5	0.56	5.52	0.3449	0.1736	7.225
6	AP8-6	0.48	10.08	0.3409	0.1612	6.622
7	AP9-2	0.56	5.52	0.3396	0.1587	6.519
8	AP9-8	0.56	5.52	0.3394	0.1615	6.680

5.3 Temperature Runs

The preparation of the system for a series of runs was described earlier. Additionally, each temperature run was preceded by vigorous boiling from the platinum test element for ten minutes at atmospheric pressure to ensure a consistent range of cavity sizes before pressurization.

In the series of tests presented, the system was pressurized to a maximum ambient pressure, $p_{a,max}$, while the bulk water temperature was held steady at 100°C. Power was then applied to the test element to elevate its temperature to 160°C. The decompression event was then initiated and a manual measurement of boiling initiation time t_b was obtained. The program used to analyze the temperature runs is provided in Appendix A. Representative results from the program are provided in Appendix E. All series are described in Table 5.3.

In series 1 the system was pressurized to a maximum pressure of 0.377 MPa. Figure 5.10 illustrates series 1, where it is observed that the temperature of the test element began to decrease almost immediately, while the measured boiling initiation time occurred after the temperature had dropped an appreciable amount.

In series 2 the system was pressurized to 0.515 MPa. The results of this series are shown in Fig. 5.11. The temperature of the test element remained constant for approximately two seconds, and the measured boiling times were close to the times at which the temperatures begin to decrease. Also apparent is the variability of the heater temperature recovery to a steady-state value.

Figures 5.12 and 5.13 illustrate series 3 and series 4, in which the system was pressurized to 0.446 and 0.584 MPa, respectively. Again, the heater temperature remained constant for a period of time after

Table 5.3. Experimental conditions for measurements to determine the effects of pressure-temperature history on boiling initiation. Initial conditions: wire temperature T_w = 160°C, ambient temperature T_a = 100°C.

Series	Run	Duration (s)	$p_{a,max}$ (MPa)	$p_a(t=0)$ (MPa)	q (MW/m^2)
1	AP2-3	20	0.377	0.377	0.427
	AP2-4	20	0.377	0.377	0.430
	AP2-5	20	0.377	0.377	0.432
2	AP3-1	20	0.515	0.515	0.424
	AP3-2	20	0.515	0.515	0.424
	AP3-3	20	0.515	0.515	0.437
3	AP3-7	20	0.446	0.446	0.419
	AP3-8	20	0.446	0.446	0.419
	AP4-1	20	0.446	0.446	0.419
4	AP4-4	20	0.584	0.584	0.408
	AP4-5	20	0.584	0.584	0.416
	AP4-6	20	0.584	0.584	0.416
5	AP7-2	20	0.377	0.377	0.407
	AP7-3	20	0.377	0.377	0.419
	AP7-4	20	0.377	0.377	0.419
	AP7-6	20	0.377	0.377	0.419
	AP7-7	20	0.377	0.377	0.419
6	AP8-4	20	1.480	0.377	0.419
	AP8-5	20	>1.480	0.377	0.414
7	AP8-7	20	1.480	0.377	0.418
	AP8-8	100	1.480	0.377	0.424
8	AP9-4	200	0.791	0.377	0.418
	AP9-6	200	0.791	0.377	0.418

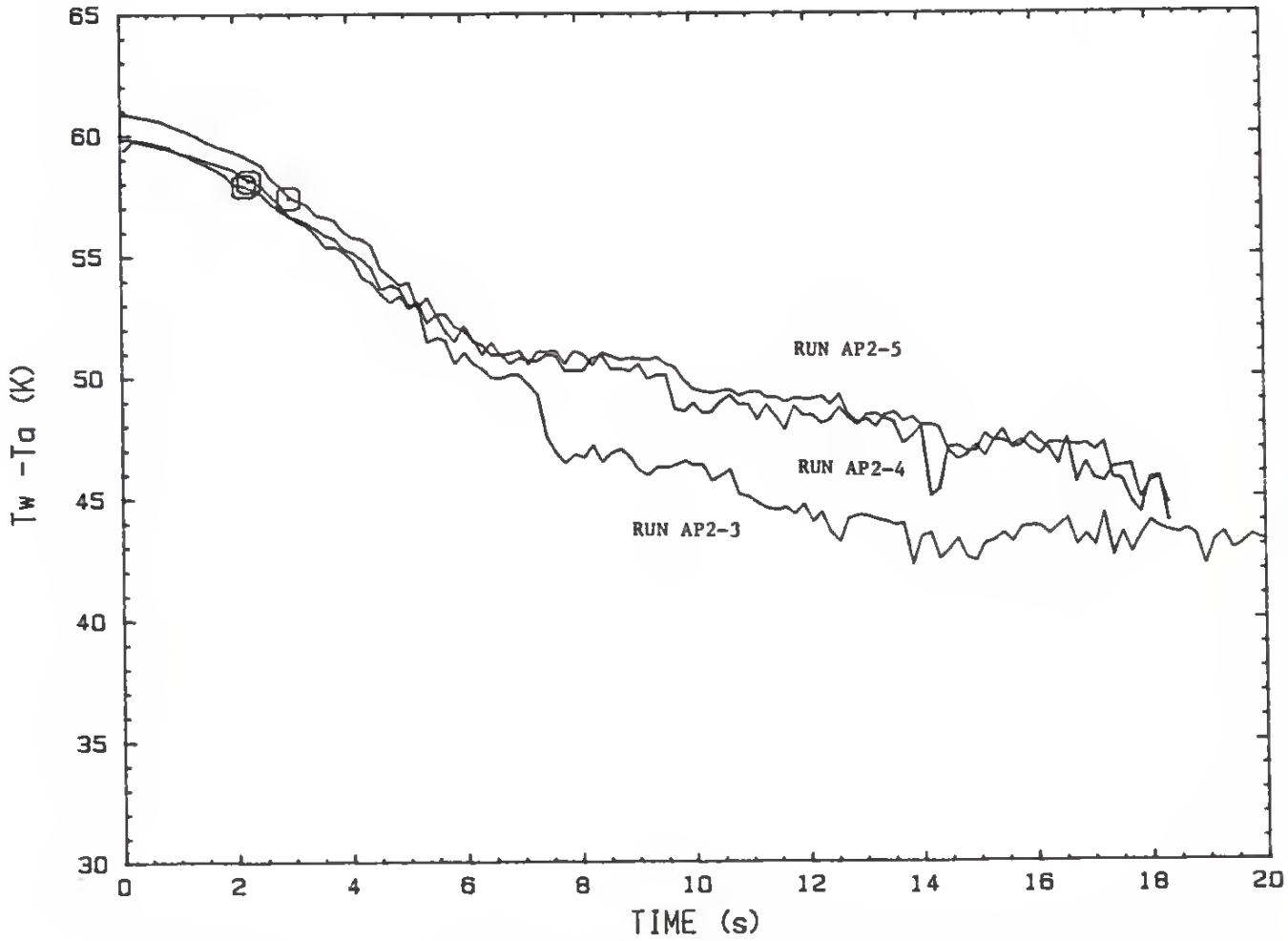

FIG. 5.10. Experimental temperature results for decompression from 0.377 to 0.101 MPa at T_a = 100°C and initial heater temperature T_w = 160°C. The reduction period of the pressure transient was on the order of 4 s. The circles mark the measured boiling initiation times.

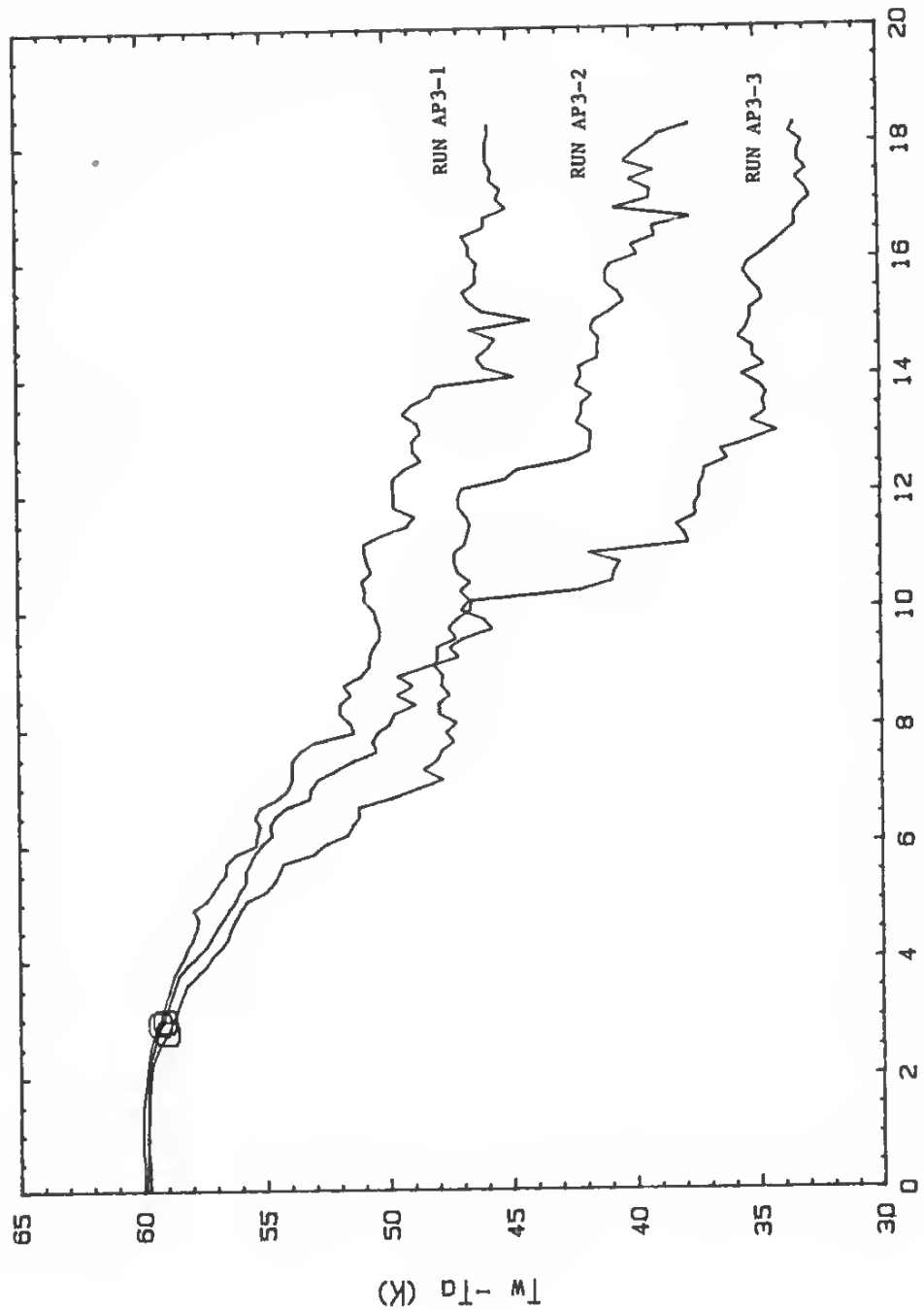

FIG. 5.11. Experimental temperature results for decompression from 0.515 to 0.101 MPa at T_a = 100°C and initial heater temperature T_w = 160°C. The reduction period of the pressure transient was on the order of 4 s. The circles mark the measured boiling initiation times.

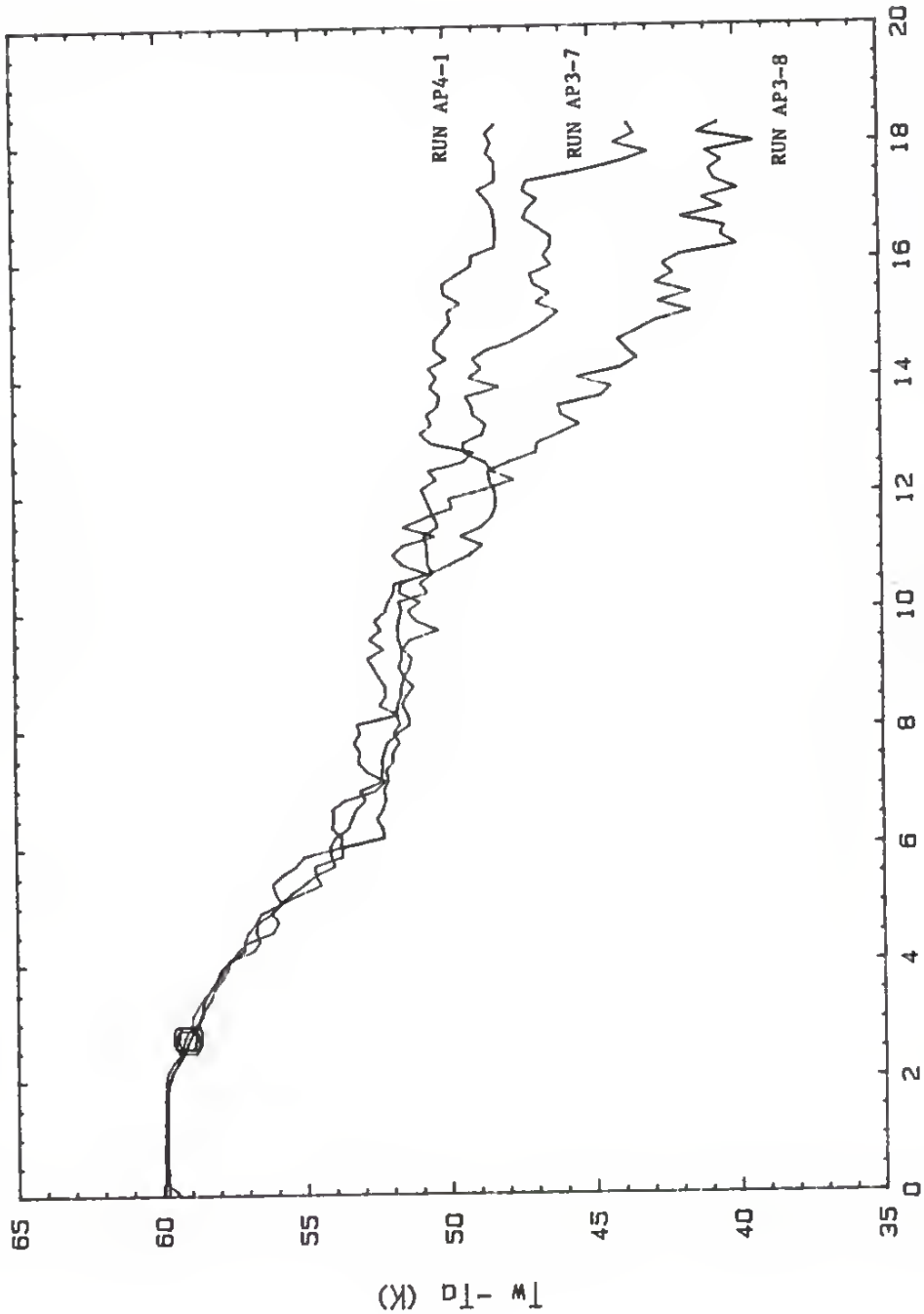

FIG. 5.12. Experimental temperature results for decompression from 0.446 to 0.101 MPa at T_a = 100°C and initial heater temperature T_w = 160°C. The reduction period of the pressure transient was on the order of 4 s. The circles mark the measured boiling initiation times.

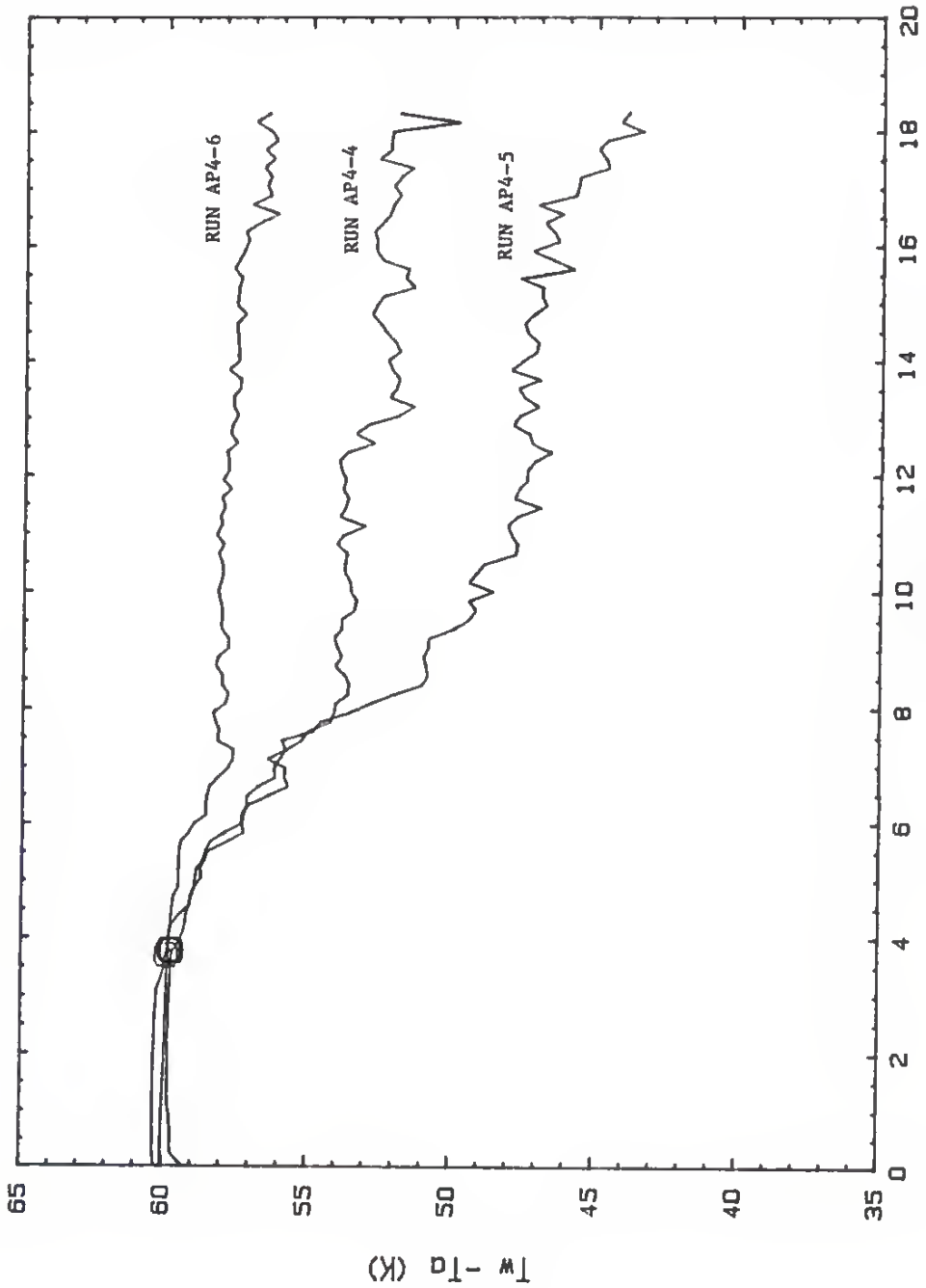

FIG. 5.13. Experimental temperature results for decompression from 0.584 to 0.101 MPa at T_a = 100°C and initial heater temperature T_w = 160°C. The reduction period of the pressure transient was on the order of 4 s. The circles mark the measured boiling initiation times.

initiation of the pressure transient, and measured boiling times were close to the points where the temperatures began to decrease. Figure 5.13 also shows particularly well the variable nature of the heater temperature recovery after boiling had begun.

Series 5-8 were performed after removal of a quantity of water from the pressurizer. The rates of decompression in these runs were less than those for series 1-4 as discussed earlier. Additionally, the procedure was varied such that the system was subjected to a maximum pressure $p_{a,max}$, then slowly returned to a starting pressure $p_a(t=0)$, the pressure at the initiation of the pressure transient.

In series 5 the maximum pressure was 0.377 MPa. Measured boiling initiation times for all runs in this series except for run AP7-6 were well after the heater temperature had begun to decrease. As in series 1, the heater temperature began to decrease almost immediately after initiation of the pressure transient. Figure 5.14 illustrates this series.

In series 6 and series 7 the maximum pressure applied was 1.480 MPa. The exception was run AP8-5, which experienced an unknown maximum pressure greater than 1.480 MPa. In these runs the measured boiling time corresponds to the time of the first audible bubble collapse. Bubbles did not appear on the visible part of the test element until after the system had returned to atmospheric pressure. In series 6 (Fig. 5.15), the heater temperature began to decrease shortly after initiation of the pressure transient, but the decrease was very gradual until the end of the pressure transient. Heater temperature fluctuations indicative of substantial nucleate boiling then appeared, but the temperature decreased minimally compared to runs with less extreme overpressures.

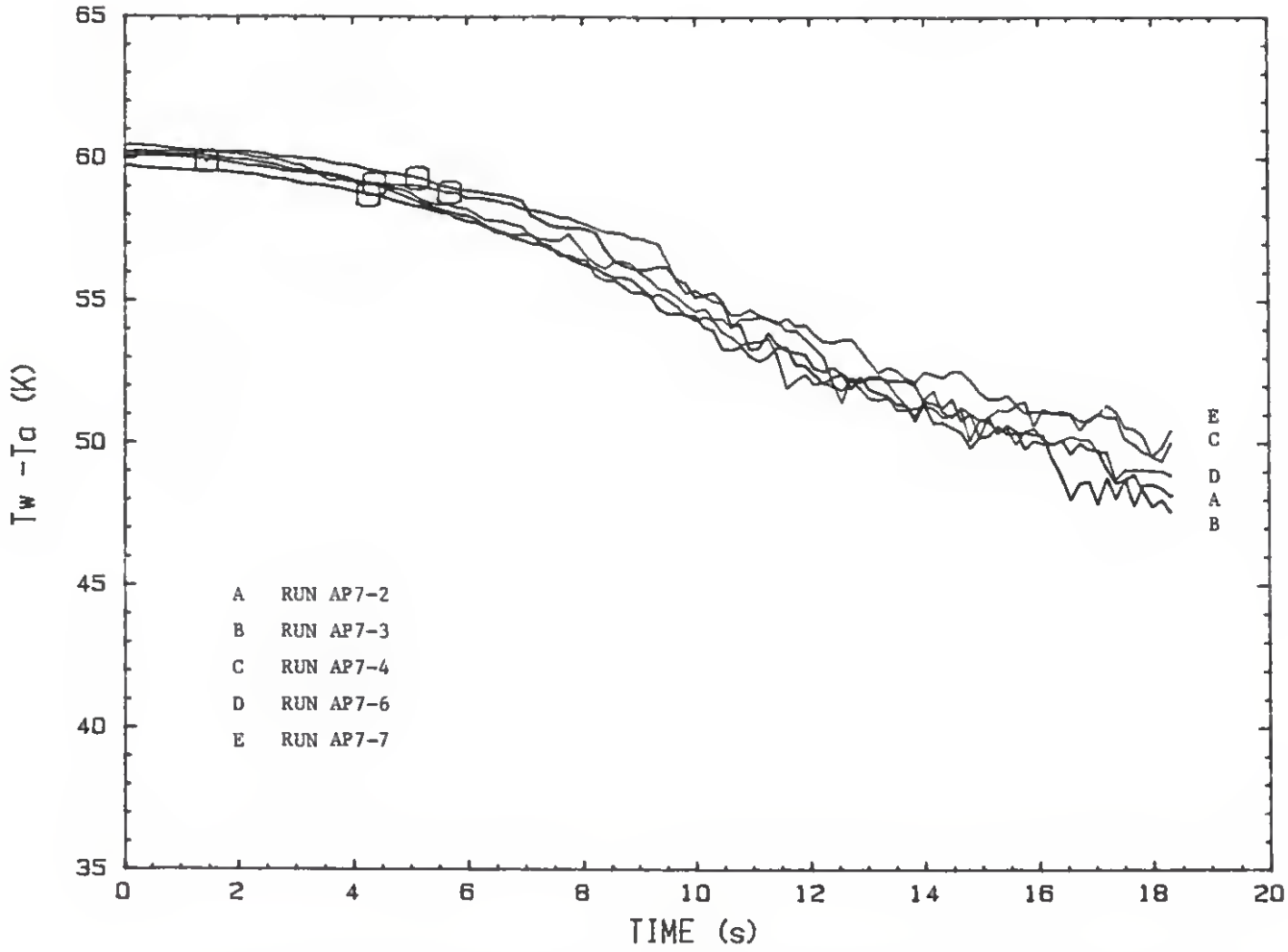

FIG. 5.14. Experimental temperature results for decompression from 0.377 to 0.101 MPa at T_a = 100°C and initial heater temperature T_w = 160°C. The maximum pressure applied was 0.377 MPa and the pressure reduction period was on the order of 6.6 s. The circles mark the measured boiling initiation times.

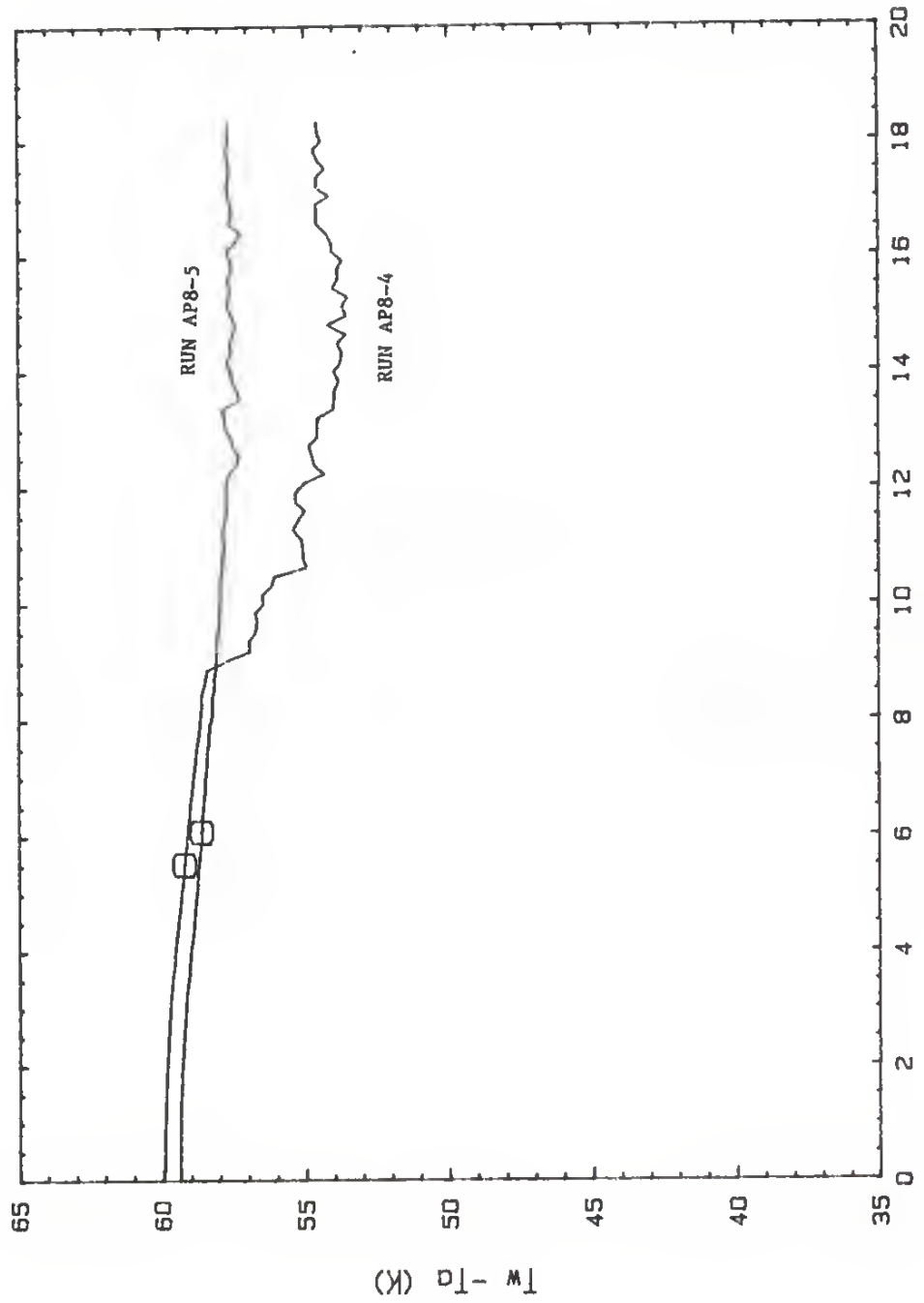

FIG. 5.15. Experimental temperature results for decompression from 0.377 to 0.101 MPa at T_a = 100°C and initial heater temperature T_w = 160°C. The maximum pressure applied was 1.48 MPa and the pressure reduction period was on the order of 6.6 s. The circles mark the measured boiling initiation times.

This behavior was also observed in series 7, in which runs of 20 s and 100 s duration were performed. The temperature behavior during the first 20 s of the event is shown in Fig. 5.16(a). Even 100 s after the initiation of the pressure transient [Run AP8-8 and Fig. 5.16(b)] the heater temperature had only decreased about 7 K, as opposed to 10-12 K drops in 20 s seen in series 5, for example.

The long-term behavior of the heater temperature was of specific interest in series 8. The maximum pressure in this series was 0.791 MPa, and the duration of the runs was 200 s. Again, no bubbles were seen until after the system had returned to atmospheric pressure. Measured boiling initiation times were before substantial nucleate boiling was indicated by the temperature analysis. The minimal decrease in the heater temperature during the first 20 s of the event is illustrated in Fig. 5.17(a). After the initial drop, the temperature reached a plateau before experiencing a more sustained decrease. The heater temperature approached the steady-state boiling temperature at the same superficial heat flux by approximately 200 s. Series 8 and the corresponding steady-state boiling temperature traces are shown in Fig. 5.17(b).

If the point at which the heater temperature starts to decrease is taken as the incipient boiling point, conditions at boiling initiation can be determined from pressure and temperature values at this time. Normally, this estimated time should be equivalent to the measured boiling initiation time, with any difference accounted for by resolution of the data analysis, human error, and reaction time in operating the chronograph. However, a significant discrepancy could exist between these two times. If the resolution limit of the analyzed data is

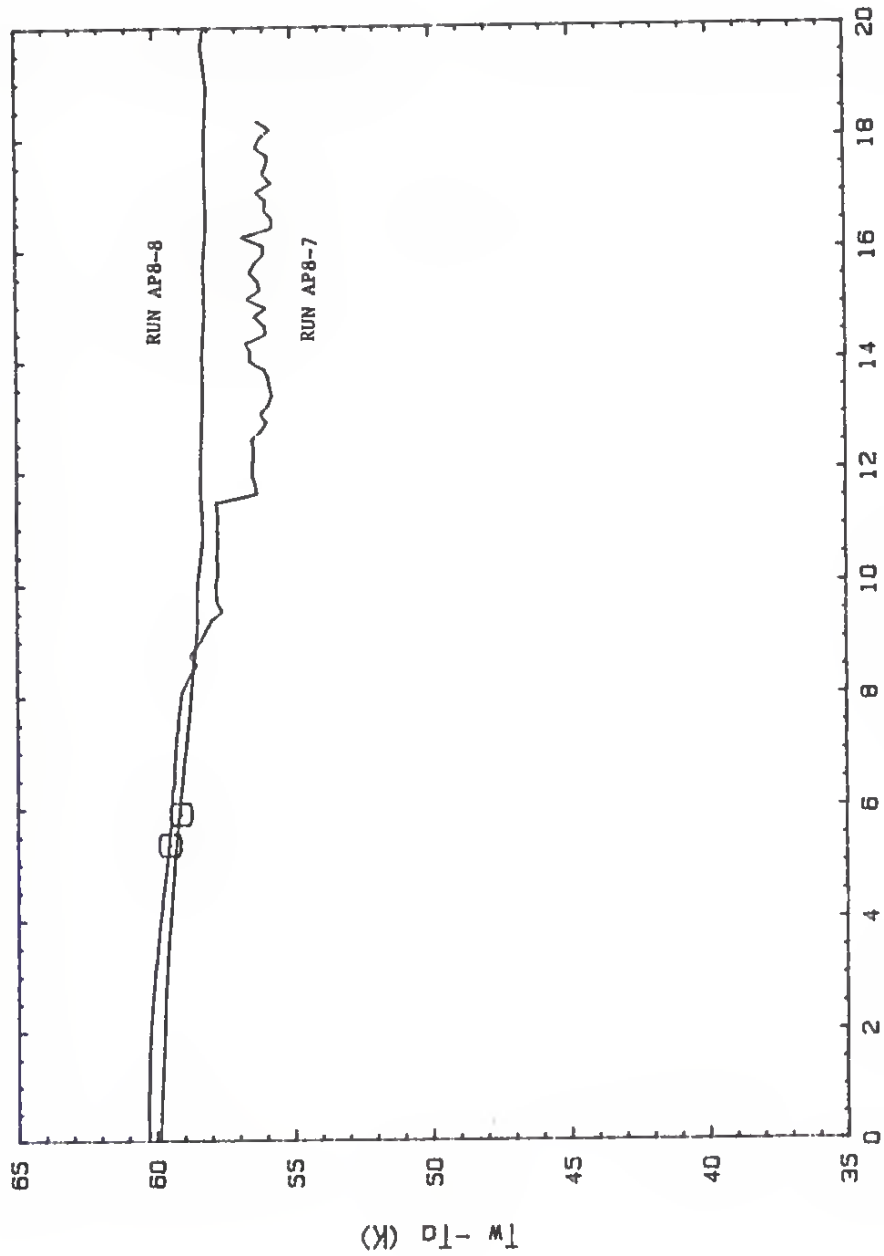

FIG. 5.16(a). Experimental temperature results showing the initial behavior of the heater temperature for T_a = 100°C and initial heater temperature T_w = 160°C. The decompression was from 0.377 to 0.101 MPa after a maximum pressure of 1.48 MPa had been applied. The reduction period of the pressure transient was on the order of 6.6 s. The circles mark the measured boiling initiation times.

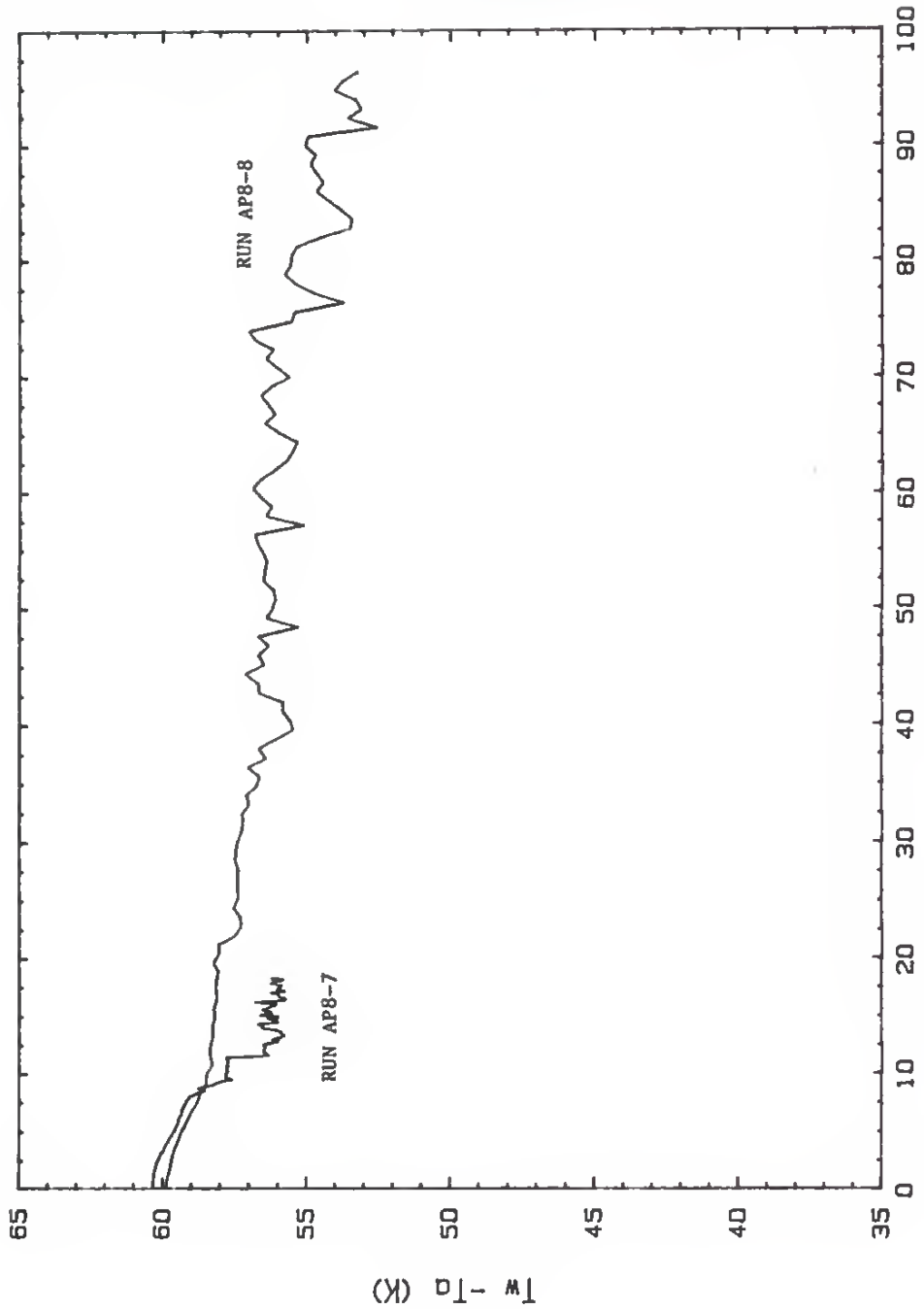

FIG. 5.16(b). Experimental temperature results showing the long-term behavior of the heater temperature for T_a = 100°C and initial heater temperature T_w = 160°C. The decompression was from 0.377 to 0.101 MPa after a maximum pressure of 1.48 MPa had been applied. The reduction period of the pressure transient was on the order of 6.6 s.

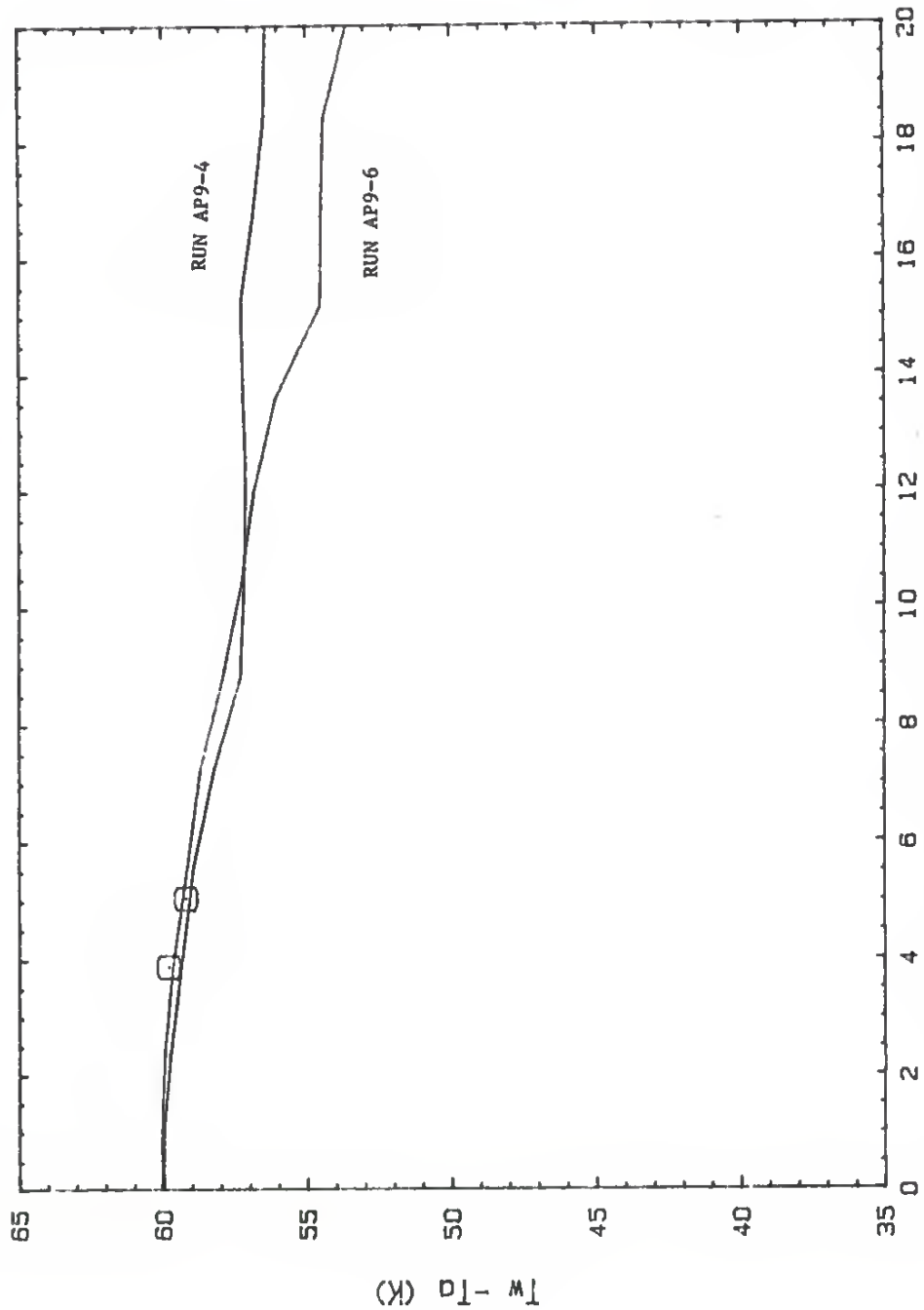

FIG. 5.17(a). Experimental temperature results showing the initial behavior of the heater temperature for T_a = 100°C and initial heater temperature T_w = 160°C. The decompression was from 0.377 to 0.101 MPa after a maximum pressure of 0.791 MPa had been applied. The reduction period of the pressure transient was on the order of 6.6 s. The circles mark the measured boiling initiation times.

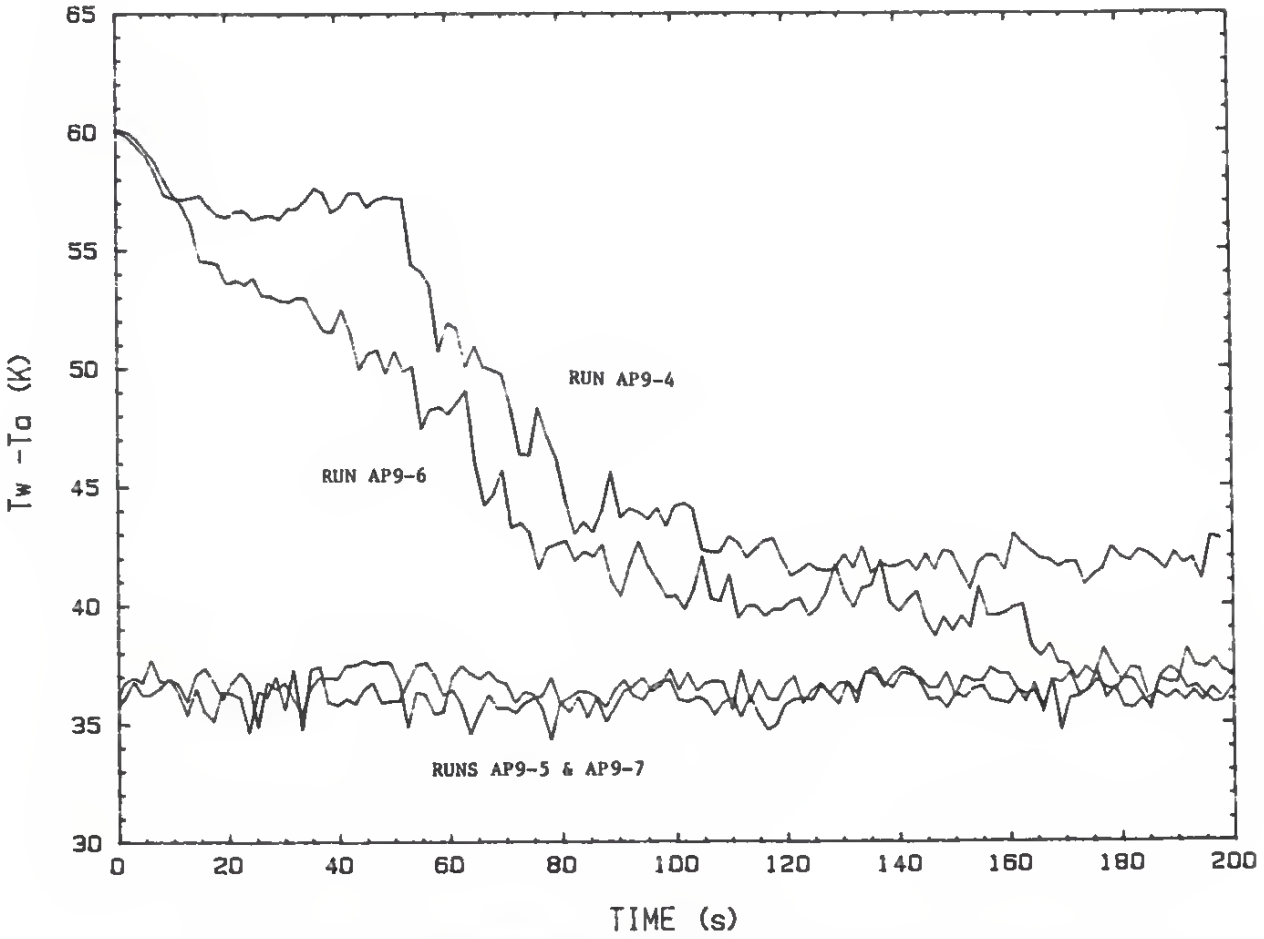

FIG. 5.17(b). Experimental tempereture results showing the long-term recovery of the heater temperature to the steady-state nucleete boiling value et T_e = 100°C. The decompression was from 0.377 to 0.101 MPe after a maximum preasure of 0.791 MPe had been applied. The initial heater temperature wes T_w = 160°C, and the reduction period of the pressure transient was on the order of 6.6 s. The euperficial heet fluxes were the eame for the trensient end the steady-state rune. The time scele of the ateady-etate resulta as ehown ie multiplied by a factor of 10.

approached, the measured value should be selected as the true boiling initiation time. If boiling initiates on a part of the test element outside the visual range and the ambient noise level precludes audio detection, the measured time would be late and the estimated value should be selected as the true boiling initiation time. Additionally, although the partial pressure of noncondensible gas is assumed to be negligible, an isolated cavity could contain a bubble of noncondensible gas. Premature non-boiling bubble formation could occur at this site. The frequency of bubble formation would not display the periodicity of true nucleate boiling. Although conditions for boiling initiation would not have been achieved according to the criteria of this work, the chronograph would have been stopped at the appearance of the first bubble. Again, the estimated boiling initiation time should be selected. Following this prescription for determining true boiling initiation times, the measured and true boiling initiation times and conditions at boiling initiation are given in Table 5.4 for all series.

Table 5.4. Results of meesurements made to determine the effects of pressure-temperature history on boiling initiation. In all cases, the heater is a platinum wire of 0.25 mm diameter and 9.6 cm length. Degassing was carried out et atmospheric pressure. True boiling initiation times are at the point the heater temperature began to show a substantial decrease. Initial conditions: wire temperature T_w = 160°C, ambient temperature T_a = 100°C.

Series	Run	Measured t_b(s)	p_b(MPa)	T_b-T_a(K)	T_b-T_s(K)	True t_b(s)	p_b(MPe)	T_b-T_a(K)	T_b-T_s(K)
1	AP2-3	2.17	0.208	57.9	36.4	0.08[a]	0.365	59.4	19.1
	AP2-4	2.95	0.173	57.4	41.7	0.08	0.365	60.8	20.5
	AP2-5	2.26	0.204	58.1	37.3	0.08	0.365	59.8	19.5
2	AP3-1	2.93	0.228	59.3	34.9	2.16	0.279	59.8	28.7
	AP3-2	2.98	0.225	59.1	35.1	2.16	0.279	59.7	28.6
	AP3-3	2.78	0.238	59.0	33.2	2.16	0.279	59.6	28.6
3	AP3-7	2.67	0.218	59.1	36.1	1.84	0.269	59.8	30.0
	AP3-8	2.75	0.214	59.0	36.6	1.84	0.269	59.8	30.0
	AP4-1	2.74	0.215	59.2	36.7	2.00	0.259	59.9	31.3
4	AP4-4	3.78	0.201	59.8	39.4	3.92	0.194	59.8	40.5
	AP4-5	3.76	0.202	59.7	39.1	3.76	0.202	59.7	39.1
	AP4-6	3.69	0.205	59.9	38.9	3.12	0.236	60.2	34.6
5	AP7-2	4.28	0.202	58.7	38.2	1.46[b]	0.299	59.5	26.1
	AP7-3	5.14	0.181	59.3	42.2	1.46	0.299	60.2	26.8
	AP7-4	4.39	0.199	59.1	39.0	1.46	0.299	60.0	26.6
	AP7-6	1.46	0.299	59.9	26.5	1.46	0.299	59.9	26.5
	AP7-7	5.7	0.170	58.8	43.6	1.46	0.299	60.2	26.8
6	AP8-4	5.52	0.161	59.2	45.7	8.88	0.110	58.4	56.1
	AP8-5	6.08	0.149	58.6	47.4	11.76 ± 0.48	0.101	57.7	57.7
7	AP8-7	5.35	0.162	59.5	45.8	8.08	0.123	59.0	53.6
	AP8-8	5.90	0.152	59.1	47.4	8.4 ± 0.8	0.120	58.6	53.8
8	AP9-4	5.05	0.174	59.2	43.3	7.2 ± 0.8	0.131	58.2	50.8
	AP9-6	3.88	0.203	59.8	39.1	7.2 ± 0.8	0.131	58.7	51.3

[a]Listed times are first times for which temperature data were calculated. The estimated time range is 0.08 to 0.40 s.

[b]Listed times are from the measured time of Run AP7-6. The estimated time range is 1.0 to 2.5 s.

6. DISCUSSION OF RESULTS

6.1 Pressure Measurement

After the initiation of decompression the pressure vessel experienced a near-exponential reduction in pressure. Pressure transients were generally reproducible to times well beyond measured boiling initiation times. The spikes that occasionally appeared in the measurements are believed to be due to spurious electronic noise. The pressure measurement system sensitivity was less than expected due to installation constraints (see Appendix C). However, the system performed consistently except in the decompressions from 0.515 MPa (series 2). The reasons for the unusual behavior in those runs are unknown; therefore the results of series 2 are not considered in the following discussion.

6.2 Estimation of Boiling Initiation Times

Consider a heater experiencing a constant power application. In the case where heat transfer from the heater to a surrounding fluid is by natural convection, the inception of nucleate boiling will enhance the heat transfer and cause the heater surface temperature to decrease. Estimated boiling initiation times were obtained by determining the times at which the test heater temperature began to show a substantial decrease. These times provided an independent means of confirming measured boiling initiation times. The accuracy of the estimated times was dependent on the techniques used to obtain and analyze the raw voltage data. Since the variations in the voltages were expected to be small compared to the initial applied voltages, the measurement system was set up to measure only the variations. The analysis of the data required averaging the data over several points to minimize masking of

changes in true voltage by electrical noise. However, the data reduction resulted in coarse time steps and thus crude estimations of the time at which the heater temperature began to decrease. Although the two methods of determining boiling initiation times should have produced the same values, this was observed only in series 3 and series 4, where the inception of boiling was accompanied by a marked change in heater temperature. In these two series, the true boiling initiation times were the measured times adjusted according to the temperature histories. These adjustments were reasonable considering reaction times and human error. In the other series, however, experimental runs generally lacked a sharp change in heater temperature at boiling initiation, and the combination of test conditions helped to produce major differences in estimated and measured times. In series 1 the temperature began to decrease almost immediately, so true boiling initiation times were the first times for which temperature data were calculated. In series 5-8 poor data resolution combined with relatively slow pressure transients required specification of a range of boiling initiation times. Table 6.1 summarizes the conditions at boiling initiation for the series considered.

6.3 Effects of Pressure-Temperature History on Boiling Initiation

Runs in each series had been preceded by vigorous boiling from the test element for 10 minutes at atmospheric pressure and bulk fluid temperature T_a = 100°C. The pressure was raised to the maximum value for each run before power was applied to the test heater to elevate its temperature.

In series 1, 3, and 4 the decompression began at the maximum pressure, and reduction periods were on the order of 4 s. The boiling

Table 6.1 Summary of results of measurements made to determine the effects of pressure-temperature history on boiling initiation. In all cases, the heater is a platinum wire of 0.25 mm diameter and 9.6 cm length. Degassing was carried out at atmospheric pressure. Initial conditions: T_w = 160°C, T_a = 100°C.

Series	$p_{a,max}$ (MPa)	$p_a(t=0)$ (MPa)	t_b(s)	p_b (MPa)	T_b-T_s (K)
1	0.377	0.377	0.08 - 0.40	0.365 - 0.330	19.7 - 23.2
3	0.446	0.446	1.84 - 2.00	0.269 - 0.259	30.2 - 31.4
4	0.584	0.584	3.12 - 3.92	0.236 - 0.194	34.4 - 40.7
5	0.377	0.377	1.0 - 2.5	0.321 - 0.260	24.1 - 31.3
6	1.48	0.377	8.88 - 12.24	0.110 - 0.101	57.7 - 60.0
7	1.48	0.377	7.6 - 9.2	0.127 - 0.114	53.6 - 56.7
8	0.791	0.377	6.4 - 8.0	0.144 - 0.121	49.9 - 55.0

initiation times increased with increasing initial pressure, and no overlapping of times was observed for the different series. Increasing initial pressure also resulted in decreasing boiling initiation pressures and increasing superheats at boiling inception.

In series 1, Fabic's hypothesis gives the largest available nucleation sites radii of r_c = 0.132 μm. This would lead to a boiling initiation pressure of 0.330 MPa and a boiling initiation superheat of 23.2 K. In series 3, r_c = 0.106 μm, leading to a boiling initiation pressure of 0.258 MPa and a boiling initiation superheat of 31.5 K. Both of these series are in excellent agreement with the Fabic model if the estimated boiling inception times are used. However, the model predicts a boiling initiation pressure of 0.114 MPa for the cavity size r_c = 0.075 μm of series 4. This pressure is substantially below that observed in this series.

In series 5-8 the pressure transient was initiated from 0.377 MPa after the initial maximum pressure was applied. Reduction periods were on the order of 6.6 s. Boiling initiation times increased with increasing initial pressure, but the range of times tended to overlap for maximum pressures of 0.791 and 1.48 MPa.

Series 5 repeated the conditions of series 1 at a slower decompression rate. Although superheats were higher and pressures were lower at the inception of boiling in series 5, the results also support Fabic's model. Series 6-8 experienced such extremes in pressure that Fabic's model predicted no boiling for the given heater temperature. The model predicted a maximum cavity radius of 0.026 μm for series 6 and series 7, which would require a heater temperature of 192.3°C to initiate boiling. Series 8 would require a heater temperature of

169.7°C to initiate boiling from a predicted maximum cavity radius of 0.053 μm. However, the heater temperature history indicated that boiling began near the end of decompression, and after an additional period of time sites were seen to commence nucleating on the visible part of the test element.

6.4 Approach to Steady-State Boiling

Even though Fabic's model greatly underpredicted boiling initiation pressures (and overpredicted boiling initiation superheats) in series 4 and series 6-8, the pressure-temperature history did affect the reactivation of nucleation sites as the runs progressed.

The models used to predict boiling conditions based on cavity size can also explain the behavior of the heater temperature as steady-state nucleate boiling is approached. Consider Eq. (2.7),

$$p_v(T_w) - p_v(T_s) = 2\sigma(T_w)/r_c. \qquad (2.7)$$

Although surface tension decreases with increasing temperature, vapor pressure is more sensitive to temperature variations and hence dominates the temperature dependence of Eq. (2.7). It is apparent that test element temperature results would be very sensitive to whether or not one or two cavities activate consistently in separate runs.

Since T_w remains constant until the inception of boiling, superheat increases with decreasing pressure until conditions for boiling are achieved. Once boiling begins, the heater cools, with the amount of cooling determined by the size and density of active sites. During the pressure transient, the cooling tends to offset the decrease in $p_v(T_s)$, thus restricting the activation of other nucleation sites.

After the decompression ends, a larger site rendered inactive by the pressure-temperature history experienced prior to the pressure transient could be activated in two ways. Vapor microbubbles created in the collapse of macroscopic bubbles in subcooled liquid could migrate from an adjacent active site and seed the cavity (33-36). If the cavity has vapor trapped at its base, activation could be accomplished either by vapor migration or by achievement of a sufficiently large local superheat to overcome the effects of pre-pressurization. Once the barrier to nucleation were breached, the cavity would remain active.

The temperature of the platinum wire test element was calculated using its resistance at 0°C (see Section 4.2). Based on measurements of the resistance at 100°C, the wire resistance at 0°C was $R_0 = 0.1961 \pm 0.0021$. This led to an uncertainty of ±2.9 K in the value of the calculated wire temperature T_w. This was a systematic error that adds to the uncertainty in boiling initiation conditions beyond that reported in Table 6.1.

The system pressure during the decompression was calculated using the recorded value of the pressure at the initiation of the event. The error in this measurement, including the ±0.25% accuracy of the pressure gauge, was estimated to be ±3.4 kPa. In addition, the pressure transducer had a linearity of ±1.0% (based on the manufacturer's performance data), and the dual mode amplifier had a range accuracy of ±1%. The combination of these sources of error led to an uncertainty in the pressure measurement of approximately ±8-9 kPa, dependent upon the magnitude of the pressure drop recorded. This error also adds to the uncertainty in boiling conditions beyond that reported in Table 6.1.

6.5 Conclusions

Although this study did not allow a quantitative comparison of results to prediction based on Fabic's theory, the results did show a clear effect of the pressure-temperature history on the initiation of boiling during pressure transients. Increasing the initial pressure tended to delay the inception of boiling, showing that lower pressures and higher superheats were necessary to initiate boiling. Since smaller cavities require greater superheat to nucleate, this is consistent with predictions that the size of the largest potential nucleation site becomes progressively smaller as greater overpressures are applied. That boiling occurred in cases where none was predicted indicates that a simple time-independent theory using constant contact angles is inadequate.

7. SUGGESTIONS FOR FURTHER STUDY

A more comprehensive study of the pressure and temperature effects on boiling initiation during pressure transients needs to be performed, with a wide range of conditions and different heater geometries. Certain changes are recommended to improve the validity and efficiency of such a study.

The test heater power supply should be upgraded with additional deep-cycle storage batteries. This would improve stability and allow application of greater power levels. More stable power supplies to provide biasing voltages are also necessary to enhance the resolution of the small voltage variations associated with this study.

An electro-acoustical device should be used in an independent method for detecting the onset of nucleate boiling. The visual technique employed in this study was hampered by a limited field of vision and reaction times. Visual detection also becomes increasingly unreliable as pressure reduction periods decrease.

A much more sensitive pressure transducer should be installed. This would greatly improve the response of the pressure measurement system and minimize amplifier drift problems.

A four-channel recording digital oscilloscope and a captive computer system are also recommended. With a four-channel oscilloscope, all pertinent data for each experimental run could be recorded, and the reproducibility of the pressure transient would not be a major concern. A captive computer system would greatly improve the efficiency of the study, allowing each test to be analyzed during preparation for a subsequent experiment. Additionally, near immediate feedback of the effects of changes in test conditions would be available.

Finally, a study of decompression with heater temperature held constant needs to be performed, as well as an investigation of the effect of temperature on advancing and receding contact angles. These two subjects need to be addressed in order to develop a general model for boiling behavior during transient condition.

8. REFERENCES

1. Fabic, S., "Vapor nucleation on surfaces subjected to transient heating," Ph.D. Dissertation, Nuclear Engineering Department, University of California, Berkeley, 1964.

2. Winterton, R. H. S., "Nucleation of boiling and cavitation," J. Phys. D.: Appl Phys., 10, 2041-2056 (1977).

3. Weisman, J., G. Bussell, and T. Hsieh, "The initiation of boiling during pressure transients," J. Heat Transfer, Nov. 1974, pp. 535-555.

4. Gallagher, J. P. and R. H. S. Winterton, "Effect of pressure on boiling nucleation," J. Phys. D: Appl. Phys., 16 L57-L61 (1983).

5. Sakurai, A., M. Shiotsu, and K. Hata, "Transient boiling caused by rapid depressurization from initial nonboiling state," 2d Multi-Phase Flow and Heat Transfer Symposium-Workshop, Miami Beach, Florida, 16-18 April 1979.

6. Churchill, S. W. and H. H. Chu, "Correlating equations for laminar and turbulent free convection from a horizontal cylinder," Int. J. Heat Mass Transfer, 18, 1049-1053 (1975).

7. Morgan, Vincent T., "The overall convective heat transfer from smooth circular cylinders," in Advances in Heat Transfer, Vol. 11,T. F. Irvine, Jr., & J. P. Hartnett (eds.), Academic Press, New York, 1975.

8. Fujii, T., M. Fujii, and T. Honda, "Theoretical and experimental studies of the free convection around a long horizontal thin wire in air," Heat Transfer 1982, Vol II, Seventh International Heat Transfer Conference, Munich, 1982, Paper NC32, pp. 311-316.

9. Griffith, Peter, and John D. Wallis, "The role of surface conditions in nucleate boiling," Chemical Engineering Progress Symposium Series, vol. 55, No. 30, 49-63 (1960).

10. Hsu, Y. Y., "On the size range of active nucleation cavities on a heating surface," J. Heat Trans., 84, 207-216 (1962).

11. Bergles, A. E., and W. M. Rohsenow, "The determination of forced-convection surface boiling heat transfer," J. Heat Transfer, 86, 365-372 (1964).

12. Han, C-Y, and Peter Griffith, "The mechanism of heat transfer in nucleate pool boiling - Part I, bubble initiation, growth, and departure," Int. J. Heat Mass Transfer, 8, 887-904 (1965).

13. Madejski, J., "Activation of nucleation cavities on a heating surface with temperature gradient in a superheated liquid," Int. J. Heat Mass Transfer, 9, 295-300 (1966).

14. Schmidt, R. J., and R. Cole, "Comments on activation of nucleation cavities on a heating surface with temperature gradient in a superheated liquid," Int. J. Heat Mass Transfer, 13, 443-445 (1970).

15. Schultz, R. R., S. Kasturirangan, and R. Cole, "Experimental studies of incipient vapor nucleation," Can. J. Chem. Eng., 53, 408-413 (1975).

16. Schultz, R. R., and Robert Cole, "Initial bubble growth in slightly subcooled transient boiling," AIChE Symposium Series, Heat Transfer - Orlando 1980, vol. 76, Paper 199, pp. 310-317.

17. Sakurai, A, and M. Shiotsu, "Transient pool boiling heat transfer. Part 1: Incipient boiling superheat," J. Heat Transfer, 99, 547-553 (1977).

18. Cole, Robert, "Nucleate boiling heat transfer, a general survey," in Boiling Phenomena, Vol I, S. van Stralen and R. Cole (eds.), Hemisphere, New York, 1979, pp. 155-193.

19. Tolubinskiy, V. I., A. M. Kichigin, and S. G. Povsten, "Generalized equation for critical heat fluxes in free-convection boiling of liquids," Heat Transfer - Soviet Research, 8, No. 3, 23-31 (1976).

20. Tolubinski, V. I., Y. N. Ostrovskiy, and V. Y. Pisarev, "Transient heat transfer with phase transitions," Heat Transfer - Soviet Research, 11, No. 1, 18-23 (1979).

21. Johnson, H. A., "Transient boiling heat transfer to water," Int. J. Heat Mass Trans., 14, 67-82 (1971).

22. Faw, R. E. and R. J. VanVleet, "Initiation of subcooled pool boiling during pressure and power transients," Report 161, Kansas Engineering Experiment Station, Manhattan, Kansas, 1984.

23. Howell, John R. and Kenneth J. Bell, "An experimental investigation of the effect of pressure transients on pool boiling burnout," Heat Transfer - Houston, Chem. Eng. Progr., Symp. Ser., 59, 88-95.

24. Aoki, S., A. Inoue, and Y. Kozawa, "Transient boiling crisis during rapid depressurization," Proc. 5th International Heat Transfer Conference, 1974, Paper B6.3.

25. Kung, S., "Boiling heat transfer and bubble growth dynamics during radid decompression," Ph.D. Dissertation, Nuclear Engineering Department, Kansas State University, Manhattan, Kanas, 1980.

26. Hooper, F. C. and A. H. Abdelmessih, "The flashing of liquids at higher superheats," Heat Transfer 1966, Proc. 3rd Int. Heat Transfer Conf., Chicago, 1966, Vol. 4, pp. 44-50.

27. Kenning, D. B. R. and K. Thirunavukkarasu, "Bubble nucleation following a sudden pressure reduction in water," Heat Transfer 1970, Proc. 4th Int. Heat Transfer Conf., Paris-Versailles, 1970, Vol. V, Paper B2.9.

28. Lienhard, J. H., Md. Alamgir, and M. Trela, "Early response of hot water to sudden release from high pressure," J. Heat Transfer, Trans. ASME, 100, 473-479 (1978).

29. Alamgir, Md., C. Y. Kan, and J. H. Leinhard, "An experimental study of the rapid depressurization of hot water," J. Heat Transfer 102, 433-438 (1980).

30. Rohsenow, W. M., "A method of correlating heat-transfer data for surface boiling," ASME Trans., 74, 969-976 (1952).

31. Stephan, K., and M. Abdelsalam, "Heat-transfer correlations for natural convection boiling," Int. J. Heat Mass Transfer, 23, 73-87 (1980).

32. Vines, R. F., The platinum metals and their alloys, International Nickel Co., New York, 1941.

33. Mesler, Russel, "Bubble nucleation," in Encyclopedia of Fluid Mechanics, N. P. Cheremisinoff (ed.), Gulf Publishing (in press).

34. Mesler, Russell and Gregory Mailen, "Nucleate boiling in thin films," AIChE Jurnal, 23, 954-957 (1977).

35. Bergman, Theodore, and Russell Mesler, "Bubble nucleation studies, Part I: Formation of bubble nuclei in superheated water by bursting bubbles," AIChE Journal, 27, 851-853 (1981).

36. Carroll, Kenneth, and Russell Mesler, "Splashing liquid drops form vortex rings and not jets at low Froude numbers," J. Appl. Phys., 52(1), 507 (1981).

APPENDIX A

Program BOIL: Temperature Data Analysis

This program was written in Hewlett-Packard BASIC, Version 2.0, and run on the HP 9816 microcomputer. The program was originally written for analysis of power transient data from a concurrent study (22), and this capability is retained in the current version. In fact, the program parameters default to the power transient values, and changes in these values arising from choosing the pressure transient option are contained in the voltage input data set.

The voltage data for an experimental run are measured by a Nicolet Explorer III digital oscilloscope. The voltage input is converted to a corresponding channel number and stored. The channel number is obtained by dividing the sampled voltage by the conversion factor

$$V_{norm} = \{\text{Voltage Range}\}/2000 \qquad \text{Volts/channel.}$$

There are 4096 voltage channels (-2048 to +2047), which allows a full scale voltage interval greater than -VR to +VR, where VR is the oscilloscope voltage range setting. There are also 4096 memory addresses available. Channel numbers are stored sequentially at a time interval determined by the Time Per Point switch. If both input channels A and B are active, the signals are stored in the sequence ABABAB, and the time interval defines the time between each sampling of the pair AB. Thus, the channel number defines the voltage and the memory address defines the time at which the voltage was sampled.

Voltage data is originally input to the program from the oscilloscope. The data is also saved on a disk for reference. The information required from each run depends on the case considered, i.e.,

transient power or transient pressure. The former is always performed in Normal Trigger mode on the oscilloscope, so the first datum is at time zero, while the latter is always performed in the Cursor Trigger mode. In this configuration the first datum time and the event initiation time must be recorded, as well as certain equipment settings. These values are stored as the first nine points in the data file when it is saved on the disk.

The program separates the raw voltage data into the two input signals, converts the data to true voltages, and then averages the data. The voltage is found from the expression

$$V = \{\text{Channel number}\} \frac{V_{norm}}{Amp} - Vcz + V_o,$$

where Amp is the signal amplification, Vcz is the zero input voltage level for the oscilloscope, and V_o is the biasing voltage. The biasing voltage is subtracted from the signal before it is amplified and sent to the oscilloscope to permit greater precision in the measurement of the small voltage changes associated with this case. The voltages are smoothed over n points, and the averaged voltage is assigned the averaged time value. Smoothing intervals are exclusive, i.e., no datum is used more than once in the averaging process.

Program output is available in an ASCII file for hardcopy printout or in binary data files for plotting the results.

```
!############################## BOIL ################################
!##                                                                ##
!##  PROGRAN CONVERTS VOLTAGE OATA NEASUREO ACROSS A PLATINUN WIRE ##
!##  ANO A STANOARO RESISTOR TO A TEMPERATURE HISTORY OF THE WIRE. ##
!##  VOLTAGE OATA IS ORIGINALLY INPUT FROM THE NICOLET OIGITAL     ##
!##  OSCILLOSCOPE, BUT THESE OATA ARE ALSO STOREO ON A OISC FOR    ##
!##  FUTURE REFERENCE.  FRON THE TENPERATURE OATA THE WIRE         ##
!##  SUPERHEAT, THE SUPERFICIAL HEAT FLUX ANO THE NOOIFIEO         ##
!##  NUSSELT NUNBER HISTORIES ARE OETERNINEO.                      ##
!##                                                                ##
!##  PROGRAN WILL ANALYZE FOR TWO CASES: a) POWER TRANSIENTS AT    ##
!##  CONSTANT PRESSURE, and b) PRESSURE TRANSIENTS AT CONSTANT     ##
!##  POWER.  THE OISTINCTION IS: a) NORNAL TRIGGER OF O-SCOPE,     ##
!##  and b) CURSOR TRIGGER OF O-SCOPE.                             ##
!##                                                                ##
!##                                                                ##
!##  R.VANVLEET                                  KSU   NOV 1983    ##
!##                                                                ##
!##  revised for Case b and improved efficiency by                 ##
!##                                                                ##
!##  O.SCHNIOT                                   KSU   SEP 1984    ##
!##                                                                ##
!##  update: "quick & dirty" plot  (O.SCHNIOT)   KSU   JAN 1985    ##
!################################################################################
!
OPTION BASE 1
COM /Array/ Raw(4096),A(512),B(512),E(512),Z(512,4)
COM /Const/ Alph,Beta,Qbeg,Xcnd
COM /Datum/ Di,Len,Ra,Rs,Ta,Tau,T0,Va0,Vb0,VczI,Vcz2,Vnorm,P$[35]
COM /Stat/ Amp,Node,Nav,Nblock,Sigma
OIN TitIe$[80]
!
PRINT CHR$(12)
INPUT "RESET GRAPHICS (Y/N) ?",Reset$
INPUT "WHAT IS THE RUN NUMBER, e.g., RUN ?.???",TitIe$
TitIe$="RUN NUNBER "&TitIe$
PRINT TitIe$
!
!     NAIN PROGRAN
!
          CALL Param
          CALL Inpt(N$)
Tscale=Tau*2000
          IF Reset$="Y" THEN CALL Graf_set(Tscale)
PRINT TitIe$," "," ","SOURCE OATA FILE: ";N$
PRINT
PRINT "AVERAGING OATA - - -> ";Nav;" POINT AVERAGING"
          CALL Avg
PRINT "CALCULATING INITIAL WIRE RESISTANCE"
          CALL Resis
PRINT "CALCULATING PROPERTIES"
          CALL Props
          CALL Outp(N$,TitIe$)
ENO
!
!
!
SUB Param
  COM /Const/ Alph,Beta,Qbeg,Xcnd
  COM /Datum/ Di,Len,Ra,Rs,Ta,Tau,T0,Va0,Vb0,VczI,Vcz2,Vnorm,P$
  COM /Stat/ Amp,Node,Nav,Nblock,Sigma
!
!   DATA FOR THE WIRE,THE FLUIO, ANO THE SETTINGS ON THE SCOPE
!   OEFAULT FOR CONSTANT PRESSURE RUNS
!
  Rs=.2394+.00203           ! STANOARO RESISTANCE
  Di=2.5E-4                 ! WIRE OIAMETER
  Len=9.6E-2                ! WIRE LENGTH
!
  Alph=.00392
  Beta=-5.5E-7
  Xcnd=.6740                ! NEAN VALUE 70 TO 200 C IS .674 (WATER CONO)
!
```

```
590     Vnorm=.002                  ! 4V RANGE ON O-SCOPE
600     VczI=-4.                    ' ZERO INPUT VOLTAGE LEVEL
610     Vcz2=4.
620     Va0=0.                      ' BUCKING VOLTAGE
630     Vb0=0.
640   !
650     Qbeg=0.
660     Mode=I
670     Amp=1.
680     Nav=I6
690   SUBEND
700   !
710   !
720   !
730   SUB Inpt(N$)
740     OPTION BASE I
750     COM /Array/ Raw(4096),A(5I2),B(5I2),E(5I2),I(5I2,4)
760     COM /Const/ AIph,Beta,Qbeg,Xcnd
770     COM /Datum/ Di,Len,Ra,Rs,Ta,Tau,T0,Va0,Vb0,Vcz1,Vcz2,Vnorm,P$
780     COM /Stat/ Amp,Mode,Nav,NbIock,Sigma
790     DIM Raw$(4096)[5]
800   !
810     INPUT "DATA SOURCE - - - SCOPE = I, DAT FILE = 2",Tt
820     IF Tt=I THEN
830       PRINT
840       PRINT "TRIGGER MODE - - - NORMAL = 1, CURSOR = 2"
850       INPUT "(NORMAL if constant pressure run)        ",Mode
860     END IF
870             CALL Reader(Tt,N$,Raw$(*))
880     IF Raw$(I)="CURSR" THEN Mode=2
890     IF Mode<>2 THEN Raw(I)=VAL(Raw$(I))
900     FOR I=2 TO 4096
910       Raw(I)=VAL(Raw$(I))
920     NEXT I
930     IF Mode=1 THEN I040
940       Vnorm=Raw(2)
950       Ch0=Raw(3)
960       Tau=Raw(4)
970       VczI=Raw(5)/1000
980       Vcz2=Raw(6)/1000
990       Amp=Raw(7)
I000      Va0=Raw(8)
I0I0      Vb0=-Raw(9)
I020      Reserv=16
1030      P$=""
1040    BEEP 2I97.26,.3
1050    INPUT "ENTER AMBIENT TEMPERATURE (C)",Ta
1060    INPUT "ENTER INITIAL WIRE TEMPERATURE (C)",T0
I070    IF Mode=2 THEN GOTO III0
I080      INPUT "ENTER AMBIENT PRESSURE, e.g. 101.4,475.8,I397.8 (kPa)",P$
I090      INPUT "ENTER INITIAL HEAT FLUX ON THE WIRE (W/m^2)",Qbeg
1100      INPUT "ENTER SAMPLING TIME INCREMENT, E.G. IE-2 FOR 20 SEC RUN",Tau
1I10    INPUT "ENTER [4,8,I6] POINT RUNNING AVERAGE (DEFAULT = I6)",Nav
1I20    IF Mode=I THEN I250
1I30      INPUT "ENTER MAXIMUM PRESSURE",Pmax
I140      INPUT "ENTER STARTING PRESSURE FOR DECOMPRESSION",Pstart
I150      INPUT "UNITS ON VALUES JUST ENTERED - - - K = kPa, P = psig",Unit$
1160      IF Unit$="K" THEN I210
1170        Conv=((Pmax/14.696)+1)*10I.325
I180        Pmax=DROUND(Conv,5)
I190        Conv=((Pstart/I4.696)+1)*I0I.325
1200        Pstart=DROUND(Conv,5)
I2I0      IF Pstart<>Pmax THEN P$="Max "&VAL$(Pmax)&", "
1220      P$=P$&"Decompress from "&VAL$(Pstart)
I230      Neg=INT((Ch0-1-Reserv)/Nav/2)     ! ALLOWS CALCULATIONS FOR TIME<0
I240      Raw(I0)=Ch0-Nav*Neg*2             ! START CHANNEL
1250    Nch=(4096-(Raw(10)-1))/2
1260    NbIock=INT(Nch/Nav)
I270    PRINT CHR$(12)
I280    PRINT Raw$(1),Raw(2),Raw(3),Raw(4),Raw(5),Raw(6),Raw(7),Raw(8)
I290    PRINT
I300  SUBEND
```

```
1310 !
1320 !
1330 !
1340       SUB Reader(Tt,Name$,Raw$(*))
1350         OPTION BASE 1
1360         COM /Stat/ Amp,Mode,Nav,Nblock,Sigma
1370 !
1380         PRINT
1390         PRINT "PLEASE INSERT DATA DISC INTO DISC DRIVE 0"
1400         INPUT "PLEASE ENTER A UNIQUE NAME FOR THE BOAT FILE.",Name$
1410         DISP "WORKING, PLEASE WAIT."
1420         MASS STORAGE IS ":HP82901,700,0"
1430         IF Tt=2 THEN 1650
1440 !
1450         ASSIGN @Scope TO 9
1460         CONTROL 9,3;9600
1470         ASSIGN @Scope;FORMAT ON
1480         CONTROL 9,5;3
1490         CONTROL 9,4;2
1500         OUTPUT @Scope;CHR$(1);
1510        OUTPUT @Scope;CHR$(69);CHR$(48);CHR$(68);CHR$(49);CHR$(68);CHR$(48);
1520         OUTPUT @Scope;CHR$(79);CHR$(52);CHR$(48);CHR$(57);CHR$(54)
1530         OUTPUT @Scope;CHR$(2);
1540         ENTER @Scope USING "5A,X,X";Raw$(*)
1550         CONTROL 9,5;0
1560         ASSIGN @Scope TO *
1570              IF Mode=2 THEN CALL Scope_set(Raw$(*))
1580         DISP "WORKING, PLEASE WAIT."
1590         CREATE BOAT Name$,4096,5
1600         ASSIGN @Path TO Name$
1610         OUTPUT @Path USING "5A";Raw$(*)
1620         ASSIGN @Path TO *
1630       SUBEXIT
1640 !
1650         ASSIGN @Path TO Name$
1660         ENTER @Path USING "5A";Raw$(*)
1670         ASSIGN @Path TO *
1680       SUBEND
1690 !
1700 !
1710 !
1720       SUB Scope_set(Raw$(*))
1730         OPTION BASE 1
1740         BEEP 1627.60,.3
1750         INPUT "ENTER TIME FOR FIRST DATA POINT (sec)",Ch1t0
1760         INPUT "ENTER TIME OF EVENT INITIATION  (sec)",Event0
1770         INPUT "ENTER TIME INCREMENT, e.g. 1E-2 FOR A 20 s RUN ",Tau
1780         INPUT "ENTER VOLTAGE RANGE (V)",Range
1790         INPUT "ENTER DC LEVEL ZERO FOR CHANNEL A (V)",Dca
1800         INPUT "ENTER DC LEVEL ZERO FOR CHANNEL B (V)",Dcb
1810         INPUT "ENTER BUCKING VOLTAGE FOR CHANNEL A (V)",Va0
1820         INPUT "ENTER BUCKING VOLTAGE FOR CHANNEL B (V)",Vb0
1830         INPUT "ENTER SIGNAL AMPLIFICATION OF ANALOG COMPUTER",Amp
1840 !
1850         Raw$(1)="CURSR"
1860         Raw$(2)=VAL$(Range/2000)      ! Vnorm
1870         Ch0=(ABS(Ch1t0)-ABS(Event0))*2/Tau+1
1880         Raw$(3)=VAL$(Ch0)
1890         Raw$(4)=VAL$(Tau)
1900         Raw$(5)=VAL$(Dca*1000)        ! Vcz1
1910         Raw$(6)=VAL$(Dcb*1000)        ! Vcz2
1920         Raw$(7)=VAL$(Amp)
1930         Raw$(8)=VAL$(Va0)
1940         Raw$(9)=VAL$(ABS(Vb0))
1950       SUBEND
1960 !
1970 !
1980 !
```

```
1990  SUB Avg
2000    OPTION BASE 1
2010    COM /Array/ Raw(4096),A(512),B(512),E(512),Z(512,4)
2020    COM /Datum/ D1,Len,Ra,Rs,Ta,Tau,T0,Va0,Vb0,Vcz1,Vcz2,Vnorm,P$
2030    COM /Stat/ Amp,Mode,Nav,Nblock,Sigma
2040  !
2050  !   THIS SUBROUTINE SEPARATES THE DATA FOR THE STANDARD RESISTOR
2060  !   PLUS THE WIRE (A(1)) AND THE WIRE (B(1)) AND CALCULATES
2070  !   THEIR RUNNING AVERAGES
2080  !
2090    IF Mode=2 THEN Chstart=Raw(10)-1
2100    Jstart=Chstart+1
2110    FOR I=1 TO Nblock
2120      Sumx=0
2130      Sumy=0
2140      Jend=Jstart+2*Nav-1
2150      FOR J=Jstart TO Jend-1 STEP 2
2160        Sumx=Sumx+Raw(J)*Vnorm/Amp        ! CONVERT TO TRUE VOLTAGE
2170        Sumy=Sumy+Raw(J+1)*Vnorm/Amp      ! AND AVERAGE
2180      NEXT J
2190      A(I)=Sumx/Nav-Vcz1/Amp+Va0          ! SUBTRACT ZERO LEVEL AND
2200      B(I)=Sumy/Nav-Vcz2/Amp+Vb0          ! ADD BUCKING VOLTAGES
2210      Jstart=Jend+1
2220    NEXT I
2230  SUBEND
2240  !
2250  !
2260  !
2270  SUB Resis
2280    OPTION BASE 1
2290    COM /Array/ Raw(4096),A(512),B(512),E(512),Z(512,4)
2300    COM /Datum/ D1,Len,Ra,Rs,Ta,Tau,T0,Va0,Vb0,Vcz1,Vcz2,Vnorm,P$
2310    COM /Stat/ Amp,Mode,Nav,Nblock,Sigma
2320  !
2330  !   THIS SUBROUTINE CALCULATES THE INITIAL RESISTANCE OF THE WIRE
2340  !
2350    IF Mode<>2 THEN GOTO 2380
2360    Ra=-Vb0/Va0*Rs-.00277          ! FOR INITIAL FLUX ON WIRE
2370  SUBEXIT
2380  !
2390    Sumx=0                         !  NO INITIAL FLUX, USE LEAST SQUARES FIT
2400    Sumx2=0
2410    Sumy=0
2420    Sumy2=0
2430    Sumxy=0
2440    Zz=10
2450    FOR I=3 TO 12
2460      J1=(I-.5)*Nav                ! TIME
2470      R=-B(I)*Rs/A(I)-.00277
2480      Time=J1^1.25                 ! EMPIRICAL ADJUSTMENT FOR BETTER FIT
2490      Sumx=Sumx+Time
2500      Sumx2=Sumx2+Time^2
2510      Sumy=Sumy+R
2520      Sumy2=Sumy2+R^2
2530      Sumxy=Sumxy+Time*R
2540    NEXT I
2550    Beta1=(Sumxy-(Sumx*Sumy)/Zz)/(Sumx2-(Sumx^2)/Zz)
2560    Beta0=(Sumy/Zz)-Beta1*(Sumx/Zz)
2570    S=Sumy2-(Sumy^2)/Zz
2580    T=Sumx2-(Sumx^2)/Zz
2590    U=1./(Zz-2.)
2600    V=Beta1^2
2610    W=U*(S-V*T)                    ! VARIANCE ABOUT REGRESSION
2620    Sigma=SQR(W*Sumx2/Zz/T)        ! EST OF STD DEV OF INTERCEPT
2630    Ra=Beta0
2640  !
2650    BEEP 2197.26,.3
2660    PRINT " ","RA = ";Ra;" AT ";T0;" C"
2670    New=Ra
2680    INPUT "Enter new value for RA or accept default",New
2690    IF New=Ra THEN 2720
2700      PRINT "*** NEW VALUE ***","RA = ";New;"AT ";T0;" C"
2710      Ra=New
2720  SUBEND
```

```
2730  !
2740  !
2750  !
2760  SUB Props
2770    OPTION BASE 1
2780    COM /Array/ Raw(4096),A(512),B(512),E(512),Z(512,4)
2790    COM /Const/ Alph,Beta,Qbeg,Xcnd
2800    COM /Datum/ O1,Len,Ra,Rs,Ta,Tau,T0,Va0,Vb0,Vcz1,Vcz2,Vnorm,P$
2810    COM /Stat/ Amp,Mode,Nav,Nblock,Sigma
2820  !
2830  !   THIS SUBROUTINE CALCULATES THE PROPERTIES OF THE WIRE:
2840  !
2850  !     Z(J,1) = TIME
2860  !     Z(J,2) = SUPERFICIAL HEAT FLUX
2870  !     Z(J,3) = THETA  [ T(wire) - T(ambient) ]
2880  !     Z(J,4) = MODIFIED NUSSELT NUMBER
2890  !
2900    Const=Ra/(1.+Alph*T0+Beta*T0^2)    !  R(wire) AT T=0 C
2910    IF Mode=1 THEN 2990
2920      Neg=INT((Raw(3)-Raw(10))/Nav/2)
2930      PRINT " ","WIRE PROPERTY :","R(wire) [ AT T=0 C ] = ";Const
2940      New=Const
2950      INPUT "Enter new value for R(wire) or accept default",New
2960      IF New=Const THEN 2990
2970        PRINT "*** NEW VALUE ***","R(wire) [ AT T=0 C ] = ";New
2980        Const=New
2990    Bb=Alph/Beta
3000    Ba=-.5*Bb
3010    B2=Bb^2
3020    FOR I=1 TO Nblock
3030      Z(1,1)=Tau*Nav*(I-Neg-.5)
3040      Z(1,2)=A(1)*A(1)*(-B(I)/A(1)-.00277/Rs)/(Rs*3.14159*O1*Len)-Qbeg
3050        R=(-B(I))*Rs/A(I)-.00277
3060        F=B2+(4./Beta)*(R/Const-1.)
3070      Z(I,3)=Ba-.5*SQR(F)-Ta
3080      Z(I,4)=Z(1,2)*O1/(Xcnd*Z(I,3))
3090  !
3100      Er1=(Vnorm^2)/(A(1)^2)
3110      Er2=(Vnorm^2)/(B(1)^2)
3120      Er3=(Sigma^2)/(Ra^2)
3130      E(I)=(Er1+Er2+Er3)/((1-(Ra/R))^2)
3140    NEXT I
3150  SUBEND
3160  !
3170  !
3180  !
3190  SUB Outp(N$,Title$)
3200    OPTION BASE 1
3210    COM /Array/ Raw(4096),A(512),B(512),E(512),Z(512,4)
3220    COM /Datum/ O1,Len,Ra,Rs,Ta,Tau,T0,Va0,Vb0,Vcz1,Vcz2,Vnorm,P$
3230    COM /Stat/ Amp,Mode,Nav,Nblock,Sigma
3240    OIN Add$[16],He1$[80],He2$[80],He3$[80],Inb$[7],Pre$[18],PI$[80],R1$[80]
3250    OIN St$[80],S1$[80],T1$[80],W1$[80],N2$[80],Out$(3)[80],Z$(4)[10]
3260  !
3270    Npg=INT(Nblock/47)        ! INFORMATION ABOUT FILE SIZE
3280    Nx=Nblock-Npg*47
3290    IF Nx>42 THEN Nblock=Nblock-(Nx-42)
3300    IF Nx=0 THEN Npg=Npg-1
3310    Npg=Npg+1
3320    Size=19*Npg
3330    ALLOCATE G(Nblock,2)      !  "QUICK & DIRTY" PLOT
3340    Abs=3
3350    Ord=2                     !   - HEAT FLUX v THETA   if  PRESSURE = const
3360    IF Mode=2 THEN Abs=1      !   - THETA v TIME        if HEAT FLUX = const
3370    IF Mode=2 THEN Ord=3
3380    FOR I=1 TO Nblock
3390      G(1,1)=Z(1,Abs)
3400      G(I,2)=Z(1,Ord)
3410    NEXT I
3420  !
3430    BEEP 1627.60,.3
3440    PRINT CHR$(12)
3450    CALL Scr_plot(G(*))
3460    DEALLOCATE G(*)
```

```
3470  !
3480    INPUT "Do you wish to have a HARD COPY of the numbers ? ( Y/N ).",Ans$
3490    IF Ans$<>"Y" THEN 4060
3500    PRINT Title$," "," ","SOURCE DATA FILE: ";N$
3510    PRINT
3520    PRINT "####      PLEASE INSERT A DISC INTO DISC DRIVE 1"
3530    PRINT
3540    PRINT "AN ASCII FILE WILL BE CREATED ON THE DISC. THIS FILE CAN THEN"
3550    PRINT "BE TRANSFERED TO THE MAIN COMPUTER FOR PRINT OUT."
3560    INPUT "PLEASE ENTER A UNIQUE NAME FOR THE ASCII FILE.",As$
3570    Pre$="                  "
3580    Add$="                "
3590    Inb$="       "
3600    St$="               ##################################################"
3610    Hel$="                  TIME      HEAT FLUX     THETA        NUSSELT"
3620    He2$="                   (s)       (W/m^2)       (C)         NUMBER"
3630    He3$="                                PAGE "
3640    Ra$=VAL$(Ra)
3650    Ra$=Ra$[1,7]
3660    P1$=Add$&"PRESSURE       = "&P$&" kPa"
3670    R1$=Add$&"INITIAL RESIS. = "&Ra$&"  OHMS AT  "&VAL$(T0)&" C"
3680    Sigma$=VAL$(Sigma)
3690    Sigma$=Sigma$[1,7]
3700    S1$=Add$&"SIGMA          = "&Sigma$
3710    T1$=Add$&"AMBIENT TEMP.  = "&VAL$(Ta)&" C"
3720    W1$=Add$&"WIRE LENGTH    = "&VAL$(Len)&" M"
3730    W2$=Add$&"WIRE DIAMETER  = "&VAL$(D1)&" M"
3740    Npg=1
3750    Lin=1
3760    MASS STORAGE IS ":HP82901,700,1"
3770    CREATE ASCII As$,Size
3780    ASSIGN @Path TO As$
3790    OUTPUT @Path;Add$&Title$,Inb$,W1$,W2$
3800    OUTPUT @Path;T1$,P1$,R1$
3810    OUTPUT @Path;S1$,Inb$,St$,Inb$,Hel$
3820    OUTPUT @Path;He2$,Inb$,St$,Inb$
3830    FOR I=1 TO Nblock STEP 3
3840              CALL Dec(I,Z$(*))
3850      Out$(1)=Pre$&Z$(1)&Inb$&Z$(2)&Inb$&Z$(3)&Inb$&Z$(4)
3860        IF I+1<=Nblock THEN CALL Dec(I+1,Z$(*))
3870      Out$(2)=Pre$&Z$(1)&Inb$&Z$(2)&Inb$&Z$(3)&Inb$&Z$(4)
3880        IF I+2<=Nblock THEN CALL Dec(I+2,Z$(*))
3890      Out$(3)=Pre$&Z$(1)&Inb$&Z$(2)&Inb$&Z$(3)&Inb$&Z$(4)
3900      IF (I+1)>Nblock THEN Out$(2)=Add$
3910      IF (I+2)>Nblock THEN Out$(3)=Add$
3920      OUTPUT @Path;Out$(1),Out$(2),Out$(3)
3930      Lin=Lin+1
3940      IF Npg=1 AND Lin=15 THEN GOTO 3960
3950      IF Lin=17 THEN
3960        OUTPUT @Path;Inb$,Inb$,Inb$,Inb$,Inb$,Inb$,Inb$,Inb$
3970        T1$=Add$&Title$&He3$&VAL$(Npg+1)
3980        OUTPUT @Path;T1$,Inb$,St$,Inb$
3990        OUTPUT @Path;Hel$,He2$,Inb$,St$,Inb$,Inb$
4000        Lin=1
4010        Npg=Npg+1
4020      END IF
4030    NEXT I
4040    MASS STORAGE IS ":HP82901,700,0"
4050    BEEP 1302.08,.3
4060  !
4070    INPUT "Do you wish to have a PLOT of the numbers (Y/N) ?",Ans$
4080    IF Ans$<>"Y" THEN 4610
4090    PRINT CHR$(12)
4100    PRINT Title$," "," ","SOURCE DATA FILE: ";N$
4110    PRINT
4120    PRINT "####      PLEASE INSERT A DISC INTO DISC DRIVE 1"
4130    PRINT
4140    PRINT "BOAT FILES WILL BE CREATED ON THE DISC. THESE FILES CAN THEN"
4150    PRINT "BE PLOTTED USING THE GENERAL PLOTTING PROGRAM"
4160    PRINT
```

```
4170    PRINT "THE TYPE OF PLOTS POSSIBLE ARE:"
4180    PRINT
4190    PRINT "          1 = NUSSELT NUMBER vs TIME"
4200    PRINT "          2 = HEAT FLUX vs THETA"
4210    PRINT "          3 = BOTH PLOTS 1 AND 2   (plot 1 recorded first)"
4220    PRINT "          4 = HEAT FLUX vs TIME"
4230    PRINT "          5 = THETA vs TIME"
4240    PRINT "          6 = BOTH PLOTS 4 AND 5   (plot 4 recorded first)"
4250    INPUT "CHOOSE THE TYPE OF PLOT YOU WISH.",Qq
4260        IF Mode=1 THEN CALL Mani
4270    Format$="MZ.DDDE,$"
4280    ALLOCATE G(Nblock,2)
4290    MASS STORAGE IS ":HPB2901,700,1"
4300    IF Qq=1 OR Qq=3 THEN 4340
4310    IF Qq=2 THEN 4370
4320    IF Qq=4 OR Qq=6 THEN 4400
4330    IF Qq=5 THEN 4430
4340      Abs=1
4350      Ord=4
4360    GOTO 4460
4370      Abs=3
4380      Ord=2
4390    GOTO 4460
4400      Abs=1
4410      Ord=2
4420    GOTO 4460
4430      Abs=1
4440      Ord=3
4450  !
4460    INPUT "PLEASE ENTER A UNIQUE NAME FOR THE BOAT FILE.",Bd$
4470    FOR D=1 TO Nblock
4480      G(D,1)=Z(D,Abs)
4490      G(D,2)=Z(D,Ord)
4500    NEXT D
4510    CREATE BOAT Bd$,(2*Nblock),9
4520    ASSIGN @Path TO Bd$
4530    OUTPUT @Path USING Format$;G(*)
4540    ASSIGN @Path TO *
4550    PRINT
4560    PRINT "BOAT file: ";Bd$,Nblock;" points","Data format: MZ.DDDE"
4570    IF Qq=3 THEN 4370
4580    IF Qq=6 THEN 4430
4590    DEALLOCATE G(*)
4600    MASS STORAGE IS ":HPB2901,700,0"
4610    BEEP 5126.94,.1
4620    PRINT "      END"
4630  SUBEND
4640  !
4650  !
4660  !
4670      SUB Dec(I,Z$(*))
4680        OPTION BASE 1
4690        COM /Array/ Raw(4096),A(512),B(512),E(512),Z(512,4)
4700  !
4710  !       THIS SUBROUTINE ENSURES THAT ALL VALUES HAVE THE
4720  !       CORRECT FIELD LENGTH FOR OUTPUT
4730  !
4740        Long=5
4750        Dec$="D"
4760        Per$="."
4770        FOR J=1 TO 4
4780          Zz=Z(I,J)
4790          IF Zz<0 THEN Zz$=VAL$(DROUND(FNRound(Zz,3),5))
4800          IF Zz<0 THEN 4880
4810          Zz$=VAL$(DROUND(Zz,5))
4820          IF Zz<1 THEN 4930
4830          GOTO 4980
4840          Z$(J)=Zz$
4850          Long=6
4860        NEXT J
4870        GOTO 5070
```

```
4880 !                    FOR ZZ<0
4890         IF LEN(Zz$)>Long THEN Zz$=Zz$[1,Long]
4900         IF LEN(Zz$)<Long THEN Zz$=Zz$&Dec$
4910         IF LEN(Zz$)<>Long THEN 4900
4920       GOTO 4840
4930 !                    FOR 0<ZZ<1
4940         IF LEN(Zz$)>Long THEN Zz$=Zz$[1,Long-1]
4950         IF LEN(Zz$)<Long THEN Zz$=Dec$&Zz$
4960         IF LEN(Zz$)<>Long THEN 5040
4970       GOTO 4840
4980 !                    FOR ZZ>1
4990         P$="N"
5000         FOR F=LEN(Zz$) TO 1 STEP -1
5010           IF Zz$[F,F]="." THEN P$="Y"
5020         NEXT F
5030         IF P$="N" AND LEN(Zz$)<Long THEN Zz$=Zz$&Per$
5040         IF Zz<1.E+5 AND LEN(Zz$)<Long THEN Zz$=Zz$&Dec$
5050         IF Zz<1.E+5 AND LEN(Zz$)<>Long THEN 5040
5060       GOTO 4840
5070     SUBEND
5080 !
5090 !
5100 !
5110     DEF FNRound(Z,Np)
5120       Nu=INT(Z*10^Np+.5)              ! ROUNDING FOR Z<0
5130       Nu=Nu/(10^Np)
5140       RETURN Nu
5150     FNEND
5160 !
5170 !
5180 !
5190     SUB Nani
5200       OPTION BASE 1
5210       COM /Array/ Raw(4096),A(512),B(512),E(512),Z(512,4)
5220       COM /Stat/ Amp,Node,Nav,Nblock,Sigma
5230 !
5240 !       THIS SUBROUTINE EVALUATES THE ERROR TERM CALCULATED
5250 !       IN SUBROUTINE PROPS IN ORDER TO ELIMINATE THOSE FIRST
5260 !       VALUES THAT HAVE 5% OR MORE ERROR
5270 !
5280       Nt=0
5290       FOR I=1 TO Nblock
5300         Nt=I
5310         IF (E(I)<.05 AND Z(1,3)>0.) THEN GOTO 5330
5320       NEXT I
5330       Nblock=Nblock-Nt
5340       IF Nblock=0 THEN GOTO 5410
5350       FOR J=I TO Nblock
5360         Z(J,1)=Z(J+Nt,1)
5370         Z(J,2)=Z(J+Nt,2)
5380         Z(J,3)=Z(J+Nt,3)
5390         Z(J,4)=Z(J+Nt,4)
5400       NEXT J
5410     SUBEND
5420 !
5430 !
5440 !
5450 SUB Graf_set(Tscale)
5460   COM /Stat/ Amp,Node,Nav,Nblock,Sigma
5470 !
5480   READ X$,Y$,Xx1,Xx2,Yy1,Yy2
5490   IF Node=2 THEN READ X$,Y$,Xx1,Xx2,Yy1,Yy2
5500   IF Mode=2 THEN Xx2=Tscale
5510   GINIT
5520   GRAPHICS OFF
5530   VIEWPORT 0,130,15,100
5540   PEN 1
5550   LDIR PI/2
5560   LORG 6
5570   MOVE 0,57
5580   LABEL Y$
```

```
5590    LDIR 0
5600    LORG 4
5610    MOVE 65,15
5620    LABEL X$
5630    CSIZE 3.7,.5
5640    MOVE 15,I5
5650    LABEL Xx1
5660    MOVE I27,I5
5670    LABEL Xx2
5680    LORG 2
5690    MOVE 0,20
5700    LABEL YyI
5710    MOVE 0,98
5720    LABEL Yy2
5730    IF Mode=2 TNEN 5780
5740      Xx1=LGT(Xx1)
5750      Xx2=LGT(Xx2)
5760      Yy1=LGT(YyI)
5770      Yy2=LGT(Yy2)
5780    VIEWPORT I5,I30,20,100
5790    WINDOW XxI,Xx2,Yy1,Yy2
5800    FRAME
5810    IF Mode=I TNEN 5840
5820    MOVE 0,Yy1
5830    DRAW 0,Yy2
5840  !
5850    DATA "TNETA","NEAT FLUX",I0,100,IE4,1E6
5860    DATA " TIME","  THETA",-2,20,30,70
5870  SUBEND
5880  !
5890  !
5900  !
5910  SUB Scr_plot(G(*))
5920    OPTION BASE 1
5930    COM /Stat/ Amp,Mode,Nav,NbIock,Sigma
5940    Er$="N"
5950    Istart=I
5960    IF Mode=2 THEN 6030
5970      FOR I=I TO NbIock
5980        IF G(I,I)<0 OR G(I,2)<0 TNEN Istart=I+1
5990        IF Istart=I+I TNEN 6020
6000        G(I,1)=LGT(G(I,I))
6010        G(I,2)=LGT(G(I,2))
6020      NEXT I
6030    LINE TYPE I
6040    PEN I
6050    ALPNA OFF
6060    GRAPNICS ON
6070    MOVE G(Istart,1),G(Istart,2)
6080    FOR I=Istart TO Nblock
6090      DRAW G(I,1),G(I,2)
6100    NEXT I
6110    MOVE 0,0
6120    IF Er$="Y" TNEN 6190
6130    IF Mode=I TNEN DISP "       * * *  LOG-LOG SCALING  * * *"
6140    WAIT 5
6150    INPUT "      ERASE TNIS PLOT (Y/N) ?",Er$
6160    IF Er$<>"Y" TNEN 6190
6170    PEN -1
6180    GOTO 6070
6190    GRAPHICS OFF
6200    ALPHA ON
6210  SUBEND
```

APPENDIX B

Program PRESSURE: Pressure Data Analysis

This program was written in Hewlett-Packard BASIC, Version 2.0, and run on the HP 9816 microcomputer. Experimental parameters are included in the voltage input data set, similar to the pressure transient option of program BOIL. Manipulation of data provided by the digital oscilloscope is as described in Appendix A; however, since the entire capacity of the oscilloscope is used to record the pressure signal, separation of data by input channel is not necessary. The program structure is identical to that of BOIL, and the output is arranged such that instantaneous pressures are reported at the same experimental times as the output from BOIL.

```
1     !!!!!!!!!!!!!!!!!!!!!!!!!!  PRESSURE  !!!!!!!!!!!!!!!!!!!!!!!!!!
2     !!                                                                !!
3     !!  PRDGRAN CONVERTS VOLTAGE DATA NEASUREO FRDN A PRESSURE        !!
4     !!  TRANSDUCER (V1A A CHARGE ANPLIFIER) TO A PRESSURE HISTORY     !!
5     !!  OF THE PRESSURE VESSEL.  VOLTAGE DATA 1S DRIGINALLY INPUT     !!
6     !!  FRON THE NICOLET OIGITAL OSCILLOSCDPE, BUT THESE OATA ARE     !!
7     !!  ALSD STDREO ON A DISC FOR FUTURE REFERENCE.                   !!
8     !!  -->NDTE<--    D-SCDPE 1S CURSDR TRIGGERED.                    !!
9     !!                                                                !!
10    !!                                                                !!
11    !!  O.SCHN1OT                                 KSU    SEP I9B4     !!
12    !!                                                                !!
13    !!  update: "quick & dirty" plot  (O.SCHN1OT)  KSU    JAN I9B5     !!
14    !!!!!!!!!!!!!!!!!!!!!!!!!!!!!!!!!!!!!!!!!!!!!!!!!!!!!!!!!!!!!!!!!!
15    !
110   OPTIDN BASE I
120   CDM /Stat/ Ch0,Orift,Nav,NbIock,Pperv,Ta,Tau,Vnorm
130   CDN /Array/ A(I025),Raw(4096)
140   DIN Title$[80]
150   !
160   PRINT CHR$(12)
170   INPUT "RESET GRAPHICS (Y/N) ?",Reset$
180   INPUT "WHAT 1S THE RUN NUNBER ?",TitIe$
190   TitIe$="RUN NUNBER "&Title$
200   PRINT Title$
210   !
220   !     NAIN PROGRAN
230   !
240             CALL Inpt(N$)
250   Tscale=Tau*4000
260             IF Reset$="Y" THEN CALL Graf_set(Raw(6),Tscale)
270   PRINT Title$," "," "," SDURCE DATA FILE: ";N$
2B0   PRINT
290   PRINT "AVERAGING DATA - - -> ";Nav;" PDINT AVERAGING"
300             CALL Avg
3I0   PRINT "CALCULATING ANP DRIFT"
320             CALL Amp_drift
330   PRINT "CALCULATING PRESSURE HISTDRY"
340             CALL Pressure
350             CALL Outp(N$,TitIe$)
360   INPUT "RECALCULATE WITH SAME SOURCE DATA (Y/N) ?",Ans$
370   IF Ans$<>"Y" THEN 400
3B0   PRINT CHR$(I2)
390   GDTO 270
400   END
410   !
420   !
430   !
440   SUB Inpt(N$)
450     DPTIDN BASE 1
460     COM /Stat/ Ch0,Orift,Nav,NbIock,Pperv,Ta,Tau,Vnorm
470     CDN /Array/ A(I025),Raw(4096)
4B0     DIN Raw$(4096)[5]
490   !
500     INPUT "DATA SDURCE - - - SCDPE = 1, BDAT FILE = 2",Tt
5I0             CALL Reader(Tt,N$,Raw$(1))
520     FDR I=2 TO 4096
530       Raw(I)=VAL(Raw$(I))
540     NEXT I
550     Vnorm=Raw(2)
560     Ch0=Raw(3)
570     Tau=Raw(4)
580     Ta=Raw(5)
590     BEEP 2I97.26,.3
600     Nav=B
6I0     INPUT "ENTER [4,B,I6] PDINT RUNNING AVERAGE (DEFAULT=B) ",Nav
620     Nch=4096-Ch0-Nav/2
630     NbIock=INT(Nch/Nav)
640     PRINT CHR$(I2)
650     PRINT Raw$(I),Raw(2),Raw(3),Raw(4),Raw(5),Raw(6),Raw(7)
660     PRINT
670   SUBEND
6B0   !
690   !
700   !
```

```
710       SUB Reader(Tt,Name$,Raw$(*))
720         OPTION BASE 1
730         PRINT
740         PRINT "PLEASE INSERT DATA DISC INTO DISC DRIVE 0"
750         INPUT "PLEASE ENTER A UNIQUE NAME FOR THE BOAT FILE.",Name$
760         DISP "WORKING, PLEASE WAIT."
770         MASS STORAGE IS ":HPB2901,700,0"
780         IF Tt=2 THEN 1000
790   !
800         ASSIGN @Scope TO 9
810         CONTROL 9,3;9600
820         ASSIGN @Scope;FORMAT ON
830         CONTROL 9,5;3
840         CONTROL 9,4;2
850         OUTPUT @Scope;CHR$(1);
860        OUTPUT @Scope;CHR$(69);CHR$(48);CHR$(68);CHR$(49);CHR$(6B);CHR$(48);
870         OUTPUT @Scope;CHR$(79);CHR$(52);CHR$(4B);CHR$(57);CHR$(54)
880         OUTPUT @Scope;CHR$(2);
890         ENTER @Scope USING "5A,X,X";Raw$(*)
900         CONTROL 9,5;0
910         ASSIGN @Scope TO *
920              CALL Scope_set(Raw$(*))
930         DISP "WORKING, PLEASE WAIT."
940         CREATE BDAT Name$,4096,5
950         ASSIGN @Path TO Name$
960         OUTPUT @Path USING "5A";Raw$(*)
970         ASSIGN @Path TO *
980       SUBEXIT
990   !
1000        ASSIGN @Path TO Name$
1010        ENTER @Path USING "5A";Raw$(*)
1020        ASSIGN @Path TO *
1030      SUBEND
1040  !
1050  !
1060  !
1070      SUB Scope_set(Raw$(*))
1080        OPTION BASE 1
1090        BEEP 1627.60,.3
1100        INPUT "ENTER TIME FOR FIRST DATA POINT (sec)",Chlt0
1110        INPUT "ENTER TIME OF EVENT INITIATION  (sec)",Event0
1120        INPUT "ENTER TIME INCREMENT, e.g. 5E-3 FOR 20 SEC RUN",Tau
1130        INPUT "ENTER VOLTAGE RANGE (V)",Range
1140        INPUT "ENTER INITIAL PRESSURE (psig)",Po
1150        INPUT "ENTER FINAL PRESSURE (psig)",Pf
1160        INPUT "ENTER AMBIENT TEMPERATURE (C)",Ta
1170  !
1180        Raw$(1)="PRESS"                          ! For error if read by "80IL"
1190        Raw$(2)=VAL$(Range/2000)                 ! Vnorm
1200        Raw$(3)=VAL$((ABS(Chlt0)-ABS(Event0))/Tau)   ! Ch0
1210        Raw$(4)=VAL$(Tau)
1220        Raw$(5)=VAL$(Ta)
1230        Raw$(6)=VAL$(Po)
1240        Raw$(7)=VAL$(Pf)
1250      SUBEND
1260  !
1270  !
1280  !
1290  SUB Avg
1300    OPTION BASE 1
1310    COM /Stat/ Ch0,Drift,Nav,Nblock,Pperv,Ta,Tau,Vnorm
1320    COM /Array/ A(1025),Raw(4096)
1330    !
1340    ! THIS SUBROUTINE CALCULATES THE RUNNING AVERAGES OF THE DATA
1350    !
1360    Adj=INT(Nav/2)-1
1370    Jstart=Ch0-Adj
1380    FOR I=1 TO Nblock
1390      Sum=0
1400      Jend=Jstart+Nav-1
1410      FOR J=Jstart TO Jend                     ! CONVERT TO TRUE VOLTAGE
1420        Sum=Sum+Raw(J)*Vnorm                   ! AND AVERAGE
1430      NEXT J
1440      A(I)=Sum/Nav
1450      Jstart=Jend+1
1460    NEXT I
1470  SUBEND
```

```
1480  !
1490  !
1500  !
1510  SUB Amp_drift
1520    OPTION BASE 1
1530    COM /Stat/ Ch0,Drift,Nav,Nblock,Pperv,Ta,Tau,Vnorm
1540    COM /Array/ A(1025),Raw(4096)
1550  !
1560  !   THIS SUBROUTINE CALCULATES THE DRIFT IN THE CHARGE AMP SIGNAL
1570  !   IT IS ASSUMED THAT DEPRESSURIZATION IS COMPLETE BY THE TIME
1580  !   OF INTEREST FOR THIS CALCULATION
1590  !
1600    Sumx=0
1610    Sumx2=0
1620    Sumy=0
1630    Sumxy=0
1640    Zz=14
1650    FOR I=(Nblock-15) TO (NbIock-2)
1660      T=Tau*Nav$(I-1)                          ! TIME
1670      Sumx=Sumx+T
1680      Sumx2=Sumx2+T^2
1690      Sumy=Sumy+A(I)
1700      Sumxy=Sumxy+A(1)*T
1710    NEXT I
1720    Drift=DROUND((Sumxy-(Sumx*Sumy)/Zz)/(Sumx2-(Sumx^2)/Zz),6)
1730  SUBEND
1740  !
1750  !
1760  !
1770  SUB Pressure
1780    OPTION BASE I
1790    COM /Stat/ Ch0,Drift,Nav,Nblock,Pperv,Ta,Tau,Vnorm
1800    COM /Array/ A(1025),Raw(4096)
1810    DIM Test(1025)
1820  !
1830    X=0
1840    Amin=100
1850    FOR I=1 TO Nblock                          ! ADJUST VOLTAGE FOR DRIFT
1860      Vdrift=Tau*Nav$(I-1)*Drift
1870      Test(I)=A(I)-Vdrift
1880      IF Test(1)>Amin THEN 1910
1890      Amin=Test(1)
1900      Imin=I
1910    NEXT 1
1920    Pperv=DROUND((Raw(6)-Raw(7))/(A(1)-Amin),6)     ! psi/volt
1930  !
1940    IF X=0 THEN BEEP 2197.26,.3
1950    PRINT "  ","DRIFT = ";Drift;" Volts per second","  ","PSI/VOLT = ";Pperv
1960    New=Drift
1970    INPUT "Enter new value for DRIFT or accept default",New
1980    IF New=Drift THEN 2030
1990      Drift=New
2000      X=1
2010      DISP "RECALCULATING  ---> PSI/VOLT"
2020      GOTO 1840
2030    FOR I=1 TO Nblock
2040      A(I)=Raw(6)-(Test(1)-Test(I))*Pperv          ! CONVERT TO PRESSURE
2050      IF I>Imin THEN A(I)=A(Imin)
2060    NEXT I
2070  SUBEND
2080  !
2090  !
2100  !
2110  SUB Outp(N$,Title$)
2120    OPTION BASE 1
2130    COM /Stat/ Ch0,Drift,Nav,Nblock,Pperv,Ta,Tau,Vnorm
2140    COM /Array/ A(1025),Raw(4096)
2150    DIM Add$[16],He1$[80],He2$[80],He3$[80],Inb$[5],St$[80]
2160    DIM T1$[80],T2$[80],Out$(3)[80],Z$(4)[10]
2170  !
2180    Istart=16/Nav+1                            ! FILE SIZE INFORMATION
2190    Step=(Istart-1)*2
2200    Size=INT(Nblock/Step+.5)
2210    ALLOCATE G(Size,2)
2220    G(1,1)=0
2230    G(1,2)=Raw(6)
```

```
2240    J=I
2250    FOR I=Istart TO Nblock STEP Step
2260      J=J+I
2270      IF J>Size THEN 2300
2280      G(J,1)=Tau*Nav*(I-1)                    ! TIME
2290      G(J,2)=A(I)                             ! PRESSURE
2300    NEXT I
2310  !
2320    PRINT
2330    PRINT "  ","**************************************************"
2340    PRINT "  ","       the ""QUICK & DIRTY"" screen plot will be"
2350    PRINT "  ","    PSIG v TIME regardless of output units choice"
2360    INPUT "ENTER PRESSURE UNITS FOR OUTPUT :   K = kPa, P = psig",Unit$
2370    BEEP 1627.60,.3
2380    PRINT CHR$(12)                          ! "QUICK & DIRTY" PLOT
2390    CALL Scr_plot(G(*),Size)                !  PSIG v TIME
2400  !
2410    IF Unit$="P" THEN 2470
2420      DISP "CONVERTING    psig ----> kPa "
2430      Pperv=Pperv/14.696*101.325
2440      FOR I=1 TO Size                       ! CONVERT TO kPa (absolute)
2450        G(I,2)=(G(I,2)/14.696+1)*101.325
2460      NEXT I
2470    INPUT "Do you wish to have a HARD COPY of the numbers ? (Y/N)",Ans$
2480    IF Ans$<>"Y" THEN 3000
2490    PRINT Title$," "," ","SOURCE DATA FILE: ";N$
2500    PRINT
2510    PRINT "****      PLEASE INSERT A DISC INTO DISC DRIVE 1"
2520    PRINT
2530    PRINT "AN ASCII FILE WILL BE CREATED ON THE DISC.  THIS FILE CAN THEN"
2540    PRINT "BE TRANSFERED TO THE MAIN COMPUTER FOR PRINT OUT"
2550    INPUT "PLEASE ENTER A UNIQUE NAME FOR THE ASCII FILE ",As$
2560    Add$="                "
2570    Inb$="     "
2580  St$="             ************************         ************************"
2590    He1$="                 TIME     PRESSURE               TIME     PRESSURE"
2600    He2$="                  (s)      (psig)                 (s)      (psig)"
2610    He3$="                                PAGE "
2620    T1$=Add$&"AMBIENT TEMP.  = "&VAL$(Ta)&" C"
2630    T2$=Add$&"PSI PER VOLT   = "&VAL$(OROUND(Pperv,6))
2640    IF Unit$="P" THEN 2670
2650      He2$="                 (s)      (kPA)                  (s)      (kPa)"
2660      T2$=Add$&"kPa PER VOLT   = "&VAL$(OROUND(Pperv,6))
2670    Istart=1
2680    Iend=45
2690    Npg=1
2700    MASS STORAGE IS ":HP8290I,700,1"
2710    CREATE ASCII As$,60
2720    ASSIGN @Path TO As$
2730    OUTPUT @Path;Add$&Title$,Inb$,T1$,T2$,Inb$
2740    OUTPUT @Path;St$,Inb$,He1$,He2$
2750    OUTPUT @Path;Inb$,St$,Inb$
2760    FOR I=Istart TO Iend STEP 3
2770              CALL Dec(I,G(*),Z$(*),Size)
2780      Out$(1)=Add$&Z$(I)&Inb$&Z$(2)&Add$&Z$(3)&Inb$&Z$(4)
2790        IF I+1<=Size THEN CALL Dec(I+1,G(*),Z$(*),Size)
2800      Out$(2)=Add$&Z$(I)&Inb$&Z$(2)&Add$&Z$(3)&Inb$&Z$(4)
2810        IF I+2<=Size THEN CALL Dec(I+2,G(*),Z$(*),Size)
2820      Out$(3)=Add$&Z$(1)&Inb$&Z$(2)&Add$&Z$(3)&Inb$&Z$(4)
2830      IF I+1>Size THEN Out$(2)=Add$
2840      IF I+2>Size THEN Out$(3)=Add$
2850      OUTPUT @Path;Out$(1),Out$(2),Out$(3)
2860    NEXT I
2870    IF Iend=Size THEN 2970
2880    OUTPUT @Path;Inb$,Inb$,Inb$,Inb$,Inb$,Inb$,Inb$,Inb$,Inb$
2890    Npg=Npg+1
2900    T1$=Add$&Title$&He3$&VAL$(Npg)
2910    Istart=Iend+46
2920    Iend=Istart+44
2930    IF Iend>Size THEN Iend=Size
2940    OUTPUT @Path;T1$,Inb$,St$,Inb$,He1$
2950    OUTPUT @Path;He2$,Inb$,St$,Inb$,Inb$
2960    GOTO 2760
2970    ASSIGN @Path TO *
2980    MASS STORAGE IS ":HP8290I,700,0"
2990    BEEP 1302.08,.3
```

```
3000 !
3010   INPUT "Do you wish to have a PLOT of the numbers ? (Y/N)",Ans$
3020   IF Ans$()"Y" THEN 3200
3030   PRINT CHR$(12)
3040   PRINT Title$," "," ","SOURCE DATA FILE : ";N$
3050   PRINT
3060   PRINT "!!!!      PLEASE INSERT A DISC INTO DISC DRIVE 1"
3070   PRINT
3080   PRINT "A BOAT FILE WILL BE CREATED ON THE DISC.  THIS FILE CAN THEN"
3090   PRINT "BE PLOTTED USING THE GENERAL PLOTTING PROGRAM"
3100   INPUT "PLEASE ENTER A UNIQUE NAME FOR THE BOAT FILE ",Bd$
3110   MASS STORAGE IS ":HP82901,700,1"
3120   CREATE BOAT Bd$,(2*Size),9
3130   ASSIGN @Path TO Bd$
3140   Format$="MZ.0D0E,#"
3150   OUTPUT @Path USING Format$;G(!)
3160   ASSIGN @Path TO !
3170   MASS STORAGE IS ":HP8290I,700,0"
3180   PRINT
3190   PRINT "BOAT file: ";Bd$,Size;" points","Data format: MZ.0D0E"
3200   DEALLOCATE G(!)
3210   BEEP 5I26.94,.1
3220   PRINT "      END"
3230 SUBEND
3240 !
3250 !
3260 !
3270     SUB Dec(I,Z(!),Z$(!),Size)
3280       OPTION BASE 1
3290 !
3300 !       THIS SUBROUTINE ENSURES THAT ALL VALUES HAVE THE
3310 !       CORRECT FIELD LENGTH FOR OUTPUT
3320 !
3330       Ii=1
3340       A=0
3350       Dec$="0"
3360       Per$="."
3370       Z$(3)=""
3380       Z$(4)=""
3390       Long=5
3400       FOR J=1 TO 2
3410         Zz=Z(Ii,J)
3420         IF Zz<0 THEN Zz$=VAL$(OROUND(FNRound(Zz,3),5))
3430         IF Zz<0 THEN 3550
3440         Zz$=VAL$(OROUND(Zz,5))
3450         IF Zz<I.E-5 THEN Zz$=".0000000"
3460         IF Zz<I.0 THEN 3600
3470         GOTO 3650
3480         Z$(J+A)=Zz$
3490         Long=6
3500       NEXT J
3510       IF Ii<>I OR I+45>Size THEN 3740
3520       A=2
3530       Ii=I+45
3540       GOTO 3390
3550 !                   FOR ZZ<0
3560         IF LEN(Zz$)>Long THEN Zz$=Zz$[1,Long]
3570         IF LEN(Zz$)<Long THEN Zz$=Zz$&Dec$
3580         IF LEN(Zz$)<>Long THEN 3570
3590       GOTO 3480
3600 !                   FOR 0<ZZ<1
3610         IF LEN(Zz$)>=Long THEN Zz$=Zz$[I,Long-1]
3620         IF LEN(Zz$)<Long THEN Zz$=Dec$&Zz$
3630         IF LEN(Zz$)<>Long THEN 3710
3640       GOTO 3480
3650 !                   FOR ZZ>1
3660         P$="N"
3670         FOR F=LEN(Zz$) TO I STEP -1
3680           IF Zz$[F,F]="." THEN P$="Y"
3690         NEXT F
3700         IF P$="N" AND LEN(Zz$)<Long THEN Zz$=Zz$&Per$
3710         IF Zz<1.E+5 AND LEN(Zz$)<Long THEN Zz$=Zz$&Dec$
3720         IF Zz<1.E+5 AND LEN(Zz$)<>Long THEN 3710
3730       GOTO 3480
3740     SUBEND
```

```
3750  !
3760  !
3770  !
3780        DEF FNRound(Z,Np)
3790          Nu=INT(Z*10^Np+.5)                    ! ROUNDING FOR Z<0
3800          Nu=Nu/(10^Np)
3810          RETURN Nu
3820        FNEND
3830  !
3840  !
3850  !
3860  SUB Graf_set(P2,Tscale)
3870    GINIT
3880    GRAPHICS OFF
3890    VIEWPORT 0,130,15,100
3900    PEN 1
3910    LDIR PI/2
3920    LORG 6
3930    MOVE 0,57
3940    LABEL "PRESSURE (psig)"
3950    LDIR 0
3960    LORG 4
3970    MOVE 65,15
3980    LABEL "TIME (s)"
3990    CSIZE 3.7,.5
4000    MOVE 7,15
4010    LABEL "0"
4020    MOVE 128,15
4030    LABEL Tscale
4040    LORG 2
4050    MOVE 0,20
4060    LABEL "-5"
4070    MOVE 0,98
4080    LABEL P2
4090    VIEWPORT 7,130,20,100
4100    WINDOW 0,Tscale,-5,P2
4110    FRAME
4120    AXES 1,1,0,0,5,5,2
4130  SUBEND
4140  !
4150  !
4160  !
4170  SUB Scr_plot(G(*),Numdata)
4180    OPTION BASE 1
4190    Er$="N"
4200    LINE TYPE 1
4210    PEN 1
4220    ALPHA OFF
4230    GRAPHICS ON
4240    MOVE G(1,1),G(1,2)
4250    FOR I=1 TO Numdata
4260    IF G(1,1)=0 AND I>1 THEN 4280
4270    DRAW G(1,I),G(I,2)
4280    NEXT I
4290    MOVE 0,0
4300    IF Er$="Y" THEN 4360
4310    WAIT 5
4320    INPUT "      ERASE THIS PLOT (Y/N)?",Er$
4330    IF Er$<>"Y" THEN 4360
4340    PEN -1
4350    GOTO 4240
4360    GRAPHICS OFF
4370    ALPHA ON
4380  SUBEND
```

APPENDIX C

System Performance

Control System Performance

The ability of the control system to provide a constant power delivery (superficial heat flux) to the test element is illustrated in Fig. C1. It will be noted that, in spite of the substantial change in wire temperature (and the rapidity at which this change is possible), with associated change in wire resistance, the control system provides constant power delivery.

Pressure Measurement System Performance

The ability of the pressure measurement system to yield an accurate pressure history of an experiment depends on proper setup for test conditions. Best accuracy requires flush mounting of the pressure transducer to the test section. However, this was not possible due to the necessity of providing cooling capability for the transducer with the cooling adaptor. The choice of the amplifier time constant also affects the accuracy, and a dramatic effect on the voltage signal measured for a given pressure drop. Use of the short and medium time constant settings resulted in signal decay during the pressure transient, while use of the log time constant introduced the complication of signal drift (Fig. C2).

The effect of temperature on the measure voltage signal is illustrated in Fig. C3. The figure compares measurements at an ambient temperature T_a = 27°C to measurements at T_a = 100°C. For the long time constant setting, the drift is adversely affected by increasing temperature (no significant difference in behavior was found in the medium and short time constant cases). Additionally, as seen in Fig.

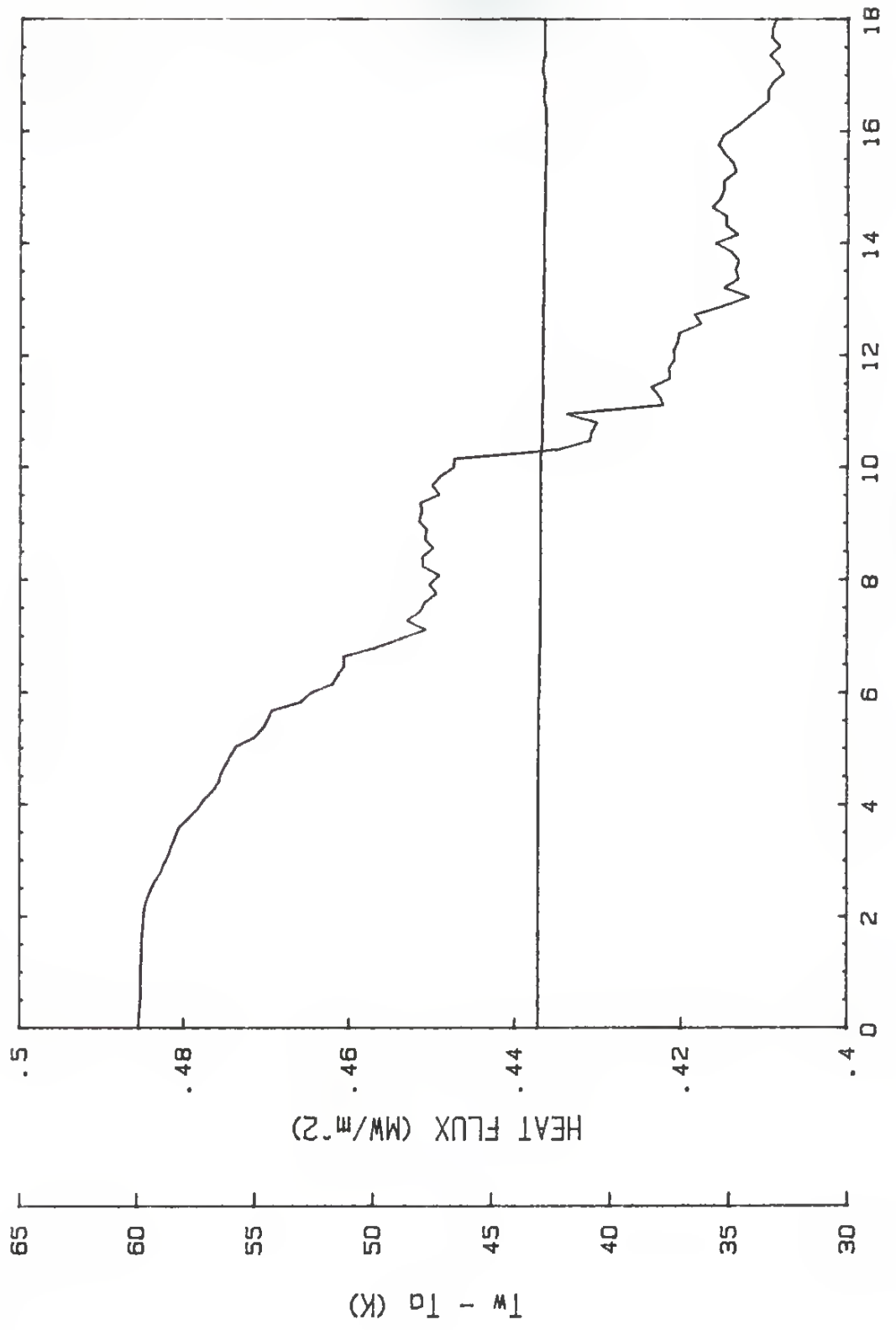

FIG. C1. Control system performance for a 20 s run. The straight line is the heat flux as a function of time. The curve is the test heater temperature aa a function of time. Results are from run AP3-3, with ambient temperature T_a = 100°C.

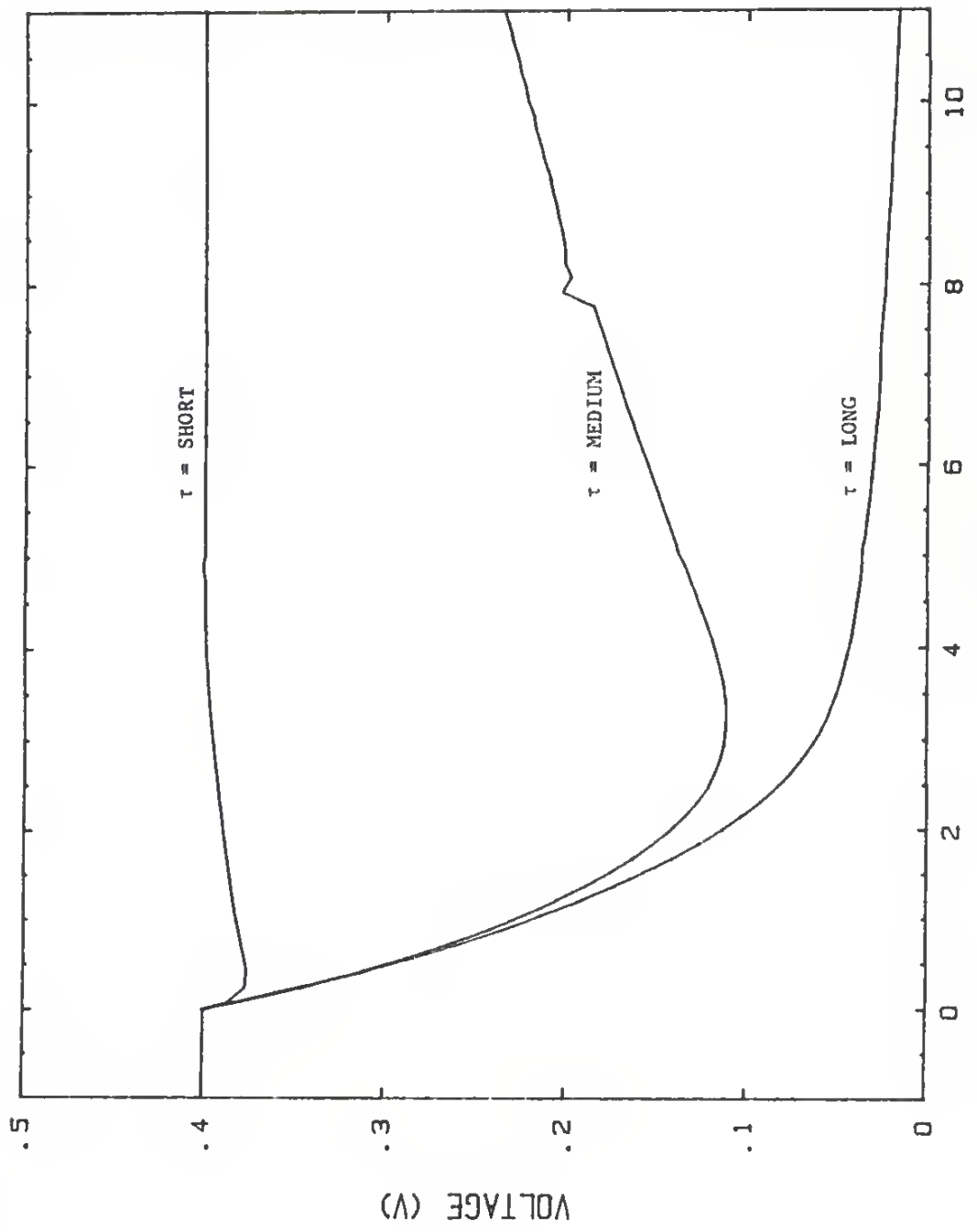

FIG. C2. Effect of pressure transducer amplifier time constant on the signal measured for a 0.377 to 0.101 MPa pressure drop at T_a = 100°C.

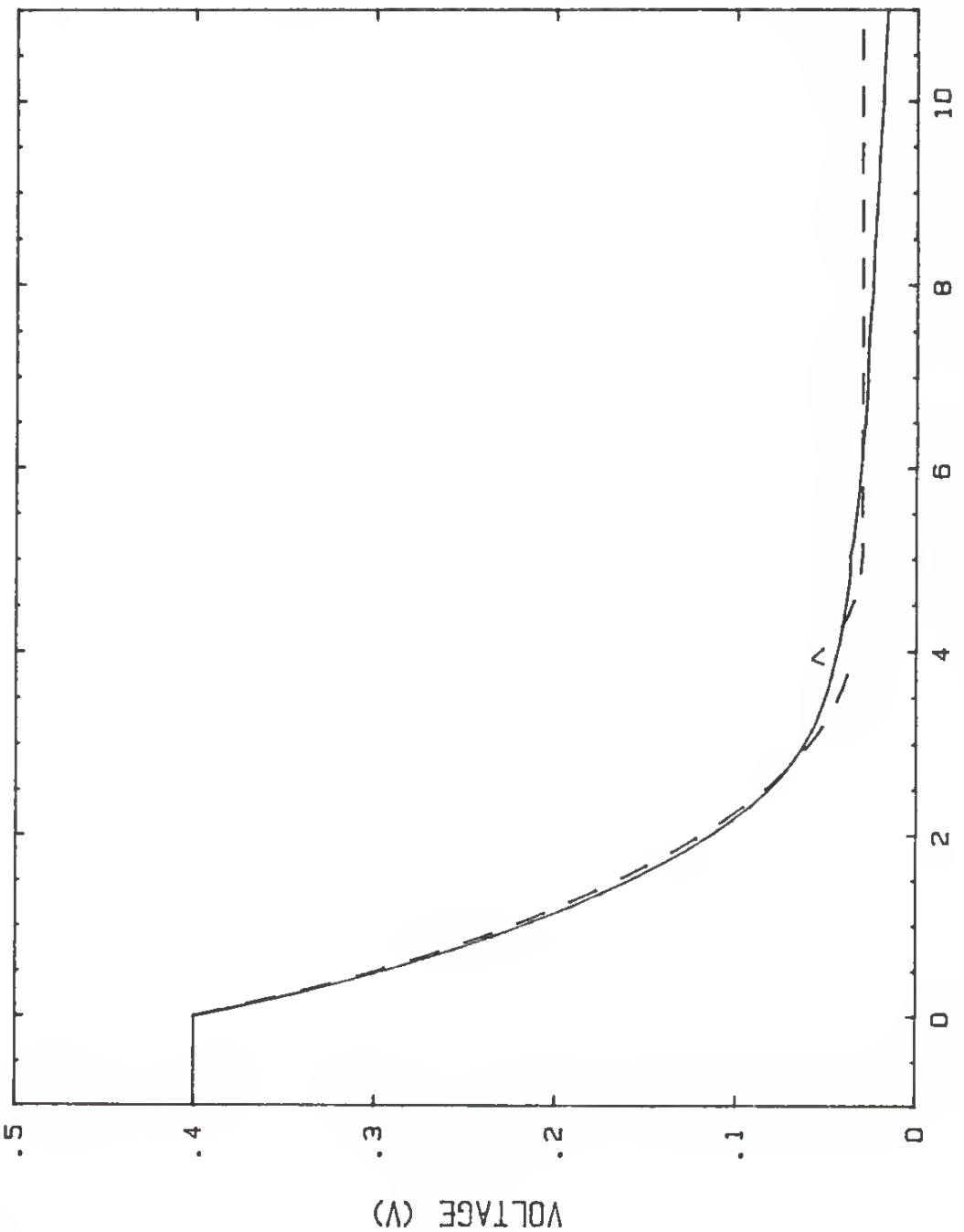

FIG. C3. Effect of ambient temperature on the signal measured for a 0.377 to 0.101 MPa pressure drop. The dashed line is the signal measured at T_a = 27°C. The solid line is the signal measured at T_a = 100°C.

C4, there was little consistency in the value of the drift beyond the individual run. Therefore, the analysis program determined the average drift for each run and corrected the data for this drift, then translated the data from voltage units to pressure units based on the observed pressure drop. Using the same data as Fig. C3, these two steps are illustrated in Figs. C5 and C6, comparing the results from a test with significant drift to the results from a test with zero drift. Figure C7 also illustrates the effect of ambient temperature on the pressure transient, comparing results for T_a = 95°C to results for T_a = 100°C.

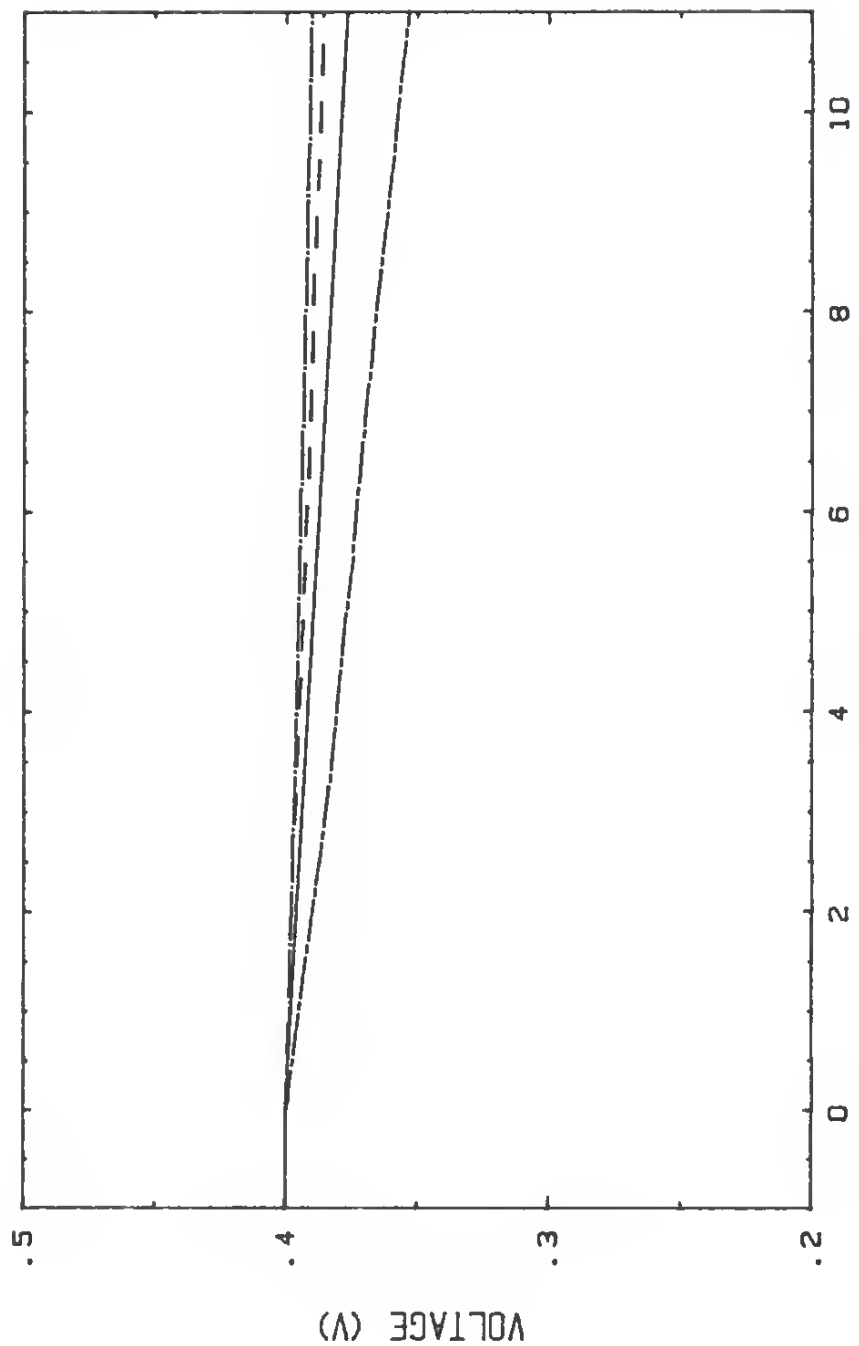

FIG. C4. Representative measurements of the pressure transducer amplifier drift at constant pressure and T_a = 100°C. The solid line is the drift of the corresponding signal shown in Fig. C3, the short dash-long dash line is data from run AP1-6, the dashed line is data from run AP9-1, and the dot-dashed line is data from run AP10-1.

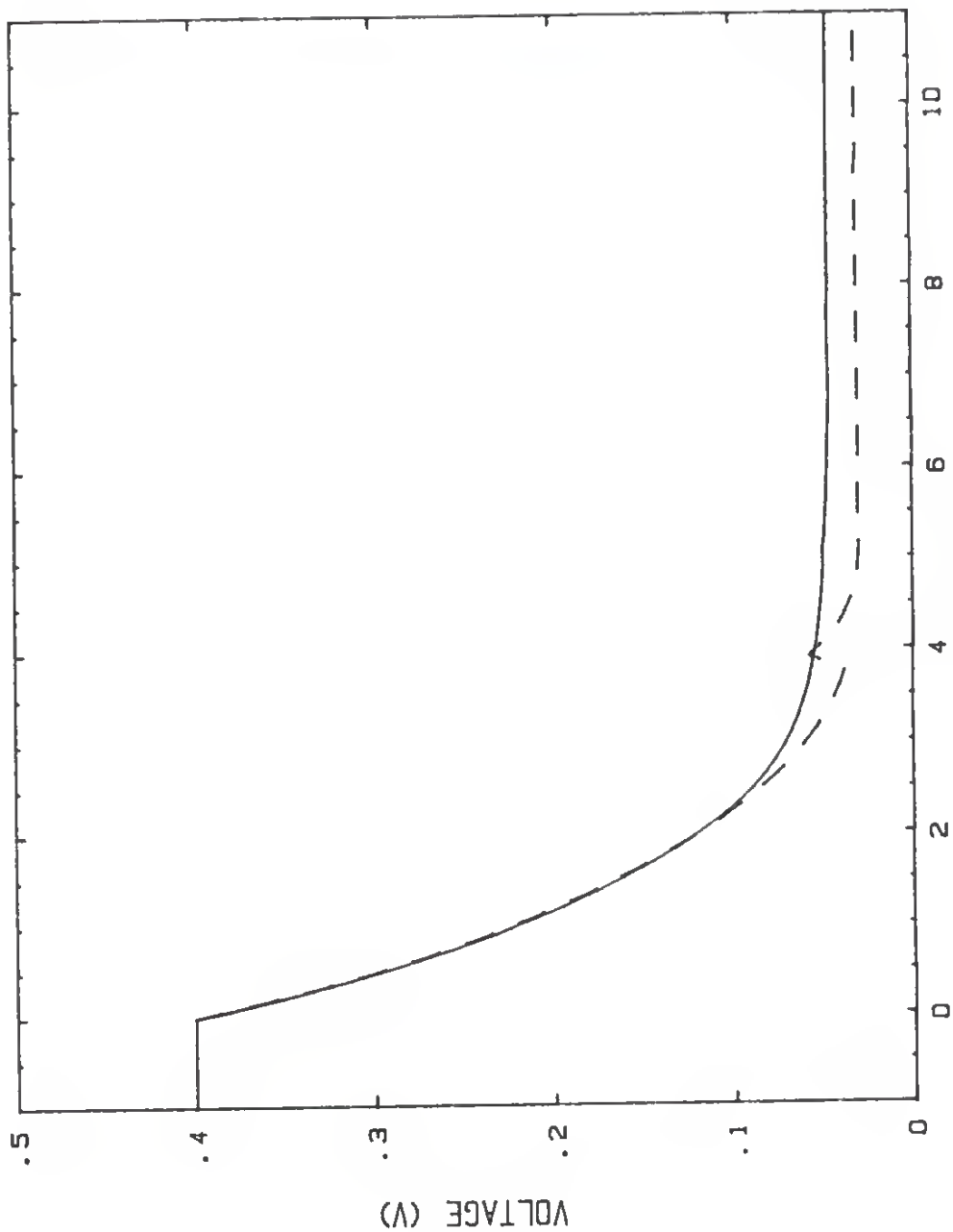

FIG. C5. Drift corrected signals for a 0.377 to 0.101 MPa pressure drop. The dashed line is the zero-drift signal measured at T_a = 27°C. The solid line is the signal measured at T_a = 100°C corrected for drift by the prescription of data analysis program PRESSURE.

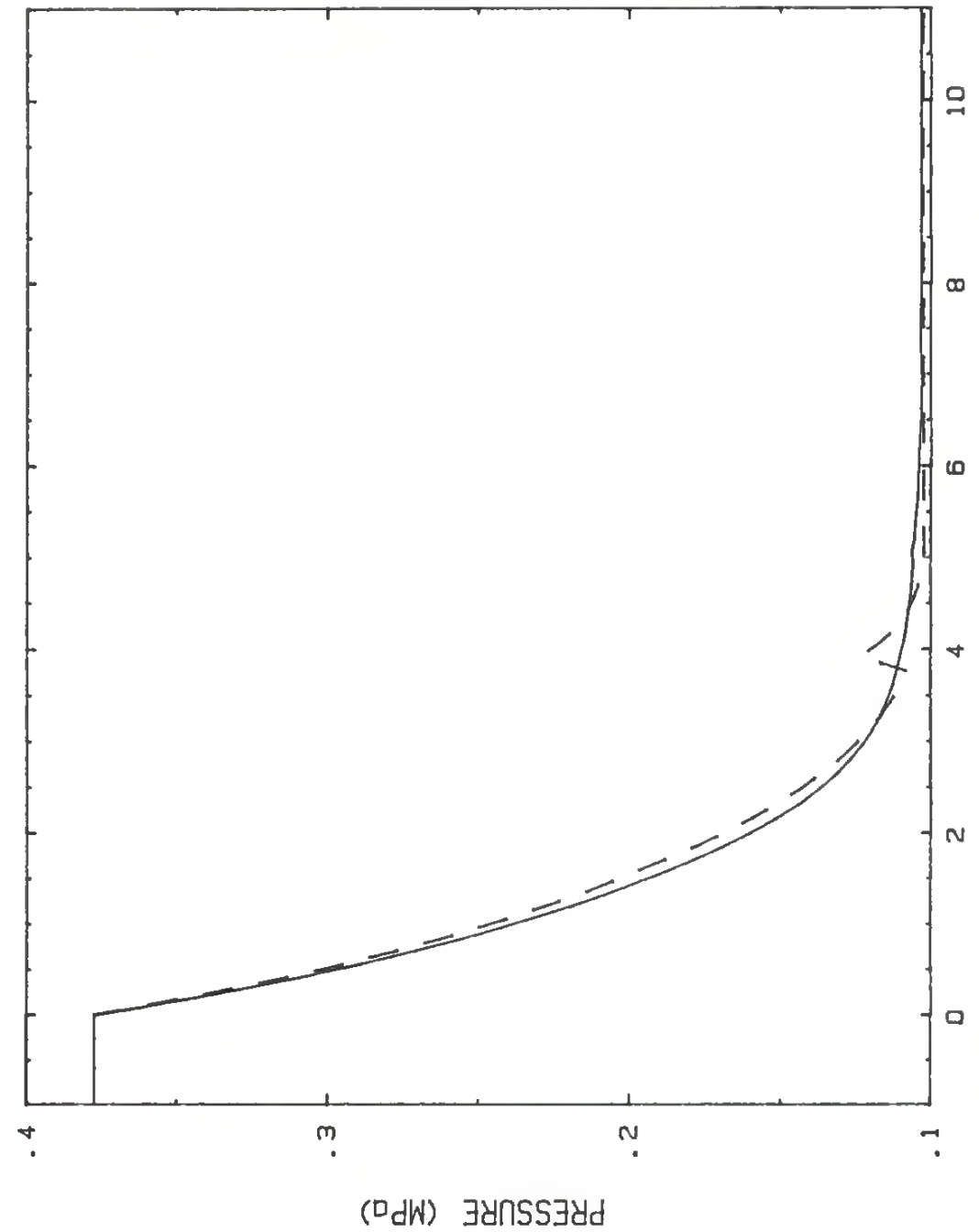

FIG. C6. Translation of data from units of voltage to units of pressure. The dashed line is the pressure history for T_a = 27°C. The solid line is the drift-corrected pressure history for T_a = 100°C.

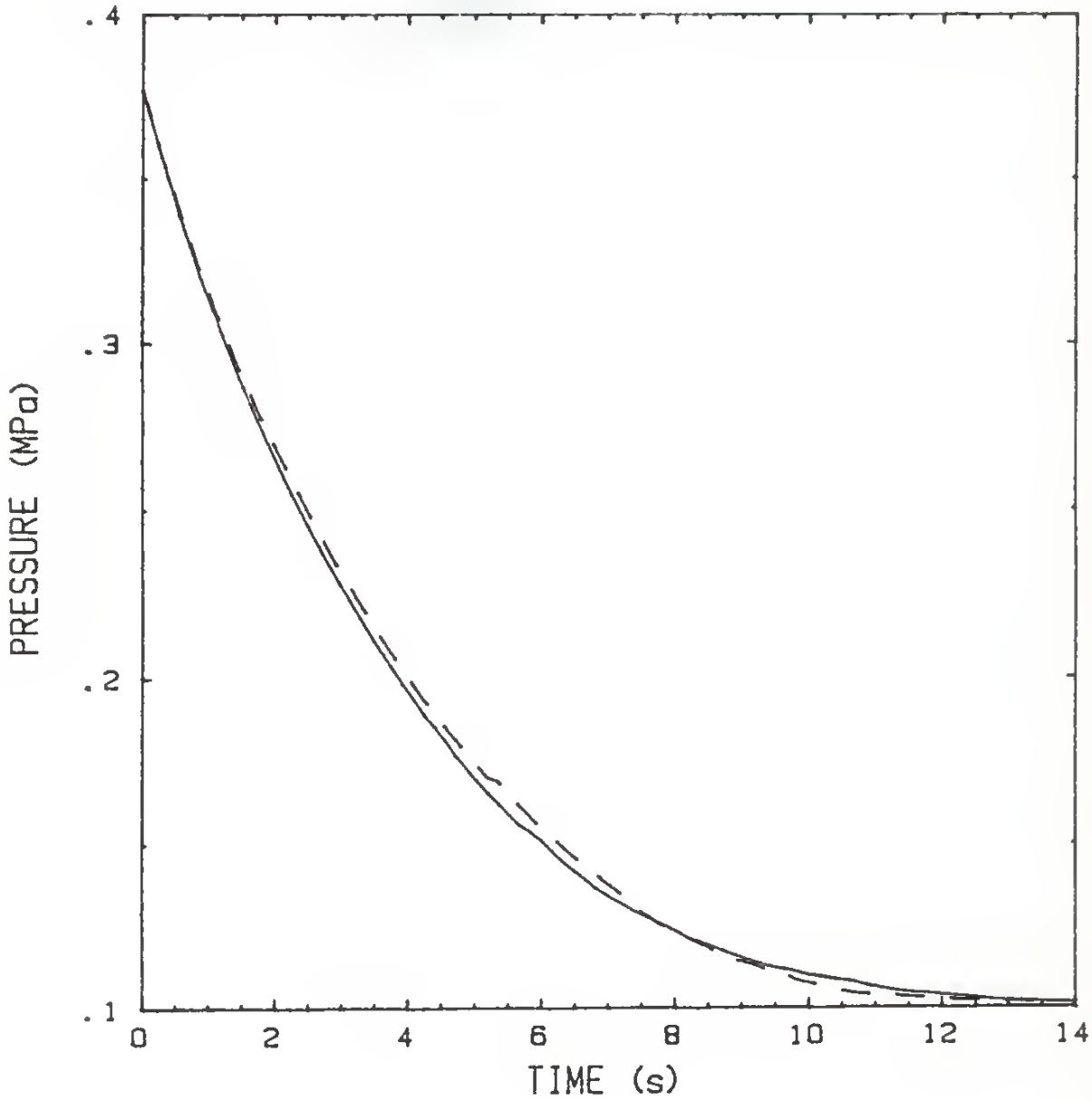

FIG. C7. Effect of ambient temperature on a 0.377 to 0.101 MPa pressure drop. The dashed line is the pressure history for T_a = 95°C. The solid line is the pressure history for T_a = 100°C.

APPENDIX D

Selected Listings of Experimental Pressure Data

Representative runs for series 1-8 (Table 5.2)

RUN NUMBER AP2-2

AMBIENT TEMP. = 100 C
KPA PER VOLT = 794.197

TIME (S)	PRESSURE (KPA)	TIME (S)	PRESSURE (KPA)
0.000	373.67	7.120	106.73
0.080	364.71	7.280	106.37
0.240	346.37	7.440	105.31
0.400	329.89	7.600	105.38
0.560	315.32	7.760	104.68
0.720	301.50	7.920	104.49
0.880	288.92	8.080	104.52
1.040	277.10	8.240	104.43
1.200	265.57	8.400	104.33
1.360	254.74	8.560	104.00
1.520	245.09	8.720	104.01
1.680	235.15	8.880	103.73
1.840	225.75	9.040	103.52
2.000	216.77	9.200	103.27
2.160	208.72	9.360	103.34
2.320	200.47	9.520	103.37
2.480	192.76	9.680	103.15
2.640	185.38	9.840	103.30
2.800	178.67	10.00	103.13
2.960	172.32	10.16	103.10
3.120	166.32	10.32	103.17
3.280	160.03	10.48	103.20
3.440	154.64	10.64	102.92
3.600	149.61	10.80	103.13
3.760	145.18	10.96	103.14
3.920	141.06	11.12	103.07
4.080	137.83	11.28	102.92
4.240	139.35	11.44	102.68
4.400	136.54	11.60	101.83
4.560	132.27	11.76	101.71
4.720	128.73	11.92	101.50
4.880	125.38	12.08	101.33
5.040	123.19	12.24	101.33
5.200	120.90	12.40	101.33
5.360	118.64	12.56	101.33
5.520	116.79	12.72	101.33
5.680	115.29	12.88	101.33
5.840	113.89	13.04	101.33
6.000	112.67	13.20	101.33
6.160	111.28	13.36	101.33
6.320	110.35	13.52	101.33
6.480	109.37	13.68	101.33
6.640	109.13	13.84	101.33
6.800	108.03	14.00	101.33
6.960	107.46	14.16	101.33

RUN NUMBER AP2-8

AMBIENT TEMP. = 100 C
KPA PER VOLT = 790.66

TIME (S)	PRESSURE (KPA)	TIME (S)	PRESSURE (KPA)
0.000	515.01	7.120	109.56
0.080	500.08	7.280	107.73
0.240	474.29	7.440	106.45
0.400	450.94	7.600	105.69
0.560	430.05	7.760	105.07
0.720	410.12	7.920	104.42
0.880	392.00	8.080	103.90
1.040	374.44	8.240	103.57
1.200	358.83	8.400	103.09
1.360	343.66	8.560	103.04
1.520	329.40	8.720	103.03
1.680	316.04	8.880	102.99
1.840	303.02	9.040	102.65
2.000	290.78	9.200	102.77
2.160	279.20	9.360	102.74
2.320	267.77	9.520	103.03
2.480	256.83	9.680	101.58
2.640	246.77	9.840	101.33
2.800	236.54	10.00	101.33
2.960	226.63	10.16	101.33
3.120	217.43	10.32	101.33
3.280	209.01	10.48	101.33
3.440	200.29	10.64	101.33
3.600	192.13	10.80	101.33
3.760	184.31	10.96	101.33
3.920	177.13	11.12	101.33
4.080	170.33	11.28	101.33
4.240	163.84	11.44	101.33
4.400	157.54	11.60	101.33
4.560	151.76	11.76	101.33
4.720	146.65	11.92	101.33
4.880	141.58	12.08	101.33
5.040	137.02	12.24	101.33
5.200	132.86	12.40	101.33
5.360	128.87	12.56	101.33
5.520	125.15	12.72	101.33
5.680	122.41	12.88	101.33
5.840	119.51	13.04	101.33
6.000	117.37	13.20	101.33
6.160	115.83	13.36	101.33
6.320	113.67	13.52	101.33
6.480	112.02	13.68	101.33
6.640	110.42	13.84	101.33
6.800	109.21	14.00	101.33
6.960	107.97	14.16	101.33

RUN NUMBER AP3-5

AMBIENT TEMP. = 100 C
KPA PER VOLT = 763.102

TIME (S)	PRESSURE (KPA)	TIME (S)	PRESSURE (KPA)
0.000	446.06	7.120	105.29
0.080	434.23	7.280	105.94
0.240	412.79	7.440	104.18
0.400	393.98	7.600	103.76
0.560	376.39	7.760	103.00
0.720	360.36	7.920	101.93
0.880	344.89	8.080	101.33
1.040	330.60	8.240	101.33
1.200	316.78	8.400	101.33
1.360	303.62	8.560	101.33
1.520	292.15	8.720	101.33
1.680	280.22	8.880	101.33
1.840	268.87	9.040	101.33
2.000	258.68	9.200	101.33
2.160	248.25	9.360	101.33
2.320	239.17	9.520	101.33
2.480	228.75	9.680	101.33
2.640	220.24	9.840	101.33
2.800	211.36	10.00	101.33
2.960	202.76	10.16	101.33
3.120	194.90	10.32	101.33
3.280	187.86	10.48	101.33
3.440	180.20	10.64	101.33
3.600	173.32	10.80	101.33
3.760	166.85	10.96	101.33
3.920	160.66	11.12	101.33
4.080	155.82	11.28	101.33
4.240	149.63	11.44	101.33
4.400	144.46	11.60	101.33
4.560	139.50	11.76	101.33
4.720	135.13	11.92	101.33
4.880	131.03	12.08	101.33
5.040	127.23	12.24	101.33
5.200	124.65	12.40	101.33
5.360	121.39	12.56	101.33
5.520	118.74	12.72	101.33
5.680	116.54	12.88	101.33
5.840	113.74	13.04	101.33
6.000	111.96	13.20	101.33
6.160	110.03	13.36	101.33
6.320	109.77	13.52	101.33
6.480	107.57	13.68	101.33
6.640	106.59	13.84	101.33
6.800	105.89	14.00	101.33
6.960	105.41	14.16	101.33

RUN NUMBER AP4-3

AMBIENT TEMP. = 100 C
KPA PER VOLT = 763.137

TIME (S)	PRESSURE (KPA)	TIME (S)	PRESSURE (KPA)
0.000	583.96	7.120	125.43
0.080	567.73	7.280	123.84
0.240	536.48	7.440	123.02
0.400	508.27	7.600	121.62
0.560	482.22	7.760	120.17
0.720	459.60	7.920	118.92
0.880	437.40	8.080	117.86
1.040	416.83	8.240	117.13
1.200	397.83	8.400	116.20
1.360	380.12	8.560	115.43
1.520	364.04	8.720	114.70
1.680	348.04	8.880	113.92
1.840	333.00	9.040	112.62
2.000	318.63	9.200	111.98
2.160	304.93	9.360	111.35
2.320	292.32	9.520	110.90
2.480	280.53	9.680	110.13
2.640	268.59	9.840	109.64
2.800	257.37	10.00	109.05
2.960	246.72	10.16	108.56
3.120	236.35	10.32	107.97
3.280	226.75	10.48	107.53
3.440	217.58	10.64	107.37
3.600	208.88	10.80	106.88
3.760	201.86	10.96	106.63
3.920	194.26	11.12	106.37
4.080	187.95	11.28	106.02
4.240	180.45	11.44	105.82
4.400	173.94	11.60	105.57
4.560	168.64	11.76	105.31
4.720	163.76	11.92	104.77
4.880	159.64	12.08	104.38
5.040	155.91	12.24	103.70
5.200	152.12	12.40	103.35
5.360	149.34	12.56	102.76
5.520	146.32	12.72	103.03
5.680	143.45	12.88	102.87
5.840	141.00	13.04	102.67
6.000	139.89	13.20	102.56
6.160	136.92	13.36	102.78
6.320	134.52	13.52	102.53
6.480	132.21	13.68	102.23
6.640	132.53	13.84	102.12
6.800	129.90	14.00	101.87
6.960	127.45	14.16	101.99

TIME (S)	PRESSURE (KPA)
14.32	101.89
14.48	101.68
14.64	101.81
14.80	101.89
14.96	101.78
15.12	101.67
15.28	101.94
15.44	101.78
15.60	101.44
15.76	101.66
15.92	101.45
16.08	101.49
16.24	101.52
16.40	101.60
16.56	101.78
16.72	101.48
16.88	101.70
17.04	101.64
17.20	101.58
17.36	101.47
17.52	101.64
17.68	101.53
17.84	101.47
18.00	101.51
18.16	101.73
18.32	101.52
18.48	101.33

RUN NUMBER AP7-5

AMBIENT TEMP. = 100 C
KPA PER VOLT = 995.193

TIME (S)	PRESSURE (KPA)	TIME (S)	PRESSURE (KPA)
0.000	377.11	7.120	146.05
0.080	373.45	7.230	144.14
0.240	362.86	7.440	142.64
0.400	354.04	7.600	141.26
0.560	344.92	7.760	139.28
0.720	336.05	7.920	137.85
0.880	327.38	8.080	136.14
1.040	319.23	8.240	135.38
1.200	311.31	8.400	133.65
1.360	303.93	8.560	132.22
1.520	296.40	8.720	130.84
1.680	289.08	8.880	129.48
1.840	282.22	9.040	128.05
2.000	275.72	9.200	126.75
2.160	269.33	9.360	125.59
2.320	263.15	9.520	124.38
2.480	260.67	9.680	123.15
2.640	253.64	9.840	122.12
2.800	247.51	10.00	121.08
2.960	241.68	10.16	119.90
3.120	236.09	10.32	118.99
3.280	231.00	10.48	117.84
3.440	225.96	10.64	116.90
3.600	220.87	10.80	116.04
3.760	216.26	10.96	115.13
3.920	211.87	11.12	114.30
4.080	207.55	11.28	113.89
4.240	202.98	11.44	112.88
4.400	198.99	11.60	112.20
4.560	194.90	11.76	111.66
4.720	191.08	11.92	111.20
4.880	187.01	12.08	110.59
5.040	183.26	12.24	110.05
5.200	179.89	12.40	109.29
5.360	176.57	12.56	108.83
5.520	173.60	12.72	108.25
5.680	170.27	12.88	107.69
5.840	167.08	13.04	107.10
6.000	163.93	13.20	106.69
6.160	161.08	13.36	106.13
6.320	158.26	13.52	105.82
6.480	155.36	13.68	105.91
6.640	152.78	13.84	105.59
6.800	150.20	14.00	105.26
6.960	147.75	14.16	104.92

TIME (S)	PRESSURE (KPA)
14.32	104.81
14.48	104.55
14.64	104.34
14.80	104.10
14.96	103.91
15.12	103.70
15.28	103.41
15.44	103.42
15.60	102.96
15.76	102.73
15.92	102.54
16.08	102.53
16.24	102.19
16.40	102.18
16.56	102.09
16.72	101.95
16.88	101.89
17.04	101.68
17.20	101.79
17.36	101.97
17.52	101.94
17.68	101.77
17.84	101.66
18.00	101.77
18.16	101.44
18.32	101.32
18.48	101.32
18.64	101.32
18.80	101.32
18.96	101.32
19.12	101.32
19.28	101.32
19.44	101.32
19.60	101.32
19.76	101.32

RUN NUMBER AP8-6

AMBIENT TEMP. = 100 C
KPA PER VOLT = 853.596

TIME (S)	PRESSURE (KPA)	TIME (S)	PRESSURE (KPA)
0.000	377.11	7.120	129.76
0.080	371.92	7.280	127.34
0.240	360.72	7.440	125.06
0.400	350.55	7.600	122.72
0.560	340.91	7.760	122.79
0.720	331.57	7.920	120.21
0.880	322.57	8.080	119.28
1.040	314.66	8.240	116.23
1.200	306.39	8.400	114.60
1.360	298.78	8.560	112.56
1.520	291.36	8.720	111.54
1.680	284.17	8.880	110.24
1.840	277.58	9.040	109.10
2.000	271.06	9.200	108.06
2.160	264.49	9.360	107.02
2.320	258.23	9.520	106.29
2.480	251.90	9.680	105.56
2.640	245.97	9.840	104.94
2.800	240.13	10.00	104.16
2.960	234.86	10.16	103.72
3.120	229.58	10.32	103.26
3.280	224.12	10.48	102.82
3.440	218.69	10.64	102.50
3.600	213.53	10.80	102.25
3.760	208.56	10.96	102.09
3.920	203.70	11.12	101.73
4.080	198.87	11.28	101.44
4.240	194.50	11.44	101.33
4.400	190.00	11.60	101.33
4.560	185.42	11.76	101.33
4.720	181.18	11.92	101.33
4.880	176.85	12.08	101.33
5.040	172.78	12.24	101.33
5.200	168.61	12.40	101.33
5.360	164.94	12.56	101.33
5.520	161.24	12.72	101.33
5.680	157.66	12.88	101.33
5.840	154.46	13.04	101.33
6.000	150.86	13.20	101.33
6.160	147.58	13.36	101.33
6.320	144.20	13.52	101.33
6.480	141.15	13.68	101.33
6.640	138.06	13.84	101.33
6.800	135.06	14.00	101.33
6.960	132.29	14.16	101.33

RUN NUMBER AP9-2

AMBIENT TEMP. = 100 C
KPA PER VOLT = 943.158

TIME (S)	PPESSURE (KPA)	TIME (S)	PRESSURE (KPA)
0.000	377.11	7.120	132.60
0.080	372.54	7.280	130.79
0.240	360.87	7.440	128.86
0.400	350.08	7.600	127.40
0.560	339.59	7.760	125.85
0.720	329.83	7.920	124.35
0.880	320.31	8.080	122.70
1.040	311.80	8.240	120.86
1.200	302.90	8.400	120.02
1.360	294.77	8.560	118.70
1.520	286.71	8.720	117.41
1.680	279.33	8.880	116.17
1.840	272.40	9.040	115.04
2.000	265.36	9.200	114.03
2.160	258.66	9.360	112.88
2.320	252.09	9.520	112.06
2.480	245.94	9.680	111.64
2.640	239.91	9.840	110.79
2.800	233.97	10.00	109.92
2.960	228.32	10.16	109.46
3.120	223.25	10.32	108.78
3.280	217.88	10.48	108.36
3.440	212.70	10.64	108.01
3.600	207.70	10.80	107.04
3.760	202.94	10.96	106.39
3.920	198.25	11.12	105.80
4.080	193.80	11.28	105.15
4.240	189.16	11.44	104.75
4.400	185.44	11.60	104.43
4.560	181.27	11.76	104.26
4.720	176.75	11.92	103.94
4.880	172.89	12.08	103.57
5.040	169.05	12.24	103.33
5.200	165.44	12.40	103.06
5.360	162.15	12.56	102.68
5.520	158.71	12.72	102.33
5.680	155.67	12.88	102.08
5.840	153.39	13.04	102.11
6.000	150.99	13.20	101.87
6.160	147.67	13.36	101.74
6.320	144.44	13.52	101.58
6.480	141.87	13.68	101.42
6.640	139.38	13.84	101.33
6.800	136.62	14.00	101.33
6.960	134.53	14.16	101.33

RUN NUMBER AP9-8

AMBIENT TEMP. = 100 C
KPA PER VOLT = 824.762

TIME (S)	PRESSURE (KPA)	TIME (S)	PRESSURE (KPA)
0.000	377.11	7.120	132.37
0.080	371.38	7.280	129.92
0.240	359.92	7.440	127.81
0.400	349.58	7.600	125.63
0.560	339.42	7.760	123.66
0.720	330.69	7.920	121.79
0.880	321.56	8.080	120.01
1.040	312.87	8.240	118.10
1.200	304.93	8.400	116.66
1.360	297.09	8.560	115.33
1.520	289.82	8.720	114.06
1.680	282.57	8.880	113.06
1.840	275.53	9.040	112.32
2.000	268.67	9.200	111.90
2.160	262.18	9.360	111.50
2.320	255.78	9.520	110.97
2.480	249.95	9.680	110.65
2.640	243.92	9.840	109.87
2.800	237.99	10.00	109.55
2.960	232.51	10.16	108.75
3.120	226.89	10.32	109.25
3.280	221.72	10.48	107.99
3.440	216.82	10.64	107.75
3.600	211.76	10.80	107.36
3.760	206.92	10.96	106.81
3.920	202.08	11.12	106.45
4.080	197.35	11.28	105.82
4.240	192.76	11.44	105.70
4.400	188.25	11.60	105.47
4.560	183.87	11.76	105.31
4.720	184.56	11.92	105.01
4.880	179.02	12.08	104.93
5.040	173.96	12.24	104.67
5.200	169.63	12.40	104.91
5.360	165.44	12.56	104.63
5.520	161.53	12.72	104.43
5.680	157.78	12.88	104.36
5.840	154.37	13.04	104.08
6.000	151.06	13.20	103.96
6.160	148.07	13.36	103.82
6.320	145.15	13.52	103.77
6.480	142.30	13.68	103.68
6.640	139.48	13.84	103.33
6.800	137.51	14.00	103.34
6.960	134.88	14.16	103.20

TIME (S)	PRESSURE (KPA)
14.32	103.19
14.48	103.04
14.64	103.15
14.80	103.16
14.96	103.16
15.12	102.99
15.28	103.08
15.44	102.78
15.60	102.62
15.76	102.77
15.92	102.55
16.08	102.52
16.24	102.49
16.40	102.14
16.56	102.07
16.72	101.91
16.88	101.94
17.04	101.99
17.20	101.79
17.36	101.82
17.52	101.75
17.68	101.72
17.84	101.68
18.00	101.71
18.16	101.74
18.32	101.62
18.48	101.57
18.64	101.66
18.80	101.55
18.96	101.41
19.12	101.48
19.28	101.57
19.44	101.68

APPENDIX E

Selected Listings of Experimental Temperature Data

First run in each of series 1-8 (Table 5.3). THETA is the platinum heater temperature less the ambient temperature. The NUSSELT NUMBER is based on the superficial heat flux.

RUN NUMBER AP2-3

WIRE LENGTH = .096 M
WIRE DIAMETER = .00025 M
AMBIENT TEMP. = 100 C
PRESSURE = MAX 377.11, DECOMPRESS FROM 373.67 KPA
INITIAL RESIS. = .316163 OHMS AT 160 C
SIGMA = 0

TIME (S)	HEAT FLUX (W/M*M)	THETA (C)	NUSSELT NUMBER
0.080	426970	59.401	2.6662
0.240	426850	59.747	2.6500
0.400	426840	59.651	2.6542
0.560	426810	59.570	2.6576
0.720	426850	59.465	2.6625
0.880	426830	59.373	2.6665
1.040	426810	59.251	2.6719
1.200	426830	59.105	2.6786
1.360	426900	58.889	2.6882
1.520	426810	58.743	2.6950
1.680	426810	58.553	2.7038
1.840	426850	58.317	2.7149
2.000	426820	57.909	2.7339
2.160	426790	57.869	2.7356
2.320	426800	57.716	2.7429
2.480	426770	57.526	2.7517
2.640	426780	57.130	2.7709
2.800	426770	56.834	2.7853
2.960	426770	56.610	2.7962
3.120	426760	56.363	2.8085
3.280	426760	56.189	2.8172
3.440	426780	55.830	2.8354
3.600	426740	55.339	2.8603
3.760	426730	55.382	2.8580
3.920	426720	55.129	2.8711
4.080	426720	54.805	2.8880
4.240	426700	54.082	2.9265
4.400	426700	53.884	2.9373
4.560	426650	53.400	2.9635
4.720	426700	53.071	2.9823
4.880	426640	53.349	2.9669
5.040	426680	52.840	2.9952
5.200	426630	53.059	2.9828
5.360	426630	51.453	3.0755
5.520	426650	51.621	3.0657
5.680	426640	51.483	3.0738
5.840	426660	50.538	3.1314
6.000	426660	50.999	3.1031
6.160	426610	50.542	3.1308
6.320	426640	50.305	3.1458
6.480	426600	49.932	3.1690
6.640	426600	49.944	3.1683

TIME (S)	HEAT FLUX (W/M*M)	THETA (C)	NUSSELT NUMBER
6.800	426610	50.093	3.1589
6.960	426590	50.061	3.1607
7.120	426580	49.658	3.1864
7.280	426560	49.218	3.2147
7.440	426490	47.480	3.3318
7.600	426450	46.815	3.3788
7.760	426440	46.422	3.4073
7.920	426470	46.776	3.3818
8.080	426460	46.644	3.3913
8.240	426460	47.179	3.3529
8.400	426460	46.464	3.4044
8.560	426450	46.860	3.3756
8.720	426460	47.009	3.3650
8.880	426450	46.687	3.3881
9.040	426460	46.106	3.4309
9.200	426450	45.919	3.4447
9.360	426430	46.260	3.4192
9.520	426450	46.210	3.4231
9.680	426430	46.362	3.4117
9.840	426480	46.617	3.4007
10.00	426450	46.315	3.4153
10.16	426440	46.348	3.4127
10.32	426450	45.684	3.4625
10.48	426440	45.910	3.4453
10.64	426480	46.151	3.4277
10.80	426460	45.099	3.5075
10.96	426420	45.013	3.5139
11.12	426450	44.759	3.5341
11.28	426440	44.546	3.5509
11.44	426450	44.452	3.5584
11.60	426450	44.588	3.5476
11.76	426420	44.289	3.5713
11.92	426450	44.732	3.5362
12.08	426450	43.979	3.5967
12.24	426460	44.384	3.5635
12.40	426430	43.564	3.6308
12.56	426420	43.162	3.6645
12.72	426490	44.138	3.5840
12.88	426470	44.261	3.5739
13.04	426460	44.212	3.5778
13.20	426450	44.071	3.5892
13.36	426460	43.989	3.5960
13.52	426440	43.854	3.6069
13.68	426460	43.928	3.6009
13.84	426450	42.186	3.7495
14.00	426430	43.401	3.6445
14.16	426430	43.522	3.6343
14.32	426450	42.438	3.7272

RUN NUMBER AP2-3 PAGE 3

TIME (S)	HEAT FLUX (W/M*M)	THETA (C)	NUSSELT NUMBER
14.48	426450	42.820	3.6940
14.64	426450	43.294	3.6536
14.80	426440	42.476	3.7239
14.96	426430	42.352	3.7347
15.12	426470	43.106	3.6696
15.28	426450	43.215	3.6602
15.44	426510	43.511	3.6359
15.60	426470	43.139	3.6669
15.76	426470	43.751	3.6156
15.92	426500	43.814	3.6107
16.08	426490	43.759	3.6150
16.24	426490	43.446	3.6412
16.40	426490	43.790	3.6126
16.56	426500	44.102	3.5870
16.72	426480	43.001	3.6787
16.88	426490	43.441	3.6416
17.04	426470	42.963	3.6819
17.20	426490	44.308	3.5703
17.36	426450	42.529	3.7193
17.52	426520	43.524	3.6348
17.68	426440	42.675	3.7065
17.84	426500	43.407	3.6445
18.00	426510	43.968	3.5981
18.16	426500	43.698	3.6202
18.32	426530	43.552	3.6326
18.48	426500	43.452	3.6408
18.64	426550	43.637	3.6257
18.80	426460	43.376	3.6468
18.96	426460	42.168	3.7512
19.12	426520	43.196	3.6625
19.28	426530	43.489	3.6379
19.44	426490	42.815	3.6949
19.60	426490	43.031	3.6763
19.76	426490	43.392	3.6456
19.92	426500	43.201	3.6619
20.08	426520	43.108	3.6699
20.24	426510	43.152	3.6661

RUN NUMBER AP3-1

WIRE LENGTH = .096 M
WIRE DIAMETER = .00025 M
AMBIENT TEMP. = 100 C
PRESSURE = CECOMPRESS FROM 515.01 KPA
INITIAL RESIS. = .316156 OHMS AT 160 C
SIGMA = C

TIME (S)	HEAT FLUX (W/M*M)	THETA (C)	NUSSELT NUMBER
-1.84	423510	59.983	2.6188
-1.68	423500	59.991	2.6185
-1.52	423530	59.977	2.6193
-1.36	423540	59.987	2.6189
-1.20	423530	59.979	2.6192
-1.04	423520	59.980	2.6191
-.880	423520	59.980	2.6191
-.720	423510	59.982	2.6189
-.560	423510	59.983	2.6189
-.400	423530	59.966	2.6197
-.240	423520	59.974	2.6194
-.080	423500	59.955	2.6201
0.080	423540	60.002	2.6182
0.240	423520	60.002	2.6181
0.400	423530	60.003	2.6182
0.560	423560	60.002	2.6184
0.720	423540	60.038	2.6167
0.880	423570	60.006	2.6183
1.040	423540	60.002	2.6182
1.200	423580	60.013	2.6180
1.360	423570	60.016	2.6178
1.520	423570	59.984	2.6192
1.680	423590	59.930	2.6217
1.840	423590	59.873	2.6242
2.000	423590	59.841	2.6256
2.160	423590	59.801	2.6274
2.320	423600	59.762	2.6292
2.480	423610	59.689	2.6324
2.640	423620	59.600	2.6364
2.800	423610	59.458	2.6426
2.960	423640	59.273	2.6511
3.120	423620	59.165	2.6558
3.280	423630	59.062	2.6605
3.440	423610	58.929	2.6663
3.600	423640	58.814	2.6717
3.760	423620	58.703	2.6767
3.920	423600	58.503	2.6857
4.080	423600	58.280	2.6960
4.240	423600	58.117	2.7035
4.400	423560	57.915	2.7127
4.560	423580	57.776	2.7194
4.720	423600	57.700	2.7230

TIME (S)	HEAT FLUX (W/M*M)	THETA (C)	NUSSELT NUMBER
4.880	423600	57.942	2.7117
5.040	423580	57.371	2.7386
5.200	423570	57.096	2.7517
5.360	423580	56.875	2.7624
5.520	423570	56.590	2.7763
5.680	423580	56.556	2.7780
5.840	423550	56.209	2.7950
6.000	423530	55.367	2.8374
6.160	423540	55.307	2.8405
6.320	423550	55.201	2.8461
6.480	423540	55.405	2.8355
6.640	423490	55.205	2.8454
6.800	423480	54.484	2.8830
6.960	423530	54.049	2.9065
7.120	423490	53.880	2.9154
7.280	423490	53.877	2.9155
7.440	423470	53.872	2.9156
7.600	423480	53.584	2.9314
7.760	423470	52.972	2.9652
7.920	423460	51.352	3.0587
8.080	423480	51.553	3.0466
8.240	423490	51.950	3.0237
8.400	423470	51.954	3.0233
8.560	423460	51.492	3.0503
8.720	423460	51.787	3.0330
8.880	423470	51.066	3.0759
9.040	423450	50.727	3.0963
9.200	423450	50.692	3.0985
9.360	423440	50.552	3.1069
9.520	423450	50.289	3.1233
9.680	423450	50.319	3.1214
9.840	423420	50.458	3.1126
10.00	423440	50.580	3.1052
10.16	423460	50.948	3.0829
10.32	423470	50.888	3.0866
10.48	423470	51.050	3.0769
10.64	423460	50.642	3.1016
10.80	423450	50.824	3.0904
10.96	423450	50.935	3.0837
11.12	423430	50.959	3.0820
11.28	423430	50.227	3.1270
11.44	423380	49.146	3.1954
11.60	423400	48.873	3.2134
11.76	423420	49.718	3.1589
11.92	423400	49.717	3.1589
12.08	423410	49.747	3.1570
12.24	423390	49.724	3.1583
12.40	423410	49.302	3.1855

TIME (S)	HEAT FLUX (W/M*M)	THETA (C)	NUSSELT NUMBER
12.56	423390	48.584	3.2324
12.72	423380	48.925	3.2098
12.88	423400	48.951	3.2083
13.04	423350	48.598	3.2312
13.20	423350	48.761	3.2203
13.36	423360	49.317	3.1842
13.52	423360	48.952	3.2079
13.68	423320	48.201	3.2576
13.84	423270	47.952	3.2741
14.00	423220	44.776	3.5059
14.16	423240	46.039	3.4099
14.32	423260	46.312	3.3899
14.48	423260	45.826	3.4259
14.64	423210	45.540	3.4471
14.80	423250	46.596	3.3692
14.96	423200	44.104	3.5591
15.12	423230	46.100	3.4053
15.28	423220	46.616	3.3675
15.44	423250	46.858	3.3504
15.60	423230	46.310	3.3899
15.76	423230	46.346	3.3872
15.92	423220	46.236	3.3952
16.08	423250	46.619	3.3676
16.24	423210	46.611	3.3678
16.40	423220	46.866	3.3496
16.56	423210	45.953	3.4160
16.72	423210	45.971	3.4147
16.88	423230	45.057	3.4841
17.04	423190	45.458	3.4531
17.20	423220	45.264	3.4681
17.36	423210	45.707	3.4344
17.52	423220	45.617	3.4413
17.68	423200	45.858	3.4231
17.84	423210	45.839	3.4245
18.00	423250	45.971	3.4225
18.16	423240	45.725	3.4333
18.32	423250	45.789	3.4285

RUN NUMBER AP3-7

WIRE LENGTH = .096 M
WIRE DIAMETER = .00025 M
AMBIENT TEMP. = 100 C
PRESSURE = DECOMPRESS FROM 446.06 KPA
INITIAL RESIS. = .316133 OHMS AT 159.9 C
SIGMA = 0

TIME (S)	HEAT FLUX (W/M**M)	THETA (C)	NUSSELT NUMBER
-1.84	418620	59.829	2.5953
-1.68	418610	59.822	2.5956
-1.52	418610	59.827	2.5954
-1.36	418620	59.817	2.5958
-1.20	418590	59.808	2.5960
-1.04	418610	59.801	2.5964
-.880	418600	59.803	2.5963
-.720	418610	59.799	2.5965
-.560	418600	59.792	2.5968
-.400	418620	59.795	2.5968
-.240	418590	59.759	2.5969
-.080	418590	59.773	2.5975
0.080	418600	59.813	2.5959
0.240	418610	59.813	2.5959
0.400	418600	59.815	2.5958
0.560	418580	59.846	2.5943
0.720	418600	59.814	2.5958
0.880	418610	59.810	2.5961
1.040	418590	59.814	2.5958
1.200	418610	59.832	2.5951
1.360	418600	59.829	2.5951
1.520	418590	59.838	2.5947
1.680	418580	59.827	2.5952
1.840	418560	59.844	2.5943
2.000	418580	59.755	2.5983
2.160	418570	59.626	2.6038
2.320	418590	59.405	2.6136
2.480	418560	59.197	2.6227
2.640	418550	59.087	2.6275
2.800	418560	58.951	2.6336
2.960	418570	58.712	2.6444
3.120	418550	58.642	2.6474
3.280	418560	58.456	2.6558
3.440	418530	58.235	2.6656
3.600	418570	58.130	2.6708
3.760	418540	57.857	2.6833
3.920	418550	57.693	2.6910
4.080	418530	57.629	2.6938
4.240	418510	57.108	2.7183
4.400	418540	57.093	2.7191
4.560	418520	56.973	2.7248
4.720	418520	56.699	2.7379

TIME (S)	HEAT FLUX (W/M**M)	THETA (C)	NUSSELT NUMBER
4.880	418480	56.536	2.7455
5.040	418480	55.382	2.7776
5.200	418500	55.207	2.8118
5.360	418450	54.458	2.8501
5.520	418460	54.641	2.8406
5.680	418430	53.975	2.8755
5.840	418420	54.119	2.8678
6.000	418420	54.139	2.8667
6.160	418420	53.964	2.8760
6.320	418420	53.484	2.9018
6.480	418410	53.352	2.9089
6.640	418370	53.214	2.9162
6.800	418370	52.894	2.9338
6.960	418380	53.094	2.9229
7.120	418380	52.309	2.9667
7.280	418380	52.295	2.9675
7.440	418350	52.321	2.9658
7.600	418380	52.215	2.9720
7.760	418350	52.120	2.9772
7.920	418360	51.772	2.9973
8.080	418320	51.334	3.0226
8.240	418300	51.408	3.0181
8.400	418340	51.592	3.0076
8.560	418320	51.454	3.0155
8.720	418320	51.198	3.0307
8.880	418330	51.553	3.0099
9.040	418310	51.328	3.0230
9.200	418320	51.233	3.0286
9.360	418340	51.572	3.0088
9.520	418350	51.300	3.0249
9.680	418300	50.326	3.0830
9.840	418300	51.108	3.0358
10.00	418360	51.392	3.0196
10.16	418310	50.961	3.0447
10.32	418350	51.680	3.0026
10.48	418330	51.613	3.0064
10.64	418310	50.744	3.0577
10.80	418350	51.602	3.0071
10.96	418350	51.899	2.9899
11.12	418340	51.532	3.0111
11.28	418330	50.435	3.0765
11.44	418330	51.537	3.0108
11.60	418340	50.756	3.0572
11.76	418300	49.925	3.1140
11.92	418340	49.952	3.1064
12.08	418290	48.721	3.1945
12.24	418250	47.689	3.2531
12.40	418310	48.446	3.2027

RUN NUMBER AP3-7 PAGE 3

TIME (S)	HEAT FLUX (W/M**M)	THETA (C)	NUSSELT NUMBER
12.56	418300	48.700	3.1859
12.72	418310	49.425	3.1393
12.88	418310	49.447	3.1379
13.04	418290	48.732	3.1838
13.20	418310	48.631	3.1906
13.36	418300	49.080	3.1613
13.52	418340	49.146	3.1573
13.68	418320	49.335	3.1451
13.84	418290	48.167	3.2211
14.00	418320	49.193	3.1542
14.16	418300	48.777	3.1809
14.32	418320	49.071	3.1620
14.48	418310	48.575	3.1942
14.64	418290	47.653	3.2559
14.80	418300	47.003	3.3010
14.96	418280	46.512	3.3356
15.12	418280	46.088	3.3664
15.28	418280	46.849	3.3117
15.44	418240	46.379	3.3450
15.60	418300	46.956	3.3043
15.76	418280	47.055	3.2971
15.92	418260	46.326	3.3489
16.08	418270	46.575	3.3311
16.24	418250	46.329	3.3486
16.40	418290	46.300	3.3510
16.56	418300	46.762	3.3180
16.72	418290	47.265	3.2826
16.88	418280	47.102	3.2939
17.04	418280	46.775	3.3169
17.20	418300	47.280	3.2817
17.36	418290	47.121	3.2926
17.52	418280	45.322	3.4232
17.68	418250	43.912	3.5329
17.84	418210	42.937	3.6128
18.00	418260	44.138	3.5149
18.16	418220	43.410	3.5736
18.32	418240	43.674	3.5521

RUN NUMBER AP4-4

WIRE LENGTH = .096 M
WIRE DIAMETER = .00025 M
AMBIENT TEMP. = 100 C
PRESSURE = DECOMPRESS FROM 583.96 KPA
INITIAL RESIS. = .316095 OHMS AT 159.9 C
SIGMA = 0

TIME (S)	HEAT FLUX (W/M**M)	THETA (C)	NUSSELT NUMBER
-1.84	408170	60.049	2.5213
-1.68	408180	60.040	2.5217
-1.52	408160	60.060	2.5207
-1.36	408200	60.065	2.5207
-1.20	408120	60.069	2.5201
-1.04	408170	60.055	2.5210
-.880	408170	60.067	2.5205
-.720	408160	60.057	2.5208
-.560	408140	60.037	2.5216
-.400	408140	60.030	2.5218
-.240	408190	60.037	2.5219
-.080	408150	60.044	2.5214
0.080	408140	60.045	2.5213
0.240	408170	60.033	2.5219
0.400	408150	60.021	2.5223
0.560	408150	60.009	2.5228
0.720	408130	60.021	2.5222
0.880	408140	59.998	2.5232
1.040	408150	59.994	2.5235
1.200	408140	59.978	2.5240
1.360	408130	59.972	2.5243
1.520	408120	59.950	2.5251
1.680	408120	59.950	2.5251
1.840	408130	59.927	2.5261
2.000	408160	59.926	2.5264
2.160	408160	59.911	2.5270
2.320	408150	59.907	2.5271
2.480	408100	59.895	2.5273
2.640	408150	59.889	2.5278
2.800	408120	59.878	2.5281
2.960	408170	59.868	2.5289
3.120	408180	59.876	2.5286
3.280	408120	59.863	2.5288
3.440	408180	59.850	2.5297
3.600	408150	59.801	2.5316
3.760	408170	59.801	2.5317
3.920	408120	59.799	2.5315
4.080	408140	59.759	2.5333
4.240	408160	59.696	2.5361
4.400	408110	59.450	2.5463
4.560	408130	59.080	2.5623
4.720	408130	59.001	2.5658

TIME (S)	HEAT FLUX (W/M*M)	THETA (C)	NUSSELT NUMBER
4.380	408110	59.921	2.5691
5.040	408130	58.691	2.5798
5.200	408140	58.745	2.5771
5.360	409120	58.547	2.5856
5.520	408110	58.434	2.5905
5.680	408100	57.759	2.6208
5.840	408120	57.203	2.6461
6.000	408110	57.326	2.6406
6.160	408130	57.282	2.6428
6.320	408120	57.109	2.6507
6.480	408100	57.090	2.6514
6.640	408120	56.729	2.6685
6.800	408090	56.131	2.6967
6.960	408090	56.170	2.6948
7.120	408070	55.971	2.7043
7.280	408060	55.730	2.7159
7.440	408090	55.200	2.7422
7.600	408090	54.994	2.7524
7.760	408040	54.209	2.7920
7.920	408040	54.081	2.7986
8.080	409010	54.026	2.8012
8.240	408030	53.599	2.8237
8.400	408030	53.586	2.8244
8.560	408030	53.729	2.8169
8.720	408060	54.070	2.7993
8.880	408040	53.937	2.8113
9.040	408050	54.009	2.8024
9.200	408030	54.124	2.7963
9.360	408060	53.842	2.8111
9.520	408020	53.843	2.8109
9.680	408000	53.399	2.8341
9.840	408020	53.329	2.8380
10.00	408000	53.559	2.8257
10.16	408010	53.582	2.8244
10.32	408030	53.773	2.8146
10.48	407990	53.784	2.8137
10.64	408030	53.668	2.8201
10.80	408020	54.054	2.7999
10.96	409040	53.819	2.8122
11.12	408000	53.054	2.8525
11.28	408000	53.952	2.8050
11.44	408030	53.750	2.8158
11.60	408030	53.675	2.8197
11.76	408020	53.855	2.8102
11.92	408000	53.745	2.8158
12.08	407980	53.924	2.8063
12.24	408030	54.001	2.8027
12.40	408000	53.708	2.8177

TIME (S)	HEAT FLUX (W/M*M)	THETA (C)	NUSSELT NUMBER
12.56	408010	52.790	2.8668
12.72	408000	53.410	2.8335
12.88	407980	52.987	2.8560
13.04	407990	51.923	2.9145
13.20	407960	51.380	2.9451
13.36	408010	52.242	2.8968
13.52	407960	52.003	2.9099
13.68	407980	51.900	2.9158
13.84	407990	52.175	2.9005
14.00	407980	52.317	2.8925
14.16	407980	51.896	2.9160
14.32	408000	52.075	2.9061
14.48	407990	52.365	2.8900
14.64	408010	52.605	2.8769
14.80	408000	52.887	2.8615
14.96	407980	52.723	2.8703
15.12	408000	52.507	2.8822
15.28	407960	51.395	2.9442
15.44	407970	51.718	2.9259
15.60	407970	51.604	2.9324
15.76	407980	52.526	2.8810
15.92	408000	52.759	2.8684
16.08	407980	52.735	2.8696
16.24	407990	52.847	2.8636
16.40	407980	52.526	2.8810
16.56	408010	52.261	2.8958
16.72	407980	52.149	2.9018
16.88	407970	51.911	2.9151
17.04	408010	52.146	2.9022
17.20	407960	51.876	2.9170
17.36	407960	51.459	2.9406
17.52	407990	52.641	2.8747
17.68	407980	52.229	2.8974
17.84	407980	52.229	2.8974
18.00	407960	52.177	2.9002
18.16	407940	49.850	3.0354
18.32	407970	51.950	2.9129

RUN NUMBER AP7-2

WIRE LENGTH = .096 M
WIRE DIAMETER = .00025 M
AMBIENT TEMP. = 100 C
PRESSURE = DECOMPRESS FROM 377.11 KPA
INITIAL RESIS. = .316161 OHMS AT 160 C
SIGMA = 0

TIME (S)	HEAT FLUX (W/M*M)	THETA (C)	NUSSELT NUMBER
-1.84	407260	59.625	2.5335
-1.68	407270	59.630	2.5333
-1.52	407260	59.627	2.5335
-1.36	407250	59.642	2.5327
-1.20	407270	59.632	2.5333
-1.04	407290	59.636	2.5332
-.880	407280	59.633	2.5331
-.720	407260	59.634	2.5331
-.560	407250	59.638	2.5329
-.400	407280	59.630	2.5334
-.240	407260	59.636	2.5330
-.080	407250	59.659	2.5320
0.080	407260	59.729	2.5291
0.240	407270	59.651	2.5325
0.400	407260	59.629	2.5334
0.560	407240	59.607	2.5342
0.720	407280	59.592	2.5350
0.880	407280	59.577	2.5357
1.040	407290	59.553	2.5367
1.200	407280	59.544	2.5371
1.360	407250	59.532	2.5374
1.520	407270	59.515	2.5382
1.680	407260	59.514	2.5382
1.840	407270	59.489	2.5394
2.000	407280	59.452	2.5410
2.160	407240	59.424	2.5419
2.320	407280	59.402	2.5431
2.480	407250	59.319	2.5465
2.640	407260	59.258	2.5492
2.800	407290	59.239	2.5502
2.960	407290	59.155	2.5538
3.120	407270	59.089	2.5566
3.280	407250	59.050	2.5581
3.440	407270	59.037	2.5588
3.600	407250	58.985	2.5609
3.760	407230	58.936	2.5630
3.920	407230	58.856	2.5664
4.080	407220	58.785	2.5695
4.240	407230	58.747	2.5712
4.400	407210	58.689	2.5736
4.560	407180	58.611	2.5768
4.720	407210	58.492	2.5823

TIME (S)	HEAT FLUX (W/M*M)	THETA (C)	NUSSELT NUMBER
4.880	407200	58.413	2.5857
5.040	407210	58.317	2.5900
5.200	407200	58.266	2.5922
5.360	407180	58.167	2.5965
5.520	407190	58.069	2.6010
5.680	407160	58.041	2.6020
5.840	407190	57.864	2.6101
6.000	407160	57.754	2.6150
6.160	407170	57.709	2.6171
6.320	407160	57.564	2.6236
6.480	407140	57.460	2.6282
6.640	407160	57.340	2.6339
6.800	407130	57.185	2.6408
6.960	407110	57.087	2.6452
7.120	407120	56.981	2.6502
7.280	407120	56.951	2.6516
7.440	407110	56.796	2.6587
7.600	407090	56.667	2.6647
7.760	407100	56.475	2.6738
7.920	407090	56.319	2.6811
8.080	407070	56.196	2.6869
8.240	407090	56.124	2.6904
8.400	407090	55.932	2.6997
8.560	407070	55.800	2.7060
8.720	407100	55.804	2.7059
8.880	407110	55.724	2.7098
9.040	407110	55.464	2.7225
9.200	407090	55.180	2.7364
9.360	407080	54.698	2.7605
9.520	407080	54.539	2.7686
9.680	407100	54.571	2.7671
9.840	407090	54.483	2.7715
10.00	407110	54.462	2.7726
10.16	407080	54.050	2.7936
10.32	407080	53.939	2.7993
10.48	407050	53.288	2.8333
10.64	407070	53.265	2.8347
10.80	407070	53.407	2.8272
10.96	407040	53.037	2.8467
11.12	407090	52.879	2.8556
11.28	407080	53.044	2.8466
11.44	407090	53.378	2.8288
11.60	407090	53.367	2.8295
11.76	407100	52.753	2.8624
11.92	407110	52.706	2.8651
12.08	407120	52.387	2.8825
12.24	407080	52.097	2.8984
12.40	407100	52.336	2.8852

RUN NUMBER AP7-2 PAGE 3

TIME (S)	HEAT FLUX (W/M**2)	THETA (C)	NUSSELT NUMBER
12.56	407C90	52.421	2.8805
12.72	407100	51.902	2.9094
12.88	407090	52.344	2.8848
13.04	407C90	51.874	2.9108
13.20	407100	51.744	2.9183
13.36	407C40	51.637	2.9238
13.52	407110	51.350	2.9407
13.68	407100	51.312	2.9428
13.84	407060	50.777	2.9736
14.00	407080	51.405	2.9373
14.16	407C30	50.694	2.9782
14.32	407070	50.702	2.9780
14.48	407C80	50.532	2.9881
14.64	407070	50.370	2.9976
14.80	407030	49.826	3.0301
14.96	407C90	50.209	3.0073
15.12	407100	50.270	3.0038
15.28	407070	50.607	2.9836
15.44	407060	50.308	3.0012
15.60	407C50	50.370	2.9975
15.76	407C60	50.363	2.9980
15.92	407080	50.283	3.0029
16.08	407C50	50.266	3.0037
16.24	407050	49.431	3.0544
16.40	407C30	48.846	3.0909
16.56	407000	48.014	3.1442
16.72	407030	48.600	3.1064
16.88	407C10	48.658	3.1026
17.04	406980	47.860	3.1541
17.20	407040	48.786	3.0947
17.36	407030	48.061	3.1414
17.52	407040	48.735	3.0980
17.68	407C00	47.803	3.1580
17.84	407000	48.529	3.1108
18.00	407C20	48.553	3.1095
18.16	407000	48.394	3.1195
18.32	407C40	48.131	3.1369

RUN NUMBER AP8-4

WIRE LENGTH = .096 M
WIRE DIAMETER = .00025 M
AMBIENT TEMP. = 100 C
PRESSURE = MAX 1480.3, DECOMPRESS FROM 377.11 KPA
INITIAL RESIS. = .316205 OHMS AT 160 C
SIGMA = 0

TIME (S)	HEAT FLUX (W/M**2)	THETA (C)	NUSSELT NUMBER
-1.84	419280	59.844	2.5987
-1.68	419300	59.848	2.5987
-1.52	419310	59.855	2.5984
-1.36	419310	59.864	2.5980
-1.20	419320	59.859	2.5984
-1.04	419290	59.866	2.5978
-.880	419310	59.871	2.5977
-.720	419290	59.880	2.5973
-.560	419280	59.872	2.5975
-.400	419290	59.888	2.5969
-.240	419270	59.885	2.5969
-.080	419830	60.093	2.5914
0.080	419250	59.932	2.5948
0.240	419260	59.895	2.5964
0.400	419280	59.900	2.5963
0.560	419260	59.900	2.5962
0.720	419280	59.898	2.5964
0.880	419280	59.894	2.5966
1.040	419260	59.879	2.5971
1.200	419290	59.877	2.5974
1.360	419260	59.859	2.5980
1.520	419280	59.850	2.5985
1.680	419290	59.841	2.5989
1.840	419280	59.828	2.5995
2.000	419280	59.810	2.6002
2.160	419270	59.790	2.6010
2.320	419300	59.773	2.6019
2.480	419290	59.761	2.6024
2.640	419250	59.730	2.6035
2.800	419280	59.719	2.6042
2.960	419270	59.694	2.6052
3.120	419280	59.676	2.6061
3.280	419280	59.646	2.6074
3.440	419280	59.620	2.6085
3.600	419290	59.587	2.6100
3.760	419270	59.545	2.6118
3.920	419280	59.530	2.6124
4.080	419280	59.491	2.6142
4.240	419260	59.459	2.6155
4.400	419250	59.419	2.6172
4.560	419260	59.385	2.6187
4.720	419270	59.350	2.6204

TIME (S)	HEAT FLUX (W/M*M)	THETA (C)	NUSSELT NUMBER
4.880	419270	59.314	2.6219
5.040	419270	59.290	2.6230
5.200	419260	59.243	2.6250
5.360	419250	59.200	2.6268
5.520	419280	59.183	2.6276
5.680	419270	59.149	2.6292
5.840	419240	59.096	2.6314
6.000	419270	59.094	2.6317
6.160	419270	59.067	2.6329
6.320	419270	59.012	2.6353
6.480	419270	58.978	2.6369
6.640	419270	58.952	2.6380
6.800	419300	58.899	2.6405
6.960	419270	58.881	2.6412
7.120	419290	58.832	2.6435
7.280	419270	58.786	2.6455
7.440	419250	58.760	2.6465
7.600	419270	58.717	2.6486
7.760	419280	58.660	2.6512
7.920	419300	58.633	2.6525
8.080	419280	58.598	2.6540
8.240	419260	58.573	2.6550
8.400	419290	58.586	2.6546
8.560	419300	58.503	2.6584
8.720	419300	58.428	2.6618
8.880	419240	58.369	2.6641
9.040	419230	57.672	2.6963
9.200	419230	56.882	2.7337
9.360	419210	56.932	2.7312
9.520	419240	56.697	2.7427
9.680	419210	56.630	2.7458
9.840	419220	56.727	2.7412
10.00	419220	56.433	2.7555
10.16	419220	56.457	2.7543
10.32	419240	56.129	2.7705
10.48	419240	56.044	2.7747
10.64	419200	54.944	2.8299
10.80	419210	55.074	2.8234
10.96	419210	55.068	2.8237
11.12	419200	55.126	2.8206
11.28	419230	55.397	2.8070
11.44	419200	55.222	2.8157
11.60	419220	54.986	2.8279
11.76	419220	55.334	2.8102
11.92	419230	55.309	2.8115
12.08	419210	55.020	2.8261
12.24	419190	54.305	2.8632
12.40	419210	54.674	2.8440

TIME (S)	HEAT FLUX (W/M*M)	THETA (C)	NUSSELT NUMBER
12.56	419200	54.766	2.8392
12.72	419250	54.856	2.8348
12.88	419230	54.543	2.8510
13.04	419210	54.557	2.8501
13.20	419180	54.519	2.8519
13.36	419190	53.974	2.8808
13.52	419200	53.964	2.8814
13.68	419210	53.926	2.8835
13.84	419190	53.781	2.8911
14.00	419220	53.967	2.8813
14.16	419200	53.717	2.8945
14.32	419200	53.679	2.8967
14.48	419200	53.841	2.8879
14.64	419190	53.543	2.9040
14.80	419210	54.193	2.8693
14.96	419190	53.541	2.9040
15.12	419210	53.694	2.8959
15.28	419210	53.493	2.9068
15.44	419210	54.016	2.8787
15.60	419210	53.823	2.8890
15.76	419200	53.866	2.8866
15.92	419210	53.680	2.8967
16.08	419240	54.061	2.8764
16.24	419240	54.076	2.8756
16.40	419240	54.265	2.8657
16.56	419230	54.590	2.8485
16.72	419240	54.565	2.8499
16.88	419240	54.607	2.8477
17.04	419240	54.139	2.8723
17.20	419240	54.593	2.8484
17.36	419230	54.582	2.8489
17.52	419250	54.275	2.8652
17.68	419200	54.552	2.8503
17.84	419220	54.705	2.8425
18.00	419230	54.413	2.8578
18.16	419200	54.542	2.8509
18.32	419260	54.564	2.8501

RUN NUMBER AP8-7

WIRE LENGTH = .096 M
WIRE DIAMETER = .00025 M
AMBIENT TEMP. = 100 C
PRESSURE = MAX 1480.3, DECOMPRESS FROM 377.11 KPA
INITIAL RESIS. = .316198 OHMS AT 160 C
SIGMA = 0

TIME (S)	HEAT FLUX (W/M*M)	THETA (C)	NUSSELT NUMBER
-1.84	417990	60.262	2.5728
-1.68	418000	60.261	2.5729
-1.52	418020	60.268	2.5727
-1.36	418020	60.266	2.5728
-1.20	418020	60.273	2.5725
-1.04	418000	60.272	2.5724
-.880	418010	60.280	2.5721
-.720	418030	60.273	2.5725
-.560	418020	60.282	2.5721
-.400	418000	60.291	2.5716
-.240	418010	60.300	2.5713
-.080	418010	60.295	2.5715
0.080	418020	60.306	2.5711
0.240	418000	60.319	2.5704
0.400	418020	60.327	2.5702
0.560	418030	60.331	2.5701
0.720	418000	60.304	2.5711
0.880	418020	60.287	2.5719
1.040	418010	60.273	2.5724
1.200	418010	60.283	2.5720
1.360	418000	60.258	2.5731
1.520	418020	60.253	2.5733
1.680	418030	60.245	2.5738
1.340	417990	60.219	2.5746
2.000	418030	60.205	2.5754
2.160	418010	60.188	2.5761
2.320	418010	60.163	2.5771
2.480	418030	60.139	2.5783
2.640	417990	60.111	2.5793
2.800	418040	60.085	2.5807
2.960	418030	60.061	2.5816
3.120	417990	60.027	2.5829
3.280	418030	59.975	2.5853
3.440	418000	59.940	2.5866
3.600	418000	59.912	2.5878
3.760	418030	59.877	2.5896
3.920	418030	59.851	2.5907
4.080	418030	59.812	2.5924
4.240	417990	59.759	2.5944
4.400	418000	59.746	2.5951
4.560	417990	59.704	2.5968
4.720	418010	59.661	2.5988

TIME (S)	HEAT FLUX (W/M*M)	THETA (C)	NUSSELT NUMBER
4.880	418020	59.616	2.6008
5.040	417980	59.586	2.6019
5.200	417990	59.538	2.6040
5.360	418010	59.532	2.6044
5.520	418010	59.490	2.6063
5.680	418010	59.455	2.6078
5.840	418010	59.434	2.6088
6.000	418010	59.416	2.6096
6.160	417990	59.399	2.6102
6.320	418000	59.381	2.6110
6.480	418010	59.307	2.6143
6.640	418000	59.332	2.6132
6.800	418020	59.296	2.6148
6.960	418010	59.283	2.6154
7.120	418030	59.238	2.6175
7.280	418000	59.232	2.6176
7.440	417990	59.164	2.6205
7.600	418010	59.164	2.6207
7.760	418000	59.108	2.6231
7.920	418020	59.065	2.6251
8.080	418010	59.034	2.6264
8.240	417970	58.968	2.6336
8.400	418010	58.716	2.6406
8.560	417970	58.496	2.6504
8.720	418000	58.777	2.6379
8.880	417980	58.509	2.6498
9.040	417960	58.279	2.6602
9.200	418000	58.128	2.6673
9.360	417960	57.947	2.6754
9.520	417970	57.556	2.6936
9.680	418000	57.767	2.6840
9.840	417960	57.808	2.6818
10.00	417950	57.804	2.6819
10.16	417970	57.696	2.6870
10.32	417990	57.739	2.6852
10.48	417980	57.780	2.6832
10.64	417940	57.702	2.6866
10.80	417970	57.738	2.6851
10.96	417970	57.754	2.6144
11.12	417970	57.692	2.6872
11.28	417990	57.758	2.6843
11.44	417980	57.803	2.6822
11.60	417960	56.293	2.7540
11.76	417940	56.378	2.7497
11.92	417930	56.489	2.7442
12.08	417950	56.471	2.7452
12.24	417960	56.425	2.7475
12.40	417940	56.420	2.7476

RUN NUMBER AP8-7 PAGE 3

TIME (S)	HEAT FLUX (W/M*M)	THETA (C)	NUSSELT NUMBER
12.56	417950	56.502	2.7437
12.72	417940	56.163	2.7602
12.88	417960	55.942	2.7712
13.04	417920	56.172	2.7596
13.20	417940	55.855	2.7754
13.36	417930	55.740	2.7812
13.52	417950	55.843	2.7761
13.68	417960	55.885	2.7741
13.84	417950	56.034	2.7667
14.00	417970	56.564	2.7409
14.16	417970	56.522	2.7428
14.32	417980	56.699	2.7343
14.48	418000	55.956	2.7708
14.64	417950	56.022	2.7672
14.80	417940	56.383	2.7495
14.96	417950	55.939	2.7714
15.12	417990	56.637	2.7375
15.28	417970	56.168	2.7602
15.44	417950	56.245	2.7562
15.60	417950	56.552	2.7413
15.76	417950	56.339	2.7517
15.92	417980	56.025	2.7673
16.08	417990	56.031	2.7671
16.24	417940	56.808	2.7289
16.40	417960	55.705	2.7830
16.56	417940	55.708	2.7828
16.72	417990	55.993	2.7689
16.88	417970	55.933	2.7718
17.04	417940	56.276	2.7546
17.20	417990	55.717	2.7827
17.36	417960	56.040	2.7664
17.52	417960	55.886	2.7740
17.68	417980	55.836	2.7766
17.84	417950	56.291	2.7540
18.00	417960	56.134	2.7618
18.16	417960	55.773	2.7797
18.32	417980	56.209	2.7582

RUN NUMBER AP9-4

WIRE LENGTH = .096 M
WIRE DIAMETER = .00025 M
AMBIENT TEMP. = 100 C
PRESSURE = MAX 790.8, DECOMPRESS FROM 377.11 KPA
INITIAL RESIS. = .316198 OHMS AT 160 C
SIGMA = 0

TIME (S)	HEAT FLUX (W/M*M)	THETA (C)	NUSSELT NUMBER
-2.40	417880	59.828	2.5908
-.800	417940	59.979	2.5846
0.800	417980	59.992	2.5843
2.400	417950	59.718	2.5960
4.000	417950	59.306	2.6140
5.600	417940	58.907	2.6316
7.200	417830	58.215	2.6622
8.800	417760	57.288	2.7048
10.40	417750	57.149	2.7113
12.00	417770	57.100	2.7138
13.60	417870	57.210	2.7093
15.20	417900	57.283	2.7060
16.80	417930	56.807	2.7288
18.40	417930	56.439	2.7467
20.00	417910	56.361	2.7503
21.60	417960	56.621	2.7380
23.20	417920	56.657	2.7360
24.80	417930	56.268	2.7550
26.40	417910	56.389	2.7489
28.00	417900	56.474	2.7448
29.60	417900	56.273	2.7546
31.20	417830	56.729	2.7320
32.80	417770	56.740	2.7311
34.40	417720	57.090	2.7140
36.00	417750	57.593	2.6904
37.60	417690	57.398	2.6992
39.20	417690	56.590	2.7377
40.80	417720	56.841	2.7259
42.40	417740	57.399	2.6995
44.00	417790	57.416	2.6991
45.60	417830	56.805	2.7283
47.20	417870	57.123	2.7134
48.80	417900	57.239	2.7080
50.40	417900	57.138	2.7129
52.00	417910	57.137	2.7129
53.60	417840	54.314	2.8535
55.20	417850	54.073	2.8663
56.80	417850	53.499	2.8970
58.40	417800	50.655	3.0593
60.00	417850	51.876	2.9877
61.60	417870	51.654	3.0006
63.20	417860	50.037	3.0975

TIME (S)	HEAT FLUX (W/M*M)	THETA (C)	NUSSELT NUMBER
64.80	417900	50.914	3.0445
66.40	417860	50.000	3.0999
68.00	417880	49.874	3.1078
69.60	417870	49.695	3.1189
71.20	417850	48.246	3.2125
72.80	417820	46.330	3.3451
74.40	417820	46.295	3.3477
76.00	417890	48.310	3.2086
77.60	417890	47.112	3.2901
79.20	417880	46.201	3.3549
80.80	417850	44.417	3.4894
82.40	417810	42.979	3.6058
84.00	417850	43.477	3.5648
85.60	417850	43.054	3.5999
87.20	417860	43.967	3.5253
88.80	417910	45.631	3.3970
90.40	417850	43.669	3.5492
92.00	417860	44.053	3.5183
93.60	417840	43.882	3.5319
95.20	417830	43.591	3.5553
96.80	417830	44.059	3.5177
98.40	417800	43.320	3.5773
100.0	417800	44.156	3.5097
101.6	417800	44.276	3.5001
103.2	417820	43.997	3.5224
104.8	417770	42.275	3.6655
106.4	417750	42.193	3.6725
108.0	417760	42.218	3.6704
109.6	417770	42.857	3.6158
111.2	417790	42.622	3.6358
112.8	417760	41.975	3.6916
114.4	417800	42.330	3.6610
116.0	417800	42.698	3.6295
117.6	417800	42.805	3.6204
119.2	417820	41.918	3.6972
120.8	417800	41.203	3.7612
122.4	417840	41.430	3.7409
124.0	417850	41.712	3.7157
125.6	417880	41.463	3.7332
127.2	417860	41.385	3.7454
128.8	417880	41.548	3.7306
130.4	417910	42.096	3.6823
132.0	417870	41.529	3.7323
133.6	417910	42.432	3.6531
135.2	417880	41.302	3.7523
136.8	417910	41.710	3.7164
138.4	417910	41.577	3.7283
140.0	417910	41.664	3.7205

TIME (S)	HEAT FLUX (W/M*M)	THETA (C)	NUSSELT NUMBER
141.6	417890	41.875	3.7016
143.2	417900	41.408	3.7434
144.8	417930	42.111	3.6811
146.4	417890	41.427	3.7416
148.0	417900	42.275	3.6667
149.6	417870	42.145	3.6776
151.2	417840	41.364	3.7469
152.8	417790	40.629	3.8141
154.4	417790	41.760	3.7109
156.0	417780	42.080	3.6826
157.6	417770	41.980	3.6913
159.2	417720	41.443	3.7387
160.8	417780	42.971	3.6062
162.4	417700	42.543	3.6418
164.0	417690	42.228	3.6688
165.6	417650	41.924	3.6951
167.2	417600	41.846	3.7016
168.8	417580	41.565	3.7264
170.4	417590	41.765	3.7087
172.0	417620	41.755	3.7098
173.6	417580	40.834	3.7932
175.2	417620	41.237	3.7564
176.8	417660	41.501	3.7329
178.4	417690	42.412	3.6529
180.0	417660	41.960	3.6921
181.6	417670	41.798	3.7065
183.2	417730	42.257	3.6667
184.8	417730	42.106	3.6799
186.4	417750	41.799	3.7071
188.0	417730	41.432	3.7397
189.6	417730	42.156	3.6755
191.2	417750	41.685	3.7172
192.8	417740	41.939	3.6946
194.4	417740	41.029	3.7766
196.0	417780	42.869	3.6148
197.6	417780	42.741	3.6257

INITIATION OF SUBCOOLED POOL BOILING DURING PRESSURE TRANSIENTS

by

DONALD L. SCHMIDT

B.S., Kansas State University, 1983

AN ABSTRACT OF A MASTER'S THESIS

submitted in partial fulfillment of the
requirements for the degree

MASTER OF SCIENCE

Department of Nuclear Engineering

KANSAS STATE UNIVERSITY

Manhattan, Kansas

1985

ABSTRACT

An experimental investigation of boiling initiation during pressure transients has been made. A platinum wire heating element of dimensions 0.25 mm diameter and 9.6 cm length was immersed in distilled and degassed water. Maximum pressures from 0.377 to 1.48 MPa were applied with the water and test element temperatures at 100°C before heating the platinum wire to 160°C. The wire experienced constant superficial heat fluxes of approximately 0.42 MW/m^2 while the system was subjected to near-exponential decompressions to atmospheric pressure. Pressure reduction periods were approximately 4 and 6.6 s, and pressure transients were reproducible over most of the pressure drop. Boiling initiation times provided conditions for boiling initiation which depended on the pressure-temperature history of the test element and the surrounding fluid. These conditions tended to be overpredicted by a model accounting for the deactivating effect of pre-pressurization on potential nucleation sites. Reactivation of nucleation sites and recovery of the test element temperature to steady-state were seen to be strongly affected by increases in the maximum pressure applied.